THE SYNTHESIS OF ^{11}C-LABELLED MELATONIN AGONISTS

FROM ^{11}C-CARBON DIOXIDE

BY

BRITA G. SCHULZE

A Thesis

Submitted to the School of Graduate Studies

in Partial Fulfilment of the Requirements

for the Degree

Master of Science

McMaster University

MASTER OF SCIENCE (1994)   McMASTER UNIVERSITY

(Chemistry)   Hamilton, Ontario

TITLE: The Synthesis of ^{11}C Labelled Melatonin Agonists

AUTHOR: Brita G. Schulze,   Diplomchemiker

                  (Technical University Bergakademie Freiberg, Germany)

SUPERVISORS: Professor Günter Firnau

                  Professor Brian E. McCarry

NUMBER OF PAGES: 118

ABSTRACT

This thesis describes the application of the radioisotope ^{11}C to the synthesis of two analogues of the neurohormone melatonin. The labelled compounds were intended to be used as tracers for the medical imaging technology Positron Emission Tomography (PET).

[^{11}C]Carbon dioxide, produced in a small on-site cyclotron by the nuclear reaction ^{14}N(p,α)^{11}C, was converted into [^{11}C]CH$_3$COCl by reaction first with CH$_3$MgBr, followed by reaction with phthaloyl dichloride. The labelled acid chloride was distilled into a solution of an amine, yielding the corresponding ^{11}C-labelled amide, which was purified by a simple solid-phase extraction method.

An apparatus was designed and built that allowed the remote synthesis with several hundred millicuries of [^{11}C]CO$_2$. The apparatus was mounted in a hot cell and operated remotely with a Macintosh Powerbook programmed in Hypercard. The apparatus and software are generic for these acylation reactions.

The individual reaction steps were optimized in terms of reaction time, solvents and equipment; radiosyntheses of a number of purified labelled acetamides were completed in 35 minutes. The radiochemical yields ranged from 15 to 20% with specific activities in the 500 mCi/μmol range at the end of the synthesis.

2-Iodo-[^{11}C-acetyl]melatonin (**11**) and 7-methoxynaphthylenyl-1-ethyl-N-[^{11}C-acetyl]acetamide (**15**) were synthesized for the first time for PET studies. It was shown that both compounds readily cross the blood-brain-barrier and penetrate into all brain tissues. Specific binding to the melatonin receptors in the suprachiasmatic nuclei of the hypothalamus could not be visualized with either one of the ^{11}C-labelled ligands because of low specific activity and high nonspecific binding.

ACKNOWLEDGEMENTS

I wish to express my thanks to Professor Günter Firnau for his excellent guidance during this project, his contributions to the construction of "the apparatus" and his participation and support in so many experiments. His encouragement especially in the beginning of this work gave me much needed confidence.

Equally, I would like to thank Professor Brian E. McCarry for the helpful discussions, which often showed me the importance of a systematic approach to a problem.

I am very grateful to my co-workers in the radiochemical laboratory of the McMaster PET Centre Dr. Raman Chirakal, Dr. Jia Juen Chen and Dr. Dilip Murthy for their scientific and moral support and their eagerness to help me in every regard.

Furthermore, I wish to thank Kinrich Chin for his excellent programming work that provided a reliable basis for operating the apparatus.

Special thanks are due to Ms. Carol Dada and Dr. Brian McCarry for their much appreciated efforts to assist my financial situation by providing me with an Ontario Differential Fee Waiver.

Above all, I wish to thank my husband Andreas for his encouragment, patience and support in the last years.

TABLE OF CONTENTS

LIST OF FIGURES

x

LIST OF TABLES

CHAPTER 1

INTRODUCTION

1.1. Melatonin and its Analogues

This section provides basic information about melatonin, its biochemistry and its biological importance. The concept of receptor agonists and antagonists will be discussed in relation to melatonin and some of its analogues.

1.1.1. Chemical Structure, Synthesis and Catabolism of Melatonin

Melatonin was first identified about 40 years ago as a neurohormone. Its structure is shown in Figure 1.
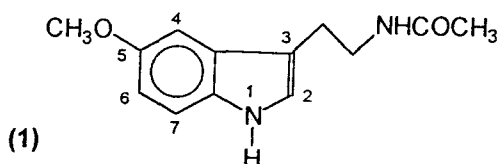
Figure 1: Chemical Structure of Melatonin

Melatonin is produced and secreted by the pineal gland and the retina. The most striking feature is the diurnal variation of its secretion, which is suppressed by environmental light (1). The hormone diffuses out of the synthesizing cells and is transported to its targets, which are high affinity receptors in the central nervous system (hypothalamus), retina and pituitary (1). Its synthetic pathway is shown in Figure 2.

The catabolism of melatonin occurs by several pathways, mainly in the liver

(Figure 3). Pathway 1 accounts for the majority of metabolized melatonin (2), while only 0.5 to 2% is metabolized according to Pathway 2 (3). The latter pathway has also been found in the eyes of non-mammalian species (4). Investigations of melatonin synthesis and catabolism have been hampered because of its short biological half-life (e.g., 12-15 min in the rat (5)).
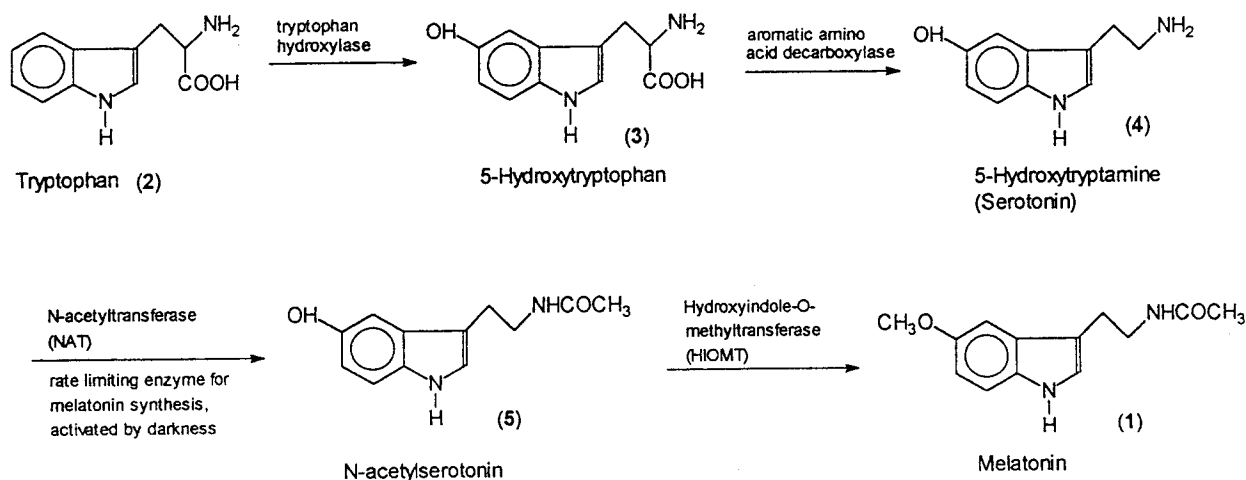
Figure 2: Biosynthesis of Melatonin
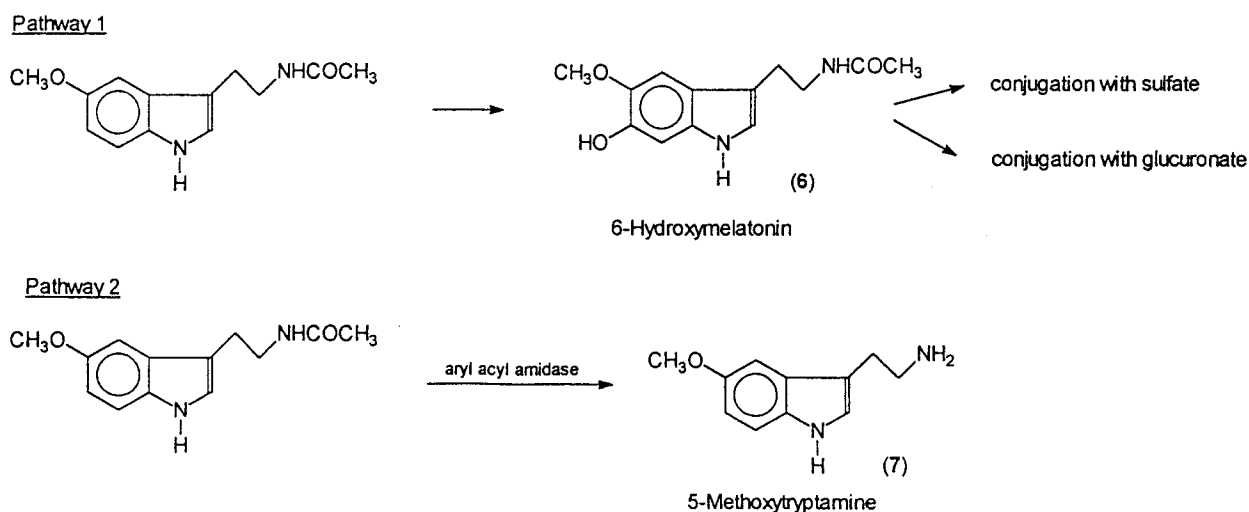
Figure 3: Catabolism of Melatonin

1.1.2. Biological Importance of Melatonin

Melatonin is rhythmically secreted by the pineal gland and the retina in most vertebrates and mammals, including man. Its signal entrains the circadian system; thus, it is an important part of the biological clock.

The circadian system induces the daily fluctuations of brain function, hormone secretion and metabolic activity. In many species it also produces seasonal rhythms of fertility and metabolism (6). The most important components of the circadian system are:

(1) the suprachiasmatic nucleus (SCN), a small structure in the hypothalamus, which contains a high concentration of binding sites for melatonin. The SCN is thought to function as a circadian oscillator (7).

(2) the pineal gland, which synthesizes and secretes melatonin into the blood stream during darkness. In non-mammalian species the pineal gland contains photoreceptors and circadian oscillators.

(3) photoreceptors in the ocular retina in mammals, which are responsible for the influence of light and darkness on the melatonin production in the pineal gland (6).

Figure 4 shows the important components and interactions of the mammalian melatonin system. The SCN is the internal clock (*Zeitgeber*) for a rhythmic production of melatonin. This production is externally triggered with the onset of darkness. If there is a considerable timeshift in the onset of darkness (e.g., flight over several time zones), it will take a few cycles until the endogenous clock is adjusted to the new dark-light cycle.

Blood plasma melatonin crosses the blood-brain-barrier and interacts with its receptors. In humans the melatonin receptors are thought to be located in the SCN. They have also been found in the retina and in the pituitary. The binding of melatonin to these receptors has various effects. Body functions are adjusted to the time of the day (e.g.,

levels of hormones, effectiveness of kidney function, etc.). In some species (seasonal reproductive animals) the reproductive system is adjusted to the time of the year.

>->->->- neuronal pathway

endogenous clock in the SCN gives signal for rhythmic melatonin production in approx. 24 hour cycle

daylight inhibits melatonin production

retinal photo-receptors respond to dark-light cycle and send out signal to produce melatonin

>->->->-

pinealocytes of pineal gland produce melatonin and secrete it into blood stream

darkness stimulates melatonin production

melatonin

catabolism in liver

physiological and behavioural effects:
-circadian entrainment
-reproduction
-endocrine function
-retinal function

>->->->->->-

reversible binding to specific receptors in CNS, retina and pituitary

Figure 4: Components of the Mammalian Melatonin System

Abnormalities of the melatonin-driven rhythmic events in man have been identified. For example, well being can be interfered with due to air travel across time zones (jet lag), shift work or sleep disorders (8). Seasonal depression is associated with a disrupted circadian rhythm. In addition, the onset of puberty is determined by the melatonin system (9).

With melatonin administration psychological and physiological effects of jet lag

could be alleviated (8). Oral melatonin doses have been given to synchronize the circadian rhythms of blind people, who lack retinal photoreceptors and suffer from sleep disorders (10). There is interest in the use of melatonin in other circadian rhythm disfunctions like delayed sleep-phase syndrome, seasonal depression and shift work syndromes (8). Recently, a melatonin-based contraceptive has been developed (9).

These facts raise interesting questions, but our understanding of the *in vivo* action of melatonin is still limited. Most experimental methods were only helpful in localization and in *in vitro* pharmacokinetic studies of melatonin receptors. For further progress a non-invasive, *in vivo* method is needed.

1.1.3. Receptor Agonists and Antagonists

Compounds can be classified as hormone receptor agonists or antagonists according to their ability to bind to the receptor and to exert a signal similar or equal to that of the hormone. An antagonist binds to the receptor, but does not exhibit any biological activity; therefore antagonists can block the receptor site. Receptor agonists show both binding and biological activity similar to that of the naturally occurring hormone.

The receptor binding affinity is characterized by the value of the binding dissociation constant K_d. The simplest model to describe the interaction of a compound with a receptor is the bimolecular reaction:

$$(1) \qquad L + R \underset{k_{-1}}{\overset{k_{+1}}{\rightleftharpoons}} RL$$
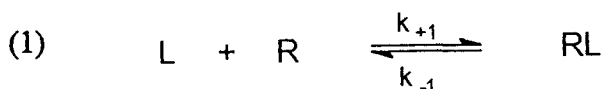
L = ligand k_{+1} = fractional rate constant of association

R = receptor k_{-1} = fractional rate constant of dissociation

RL = receptor-ligand complex

The equilibrium dissociation K_d constant is defined as (11):

$$(2) \qquad K_d = \frac{[R] \cdot [L]}{[RL]}$$

and at equilibrium:

$$(3) \qquad K_d = \frac{k_{-1}}{k_{+1}}$$

Therefore, the lower the K_d, the less the dissociation of the receptor-ligand complex under comparable experimental conditions or, in other words, the higher the affinity of the receptor for the ligand.

Heward *et al.* (12) and Frohn *et al.* (13) established some basic structure - activity relationships for melatonin and its derivatives. They found that in melatonin the methoxy group on carbon 5 is essential for the activity toward the receptor and defines it as an agonist, whereas the N-acetyl moiety, attached through an ethyl group to the C3 atom, is important for receptor binding. Therefore, compounds like N-acetyltryptamine (8) or N-acetylserotonin (5) are receptor antagonists (Figure 5). On the contrary, compounds like 5-methoxytryptamine (7) or 5-methoxyindole-3-acetic acid (9) have some melatonin-like activity, i.e., they are receptor agonists, although they bind poorly to the receptor (12). N-butyrylamide-5-methoxytryptamine (10) has a 50% higher biological activity than melatonin, which may be caused by the increased receptor affinity (13).

In later studies 2-iodomelatonin (11) and 6-chloromelatonin (12) were found to have much higher receptor affinities than melatonin (14,15). Dubocovich (16) reported a novel melatonin receptor antagonist, luzindole (13), which has a receptor affinity comparable to that of melatonin. N-(2,4-dinitrophenyl)-5-methoxytryptamine (14) has been described as an antagonist with high affinity in the rat (17), but not in the hamster (18).

Antagonists   Agonists
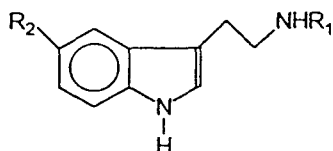
(5) : R1 = COCH₃   R2 = OH

(8) : R1 = COCH₃   R2 = H

(1) : R1 = COCH₃   R2 = OCH₃

(7) : R1 = H   R2 = OCH₃

(10) : R1 = COC₃H₇   R2 = OCH₃
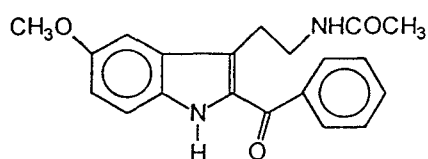
(13)
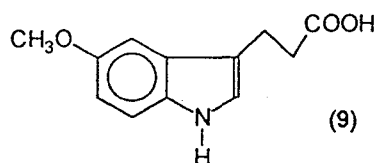
(9)
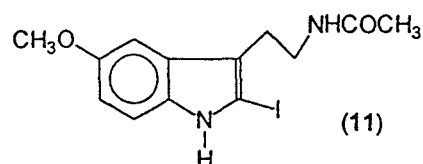
(11)
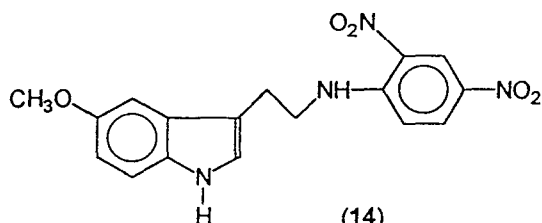
(14)
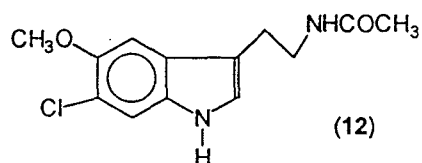
(12)
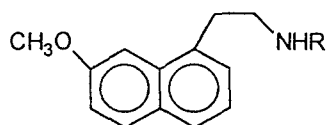
(15) : R = COCH₃
(16) : R = COCF₃
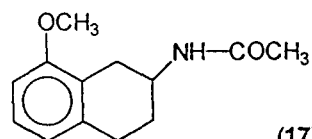
(17)

Figure 5: Melatonin Receptor Agonists and Antagonists

Both compounds have a methoxy group in the 5-position and therefore they do not fit into

the proposed structure-activity relationship (12,13). It is not clear whether in these cases

the biological activity is suppressed because of the phenolic substituents.

The pharmaceutical company SERVIER has developed a series of naphthalene derivatives that exhibit biological behaviours very similar to melatonin (19). 7-Methoxynaphthylenyl-1-ethyl-N-acetamide or S20098 (15) has a pharmacological activity comparable to that of melatonin and its receptor affinity is *ca.* 100 times higher than that of melatonin. S20755 (16) binds stronger to the melatonin receptor by five orders of magnitude (see Table 5).

Recently, some methoxy-substituted 2-amidotetralins have been found to exhibit melatonin-like effects (20). Although the reported receptor affinities of these tetralin derivatives are lower than those of melatonin or 2-iodomelatonin, the authors could demonstrate that the optimal spatial distance between the methoxy and acetamido group is a further requirement for a melatonin agonist. 2-N-acetyl-8-methoxytetralin (17) showed the best results.

1.2. Positron Emission Tomography (PET)

This section is intended to give an overview of Positron Emission Tomography and of the radioisotopes available for this technology. Compounds that are to be used as PET tracers must meet specific requirements, which dictate their chemical syntheses, analyses and methods of purification. These requirements will be discussed in more detail.

1.2.1. Isotopes for PET

PET is an imaging technology that involves radioactive tracers. The tracers (radiopharmaceuticals) require special isotopes that decay by positron emission.

The nucleus of a positron-emitting isotope is unstable; it is proton-rich in relation to its most stable isotope. By transformation of a proton into a neutron and emission of

the positron (β^+) the nucleus attains a stable proton-neutron balance. The positron has the same rest mass as an electron, but a positive charge and is regarded as the anti-matter counterpart to the electron. After ejection the positron has a certain kinetic energy, which carries it some distance. The kinetic energy decreases until the positron is almost at rest. Then, it interacts with an electron and the mass of the two is set free as "annihilation energy". Two γ-rays are emitted in almost opposite directions, each with 511 keV of energy. This process is shown in Figure 6.

The detection of the labelled compound during a PET study relies on this special feature of the two γ-rays with a distinctive energy, emitted simultaneously while the nuclide decays.
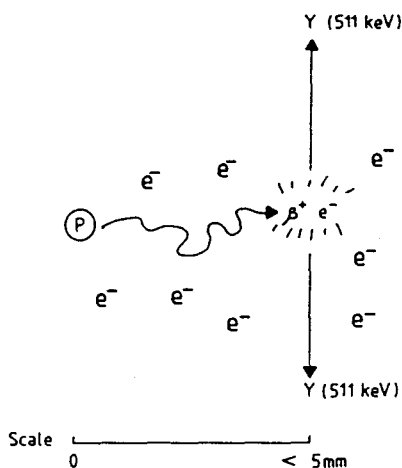
Figure 6: Decay of a Positron Emitting Radionuclide (21)

Table 1 summarizes the physical characteristics of the most commonly used positron-emitting isotopes in PET. They have the advantage of decaying almost exclusively by positron emission. The other decay mechanism, electron capture, is worthless for PET and contributes only to the radiation dose for the patient.

These nuclides are produced routinely in small, medical cyclotrons in a hospital setting. Thus, radiochemical syntheses with these isotopes to produce the respective

radiopharmaceutical can be carried out in close proximity to the clinical use.

Table 1: Isotopes used in PET Studies

Isotope	Half-life in min	Positron Emission	Decay Product
^{11}C	20.4	99.8%	^{11}B
^{13}N	10.0	100%	^{13}C
^{15}O	2.0	99.9%	^{15}N
^{18}F	109.8	96.9%	^{18}O

The half-life of ^{18}F allows relatively timely syntheses (up to 6 hours). The most extensively used F-18 labelled tracers in PET are 2-deoxy-2-[^{18}F]fluoro-D-glucose (**18**) and 6-[^{18}F]fluoro-L-dopa (**19**) (Figure 7). The half-lives of ^{15}O and ^{13}N (2 minutes and 10 minutes, respectively) limit the spectrum of possible chemical reactions. Some tracers which are used routinely in clinical investigations are [^{13}N]NH$_3$, [^{15}O]O$_2$ and [^{15}O]H$_2$O. The half-life of ^{11}C (20 minutes) permits a variety of chemical reactions, for example, methylations with $^{11}CH_3I$ or addition of $^{11}CO_2$ to various Grignard compounds.
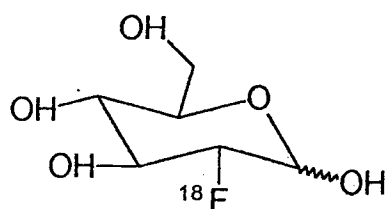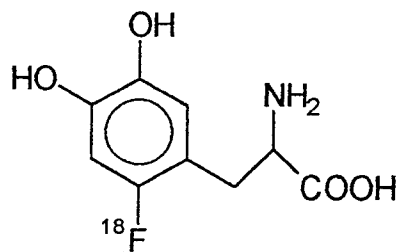
(18)   (19)

Figure 7: Examples of PET Tracers in Clinical Routine

1.2.2. Production of Isotopes

Several methods and devices exist for the production of radioisotopes. For clinical applications, cyclotrons have proven to be the most practical accelerators. They can be classified according to the energy and multiplicity of charged particles available for irradiation (21). Figure 8 shows the principle of acceleration in a schematic diagram of a cyclotron.
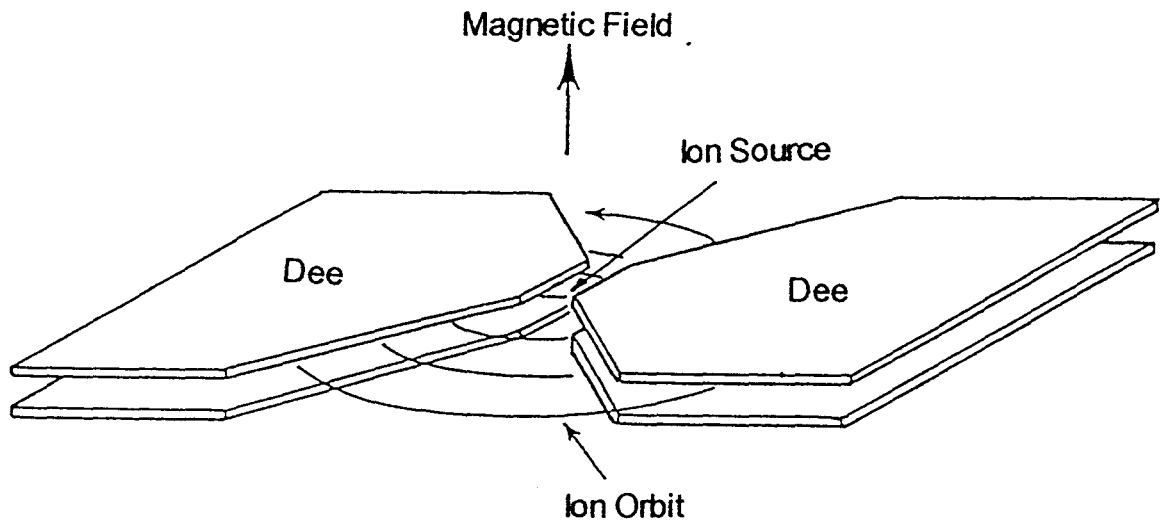
Figure 8: Principle of Ion Acceleration in a Cyclotron (22)

An ion source is located in the middle of the vacuum tank, between the so-called Dee-electrodes (Figure 8). Negative hydrogen ions are electrostatically extracted from the plasma within the ion source. The combination of an oscillating electrical field (± 30 kV) and a permanent magnetic field (1.8 Tesla) forces the hydride ion into a spiral path between the Dee-electrodes. After approximately 110 revolutions the H⁻ ion has attained an energy of 11 MeV. Then it is intercepted by a thin carbon foil, which strips away the two weakly bound electrons from the nucleus, affording a proton. The resulting proton changes its direction and streams outward, toward one of the targets for irradiation (22).

Figure 9 shows a schematic of a gas target for production of $^{11}CO_2$ (22). The target body is made of aluminum, the window that separates the pressurized target gas from the vacuum tank is made of Havar (stainless steel with a thickness of 25 μm). The target is loaded with 11.4 mL $^{14}N_2$ at 200 psi; this pressure rises to 450 psi during irradiation. The target body is cooled with water and the Havar window is cooled by a helium gas stream. Gas targets have usually a conical shape as seen in Figure 9; this shape tends to minimize scattering effects that occur when the incoming protons hit the target wall.
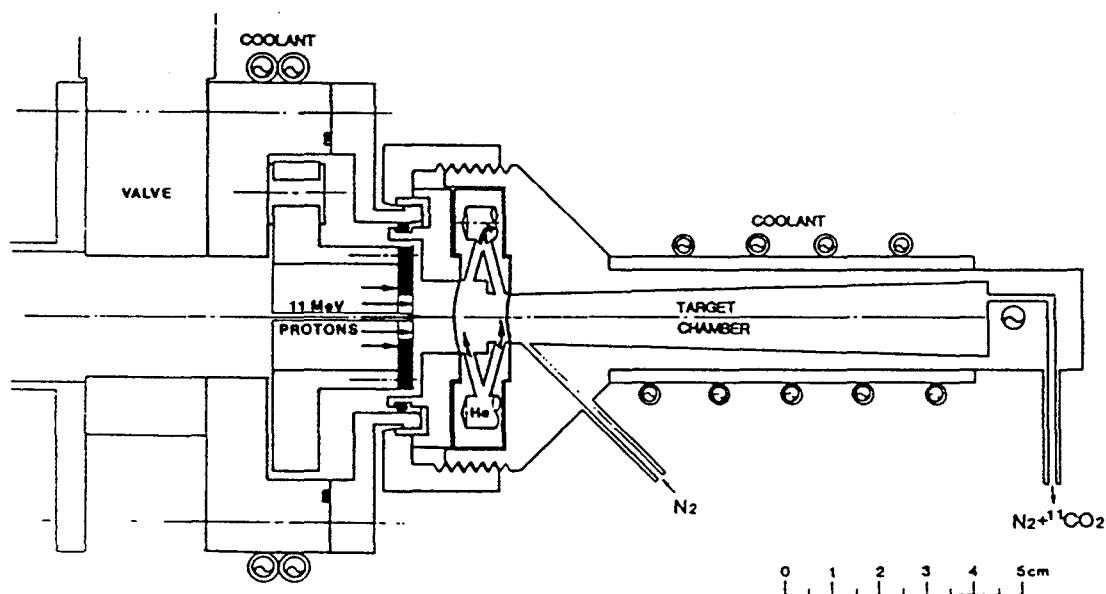
Figure 9: Schematic of a Gas Target for Production of $^{11}CO_2$

Table 2 shows the more common isotopes and the methods for their production. Most of the nuclear reactions can be carried out with low energy protons (< 20 MeV). This means that positron-emitting isotopes for medical use can be produced with small, easy to operate, low energy (10 to 20 MeV), proton-only cyclotrons.

Table 2: Production of Positron Emitting Isotopes

Isotope	Nuclear Reaction for Production[A]	On-line Product Precursor for Further Syntheses
^{11}C	^{14}N (p,α) ^{11}C	$[^{11}C]CO_2$ $[^{11}C]CH_4$
^{13}N	^{13}C (p,n) ^{13}N ^{16}O (p,α) ^{13}N ^{12}C(d,n) ^{13}N	$[^{13}N]NH_4^+$ $[^{13}N]NO_3^-$ $[^{13}N]NO_2^-$
^{15}O	^{15}N (p,n) ^{15}O	$[^{15}O]O_2$ $[^{15}O]CO$ $[^{15}O]CO_2$ $[^{15}O]H_2O$
^{18}F	^{18}O (p,n) ^{18}F	$[^{18}F]F^-$ $[^{18}F]F_2$

[A] The isotope in front of the bracket indicates the starting material. The first letter in the bracket stands for the particle which irradiates the starting material, the second one stands for the emitted particle during irradiation. The produced radioisotope is indicated after the brackets. Abbreviations: p = proton, α = alpha-particle (helium nucleus), n = neutron.

1.2.3. Principles of PET

In a PET study, the patient receives an intravenous injection of the tracer that is labelled with a positron-emitting isotope. The organ of interest (usually the brain or the heart) is monitored by the tomograph, consisting of several rings of γ-ray detectors. This is schematically depicted in Figure 10.

The Siemens-CTI Tomograph (model 953), used at the McMaster University PET Centre consists of 15 detector rings. Each ring has 384 individual detectors. Two

opposing detectors will register one event at the line between them when they each are hit by a γ-ray "simultaneously" (i.e., within the coincidence time of a few nanoseconds). Millions of coincidence events are registered during a PET scan.
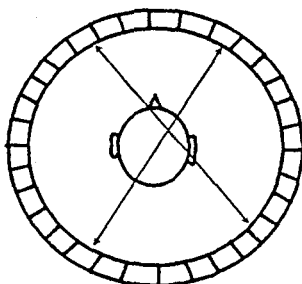
Figure 10: Schematic of the Human Head in the Detector Ring of a Tomograph (arrows indicate the coincident γ-rays)

Due to attenuation by body tissue and bone some 511-keV-γ-rays of the injected PET tracer are lost or arrive at the detector with decreased energy. Therefore, the attenuation for every line of coincidence is measured for each patient prior to the PET scan. The radiation source for this transmission scan is ^{68}Ge/^{68}Ga in secular equilibrium, where ^{68}Ga produces 511-keV-γ-rays. This radiation source is in the detector ring moved around the organ; at each position the opposite detector will register more or less attenuated γ-rays. This information is then used during the image reconstruction process.

After data accumulation the coincidence lines between detectors across the tomograph circle are "backprojected" to reconstruct the distribution pattern of radioactivity in the original object. This pattern is displayed as cross-sectional slices through the organ of interest as colour-coded images. A modern PET scanner monitors up to 31 slices simultaneously, covering a width of ca. 15 centimetres *in vivo*. The spatial resolution ranges from 4 to 7 millimetres.

1.2.4. Specific Requirements for PET Tracers

PET tracers have several important characteristics which distinguish them from other pharmaceuticals. A discussion and an explanation of these characteristics is necessary before imaging of melatonin receptor sites can be addressed. This section reviews the following requirements:

(1) purity, sterility, apyrogenity

(2) high radiochemical yield

(3) high specific activity

(4) high binding affinity

(5) high binding selectivity

(6) blood-brain-barrier permeability

(7) slow metabolism, fast clearance

(8) no toxic or pharmacologic effects.

1) Purity, sterility, apyrogenity

Since the tracer will be injected intravenously, it must be chemically pure, sterile and apyrogen (apyrogen means free of small particles like cell remnants, which would cause inflammation). Because of the short half-lives of the isotopes available, the labelled compound must be injected into the patient before its purity, sterility and apyrogenity can be checked. Therefore extreme care in the purification of the tracer and a high degree of reproducibility during the synthesis are necessary.

2) High radiochemical yield

The radiochemical yield gives information about the percentage of produced radioactive tracer that is associated with the product and should be as high as possible. It is calculated as the ratio of product activity over starting activity, both decay corrected to a common time point:

$$(4) \quad radiochemical \; yield = \frac{(product \; activity)_{t=0}}{(starting \; activity)_{t=0}} \times 100$$

3) High specific activity

PET requires tracers with high specific activity for receptor studies. The specific activity is defined as the activity of labelled compound divided by the amount of unlabelled compound present in the product:

$$(5) \quad specific \; activity = \frac{activity}{chemical \; quantity}$$

Data containing an amount of activity must bear a reference to a common time point to allow their evaluation. Therefore, the specific activity can be expressed as either

a) corrected to end of bombardment (EOB): a correction for the radioactive decay since the end of bombardment in the accelerator has been made.

b) corrected to end of synthesis (EOS): no correction for radioactive decay during the time of synthesis was made and the value expresses the actual specific activity at a certain time.

The theoretical specific activity is inversely proportional to the half-life of the nuclide and can be calculated as shown in the example for 1 Curie of ^{11}C. A Curie is defined as 3.7×10^{10} decompositions per second (dps). The radioactive decay obeys the differential relation:

$$(6) \quad -\frac{dN}{dt} = \lambda \times N \approx -\frac{\Delta N}{\Delta t}$$

N = number of ^{11}C nuclei $\quad\quad\quad$ Δt = 1 second

λ = decay constant = 0.693 / $t_{1/2}$ $\quad\quad$ $t_{1/2}$= half life in seconds = 1200 s

For 1 Curie we can write:

$$(7) \qquad -\frac{\Delta N}{\Delta t} = 3.7 \times 10^{10} \; dps$$

Thus, $\qquad\qquad 3.7 \times 10^{10} = \lambda \times N$

$$N = 6.4 \times 10^{13} \text{ atoms}$$

or $\underline{N = 106.3 \text{ pmol}}$

A_0 = Avogadro number = 6.022×10^{23}

Therefore, the specific activity would be

$$(8) \qquad \frac{1 \; Ci}{106.3 \; pmol} = \frac{x}{1 \; mol}$$

$$\underline{x = 9.4 \times 10^6 \text{ Ci / mmol}}$$

These calculations illustrate that the actual quantities of labelled material will be at most in the picomolar range, which allows to quantify them only by measuring their radioactivity .

The actual specific activity of a compound depends strongly on its preparation. The shorter the half-life of an isotope, the more important becomes the time factor. This is illustrated in Table 3. For example, during handling of gaseous radioactive compounds such as $[^{11}C]CO_2$ dilution with $^{12}CO_2$ is unavoidable. A ratio of labelled vs. unlabelled product of 1:10,000 or greater is commonly encountered.

There is a limit to the quantity of radioisotope that can be produced in a cyclotron, for example 1500 mCi of ^{11}C with the McMaster cyclotron. On the other hand, there is a minimum amount of radioactivity that must be incorporated in a PET

Table 3: Values for the Specific Activity of some Isotopes

Isotope	Half Life	Theoretical Specific Activity [Ci/mmol]	Spec. Act. in Practice [Ci/mmol]
^{14}C	5600 years	0.062	0.06[A]
^{125}I	60 days	2170	2000[A]
^{32}P	14 days	9317	6000[A]
^{18}F	110 min	1.71 x 10^6	10-12[B]
^{11}C	20.4 min	9.4 x 10^6	500[C]

[A] value given by manufacturer (Amersham) for the respective labelled product

[B] approximate value achieved in the laboratory of the McMaster PET group after production of 200 mCi of [^{18}F]F$_2$ in a cyclotron, followed by a 2 hour synthesis of 6-[^{18}F]fluoro-L-DOPA (personal communication with Dr. Raman Chirakal)

[C] approximate value after production of 450 mCi of [^{11}C]CO$_2$ in a cyclotron, followed by a 30 minute synthesis of a C-11 labelled melatonin agonist

tracer for sufficient imaging (10 to 20 mCi, depending on the isotope). Therefore, chemical synthesis, purification and preparation for injection must be accomplished within 2-3 half-lives of the respective isotope.

One can classify PET tracers in three categories:

a) flow tracer, e.g., [^{15}O]H$_2$O, [^{13}N]NH$_4$$^+$

b) metabolism tracer, e.g., [^{18}F]fluoro-2-deoxyglucose, 6-[^{18}F]fluoro-L-dopa

c) receptor binding tracer, e.g., [^{18}F]fluoropropylspiperone.

Tracers of the first two categories help to elucidate metabolism or blood flow; a sufficient amount of activity must be injected to yield a high count rate in the scanner, but their specific activity is of little importance.

Tracers for receptor binding **compete** with naturally present compounds in the

body for a limited number of binding sites. If the tracer is too dilute with unlabelled compound (i.e., low specific activity), there will not be enough accumulation of activity in the area of interest and PET imaging is not possible. For these compounds a high specific activity is very important.

Both the specific activity and the radiochemical yield depend strongly on the chemical synthesis; possible synthetic pathways are dictated by the time that is available to work with the respective isotope. Therefore, a loss in radiochemical yield is often accepted if the reaction time can be decreased or if the specific activity can be increased. This will be further discussed in Section 1.3.2.

4) High binding affinity (for tracers involved in a competition for binding sites)

For imaging of receptor binding sites, the radioactively labelled tracer should bind strongly to the receptor, which requires a low K_d value (see Section 1.1.3.).

5) High binding selectivity (for tracers involved in a competition for binding sites)

The specific binding of a ligand to the receptor must be high, its nonspecific binding (to other tissue components or to walls of glass test tubes in an *in vitro* experiment) should be low. In an *in vitro* binding assay only the total binding is observed; it consists of a hyperbolic curve at low ligand concentrations (specific binding), which becomes a straight line at higher concentrations of ligand (nonspecific binding, Figure 11 (11)). The nonspecific binding is proportional to the concentration of added ligand and does not depend on the existence of binding sites. Therefore, if the ligand concentration is low enough (approximately its K_d value), its nonspecific binding can be neglected.

6. Blood-brain-barrier Permeability

The blood-brain-barrier prevents the diffusion of proteins and neutral molecules into the intercellular space in the brain (23). For glucose and amino acids, specific trans-membrane active transport mechanisms exist, otherwise only lipid soluble compounds would gain access to the brain by diffusion. If a new PET tracer for the brain is

Figure 11: Specific and Nonspecific Binding in a Receptor Binding Study (11)

developed, its ability to cross the barrier is a first basic requirement. With a PET study quantitative relationships can be obtained about tracer concentrations in blood and brain, which allows to evaluate the ability of the compound to cross the blood-brain-barrier.

7. Slow Metabolism and Fast Clearance

The metabolic decomposition and clearance of the PET tracer should be slow from the organ of interest to allow enough time for imaging. In contrast, the clearance of the tracer and its degradation products should be fast from the tissue surrounding the organ of interest. Both of these parameters must be determined experimentally.

8. No Toxic or Pharmacologic Effects

The synthesized tracer must not have any toxic or pharmacological effects. Carbon-11 labelled PET tracers have a high specific activity, in the range of 500 to 5000 mCi/μmol. A quantity of 10 to 20 mCi is injected in a typical PET study. Therefore, the net chemical quantity administered is in the range of 2 to 40 nmol or 30 to 600 pmol per kg body weight. Pharmacological or toxic effects can not be expected to be observed at

those concentrations.

In addition, the product must be analyzed for the presence of radioactive and non-radioactive impurities that may have arisen during synthesis.

1.3. Candidates for PET Imaging of Melatonin Receptors

This section will discuss melatonin receptor agonists that have proven to be good receptor ligands *in vitro* (low K_d value). From these compounds candidates were chosen for ^{11}C labelling in this thesis.

1.3.1. Review of Experiments to Visualize Melatonin Receptors

The investigation of melatonin receptors has long been hampered by the lack of high affinity ligands for the melatonin receptor. Using the low affinity ligand [3H]melatonin (K_d in the nanomolar range), investigators were able to identify binding sites in brain homogenates (24,25) and by *in vitro* autoradiography. In the latter method slices of brain were dipped into a solution of radioactively labelled melatonin. Afterwards the solution was rinsed off and a film was exposed to the organ slices. Areas with accumulated radioactivity (melatonin) caused blackening of the film and the regions of accumulated melatonin were detected. Because of the low specific activity (*ca.* 30 Ci/mmol) results have not been very consistent.

These studies were improved considerably by the development of 2-[125I]iodomelatonin (26,27), a receptor ligand with higher affinity (K_d in the picomolar range) and increased specific activity (*ca.* 2000 Ci/mmol).

Application of 2-[125I]iodomelatonin in *in vitro* autoradiography allowed localization of melatonin binding sites in the SCN and the median eminence region of the rat hypothalamus (28). Subsequently, these techniques were refined and slightly varying binding sites for different species could be established.

In some cases two or more research groups have reported different melatonin binding sites for one species, which shows the difficulty in ascribing the fast and reversible binding process to a structure with the dimensions of a few millimetres; for example, binding sites in rats were found in the median eminence of the hypothalamus (28) and in the pars tuberalis (29).

So far, little work has been done to investigate melatonin binding in humans. Reppert *et al.* (30) did postmortem autoradiography studies with 2-[^{125}I]iodomelatonin in the brains of fetuses and adults and identified melatonin binding sites in the SCN. Their autoradiography showed the suprachiasmatic nuclei in humans as two oval spots, each approximately 0.5 mm wide and 2 mm long and 4 mm apart from each other. Yuan *et al.* (31) investigated in postmortem fetuses binding and pharmacological characteristics of 2-[^{125}I]iodomelatonin and found the highest number of sites in the hypothalamus (which contains the SCN).

An *in vivo* approach with PET has first been made by LeBars *et al.* (32,33). Melatonin, labelled with the positron emitting isotope ^{11}C, was injected into a volunteer whose brain was monitored by PET. The images did not show the expected accumulation of ^{11}C at the receptor site in the hypothalamic area. Several reasons may explain the failure of this experiment:

(1) The specific activity of the labelled melatonin was not high enough and there was too much unlabelled material competing for the receptor sites.

(2) The binding of melatonin to the receptors is not strong enough (i.e., K_d is too high).

(3) The biological half-life of melatonin is very short and the compound was catabolized too rapidly.

(4) The authors attempted to visualize an area with dimensions below the resolution of the PET scanner. The spatial resolution of a modern tomograph is 4 -

7 mm, and the contrast of radioactivity (i.e., the signal to noise ratio) might not have been high enough to visualize that small area.

Similarly, attempts to use melatonin fluorinated with ^{18}F in 4-position (34) (20) for imaging the SCN in human brain did not succeed (Firnau, unpublished). In this case most likely the specific activity of 6-[^{18}F]fluoromelatonin (0.235 Ci/mmol) was too low and the PET image did not show accumulation of radioactivity in the hypothalamic area. The low specific activity is unavoidable because of the fluorination procedure (Figure 12) which uses [^{18}F]F$_2$ gas containing cold carrier fluorine.

Figure 12: Fluorination of Melatonin (34)

In a further experiment, LeBars *et al.* (35) tried to overcome the problems of fast *in vivo* metabolism and of low specific activity by acetylating 6-fluoro-5-methoxytryptamine with [^{11}C]CH$_3$COCl. Since the melatonin degradation starts with 6-hydroxylation, 6-fluoromelatonin has a longer biological half-life (27 min in the rat) (5). So far they have not reported successful PET imaging with this tracer. Table 4 summarizes the experimental work thus far to prepare melatonin and its analogues labelled with positron emitting isotopes.

Table 4: Experiments to Label Melatonin and some of its Analogues with Positron Emitting Isotopes

Isotope	Melatonin Derivative	Specific Activity at EOS in mCi/µmol	Radioch. Yield	Applied in PET	Ref.
^{11}C	melatonin	268	25%	yes; no specific binding	(32,33)
^{11}C	6-fluoro-melatonin	43	35%	no	(35)
^{18}F	4-fluoro-melatonin	0.235	19%	yes; accumulation of activ. in hypothal., but no identification	(34) Firnau, unpubl.
^{18}F	6-fluoro-melatonin	0.235	8%	no	(34) Firnau, unpubl.

1.3.2. New Prospective Candidates for PET Imaging of Melatonin Binding Sites

The visualization of melatonin binding sites *in vivo* requires a PET tracer suitable for a competition experiment; therefore it is desirable that the tracer has a high specific activity. The lowest specific activity with which imaging would still be possible can be estimated from (1) the number of melatonin binding sites in the brain and from (2) the required count rate that would give a detectable signal during a PET study. These two requirements can be connected as follows:

Yuan *et al.* (31) reported the maximum number of binding sites in the hypothalamus of a human fetus as 5.4 fmol/mg protein or 216 fmol/g brain tissue,

which is approximately 216 fmol/cm³ tissue (1 g wet brain tissue contains *ca.* 40 mg protein). We can assume a receptor occupancy of 10%, therefore 21.6 fmol of ligand can be bound in 1 cm³ of tissue. The tomograph would need about 10 nCi per cm³ or per gram brain tissue for a statistically significant count rate.

Therefore the labelled compound must have a minimum specific activity of:

$$(9) \quad spec.\ activity = \frac{10^{-8} Ci \times cm^3}{216 \times 10^{-15} mol \times cm^3 \times 0.1} = 460 \frac{Ci}{mmol}$$

While this value is only an estimate, it could be achieved with ^{11}C-containing melatonin derivatives, but not with ^{18}F-labelled compounds that have been made from electrophilically reactive $[^{18}F]F_2$ (see Table 4). Therefore, labelling with ^{11}C has been the focus of the work in this thesis.

As explained in Chapter 1.2.4, the specific activity of compounds labelled with positron-emitting isotopes will decrease with time. If a compound were to be labelled with ^{11}C, the maximal time available for synthesis can be calculated as follows: Let's assume that approximately 750 mCi of $[^{11}C]CO_2$ can be produced with our cyclotron. With an acetylation procedure similar to that described by LeBars (32), a radiochemical yield of 25% or about 188 mCi could be expected. Injection of 15-20 mCi of a ^{11}C-labelled tracer would allow PET scanning for 60 to 90 minutes.

The radioactive decay of an isotope obeys the relation

$$(10) \quad A = A_0 \times EXP\left(-\frac{0.693 \times t}{t_{\frac{1}{2}}}\right)$$

A = remaining activity at time t
A_0 = starting activity at time t_0
t = time $t_{1/2}$ = half life

If equation 10 is applied to 188 mCi (=25% of 750 mCi), 74 min are available for the synthesis of 15 mCi labelled product. If a radiochemical yield of only 10% can be achieved, the available time decreases to 47 minutes.

Table 5: Equilibrium Dissociation Constants K_d of some Melatonin Analogues

Animal; Organ	Melatonin Analogue	K_d in M	Reference
rabbit; retina	luzindole (13)	2×10^{-8}	(16)
bovine; medial basal hypothalamus	[^{3}H]melatonin (1)	1.2×10^{-8}	(24)
rat; hypothalamus	[^{3}H]melatonin (1)	8.7×10^{-9}	(36)
ovine; pars tuberalis	S20098 (15)	8.1×10^{-11}	(19)
ovine; pars tuberalis	2[^{125}I]-iodomelatonin (11)	2.5×10^{-11}	(29)
rat; median eminence (PT)	2[^{125}I]-iodomelatonin (11)	2.1×10^{-11}	(28)
human; hypothalamus	2[^{125}I]-iodomelatonin (11)	2.1×10^{-11}	(31)
human; brain	2[^{125}I]-iodomelatonin (110	1.4×10^{-11}	(31)
ovine; pars tuberalis	S20755 (16)	4.2×10^{-13}	(19)

Another selection criterion for a candidate suitable for visualization of melatonin receptors is its binding dissociation constant K_d, which should be as low as possible.

Table 5 shows some selected K_d values. Since these K_d values were established in different binding assays, using different animals, care must be taken in comparing them directly with each other. Nevertheless, they give an idea about the order of magnitude of binding affinity.

The results show, that the binding constant of 2-iodomelatonin is approximately three orders of magnitude smaller than that of melatonin, which makes it a very promising ligand for *in vivo* PET imaging. Similarly, the naphthalenic ligand S20755 has a binding constant which is 10^5 times better that of melatonin.

1.4. Strategies for the Synthesis of 2-Iodo-5-methoxytryptamine (22)

The data in Section 1.3. showed that 2-iodomelatonin (11) is the most successful ligand used for melatonin receptor investigations because of its high receptor affinity. Therefore, it was decided to investigate 2-iodomelatonin as a PET tracer in this thesis. In order to incorporate ^{11}C in the amide function of the compound, the free amine 2-iodo-5-methoxytryptamine (22) had to be synthesized in order to be used as the precursor in the ^{11}C acetylation reaction.

The following possibilities for the preparation of (22) were considered:

1. Deacetylation of 2-iodomelatonin

2. Iodination of 5-methoxytryptamine (7)

3. Total synthesis

They are summarized in Figure 13 and discussed in this section.

1.4.1. Deacetylation of 2-Iodomelatonin

The cleavage of an amide bond requires more rigorous conditions than those needed for ester hydrolysis (37). However, in the case of iodomelatonin strongly basic or acidic conditions are likely to liberate iodine or to destroy the indole moiety. For
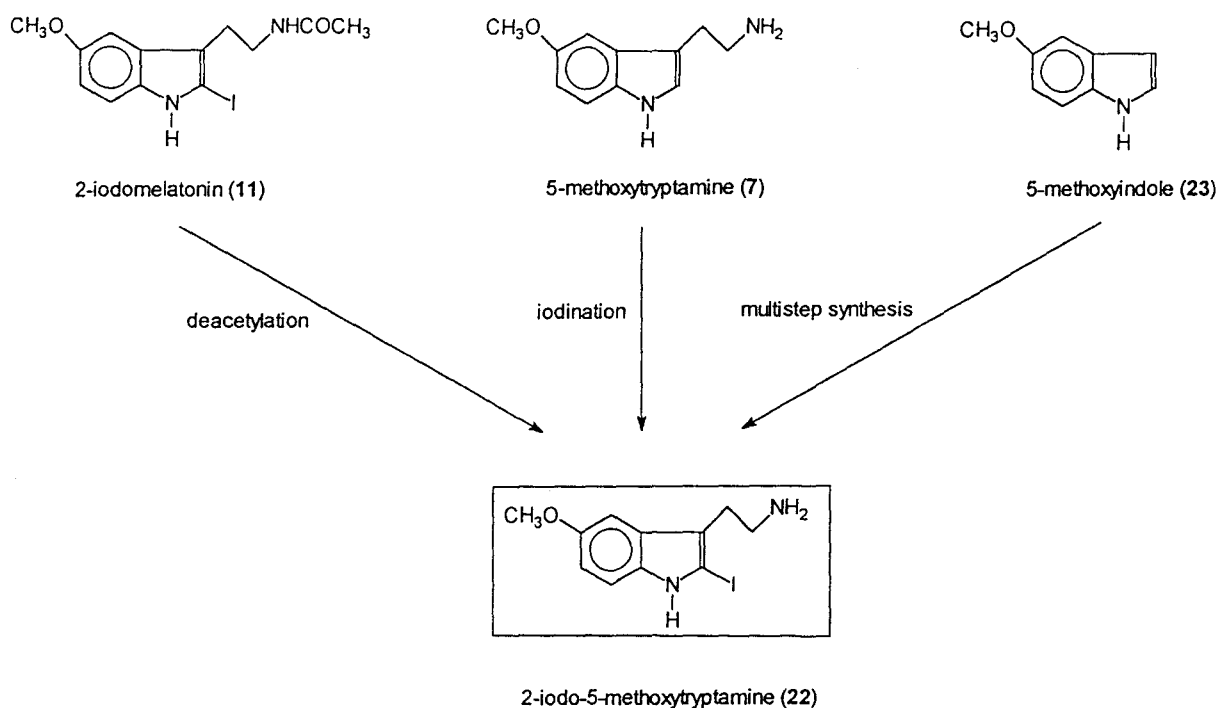
Figure 13: Approaches to the Synthesis of 2-Iodo-5-methoxytryptamine (**22**)

example, the instability of 2-haloindoles under acidic conditions has been used to prepare oxindoles (**38**). The authors report that 2-bromoskatole (**25**) was stable in strong base when ethanol was the solvent. Figure 14 illustrates the variety of solvent-dependent possible reactions of 2-haloindoles.

In another case (**39,40**) the alkaline stability of 2-haloindoles was investigated more thoroughly. The authors report that α-N-(trifluoroacetyl)-2-halo-L-tryptophan methyl ester (**29**) can not be hydrolysed in alkaline solution; after exposure to 1N NaOH solution TLC showed several ninhydrin positive products (Reaction 1 in Figure 15). The authors did not report a reaction time or a temperature. On the other hand, α-N-(trifluoroacetyl)-1-methyl-2-halo-L-tryptophan methyl ester (**30**) could be hydrolysed in aqueous methanolic solution with equimolar amounts of NaOH to (**31**) (again no specification of reaction time or temperature, but presumably they were similarly to
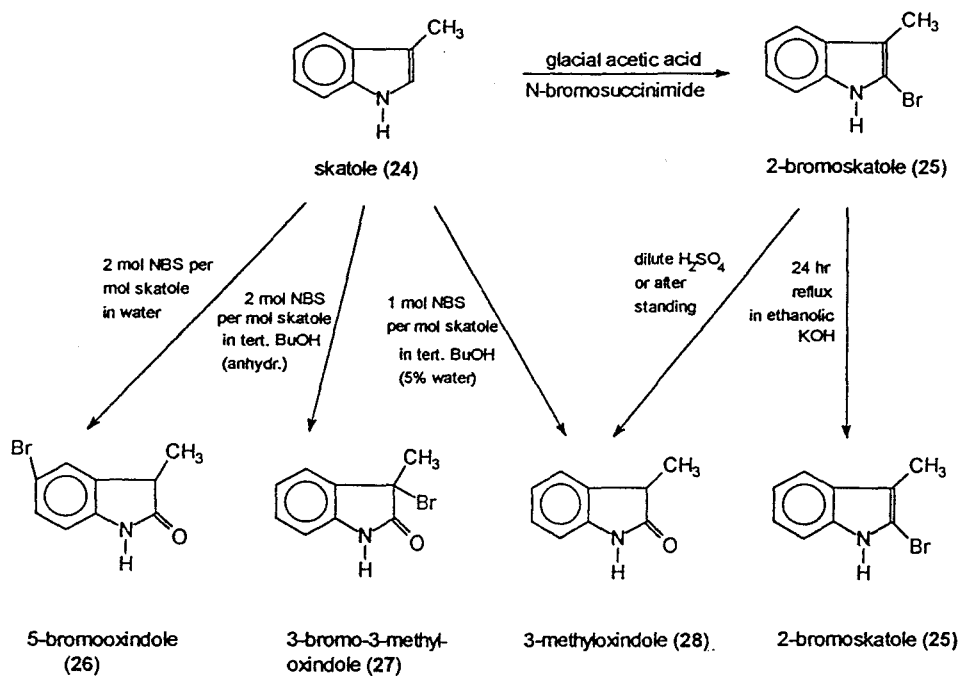
Figure 14: Syntheses of 2-Oxindoles from a Skatole or 2-Haloskatole
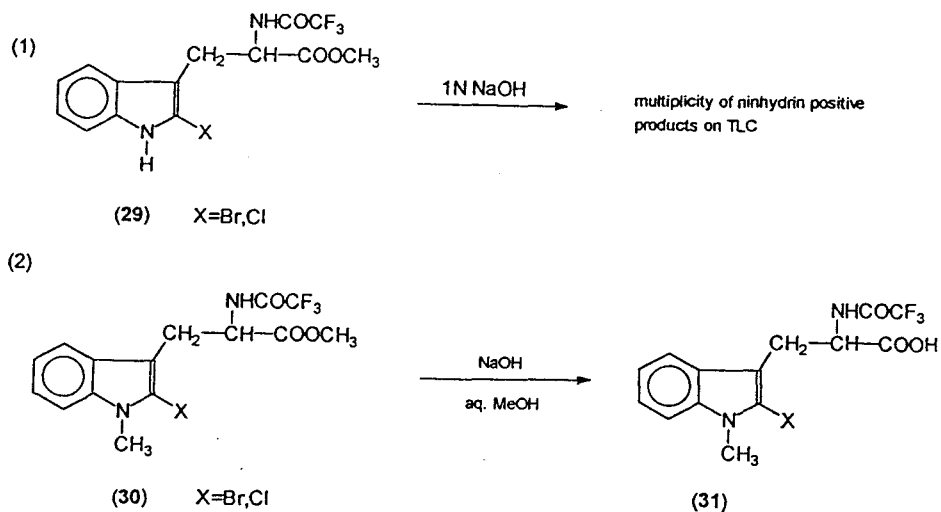
Figure 15: Stability of 2-Haloindoles in alkaline Media (40)

reaction 1 in Figure 15). These results indicate that

- in strong alkaline medium ionization of the indole nitrogen contributes to its decomposition

- the trifluoroacetyl group is less labile to alkaline hydrolysis conditions than the methyl ester group (see reaction 2 in Figure 15); relative to the trifluoroacetamide, an acetamide would require even more drastic conditions to affect hydrolysis.

These studies were done with bromine or chlorine in 2-position; therefore, care must be taken in inferring from the stability of those compounds, that a 2-iodinated indole derivative will be stable under the same conditions. On the other hand, under conditions where even a 2-chlorinated tryptophan derivative decomposes (e.g., reaction 1 in Figure 15), 2-iodinated melatonin will probably not be stable.

An alternative method for deacetylation uses specific enzymes which allow much milder reaction conditions. Phillips and coworkers (39) used carboxypeptidase A for cleavage of the N-acetyl bond and α-chymotrypsin for cleavage of the ester bond (Figure 16) of α-N-(trifluoroacetyl)-2-halo-L-tryptophan methyl ester (29). However, examples of the application of carboxypeptidase to cleave the N-acetyl bond in melatonin or 2-iodomelatonin have not been reported.

Cahill and coworkers (41) have found a melatonin deacetylating enzyme, which appears to be related to acetylcholinesterase (EC 3.1.1.7) and aryl-acylamide amidohydrolase (EC 3.5.1.13). The presence of this enzyme was shown in cultured eyecups of *Xenopus laevis* (41) and later in the eyecups of representatives from three other vertebrate classes, excluding mammals (42). Until now the enzyme has not been isolated or purified; further, it could not be localized to specific cell types in the retina (4).

Bertholet and Hirsbrunner (1985) described the successful deacetylation of melatonin under basic and aprotic conditions (Figure 17).
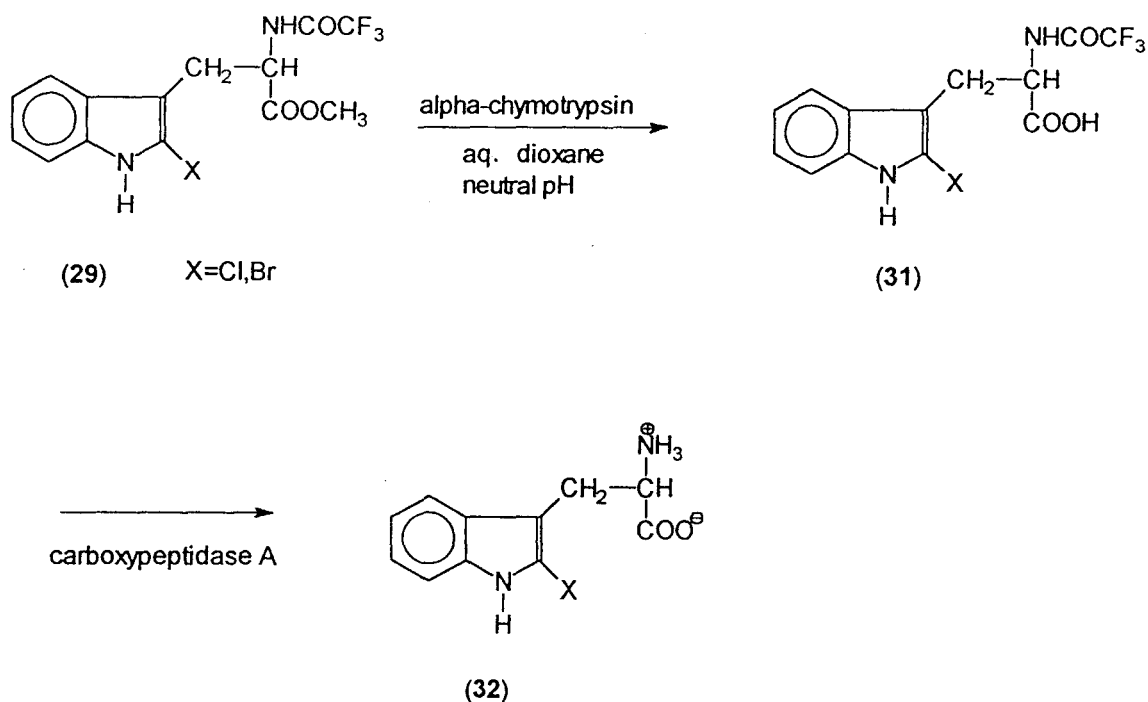
Figure 16: Synthesis of 2-Halotryptophans by Enzymatic Cleavage (39)
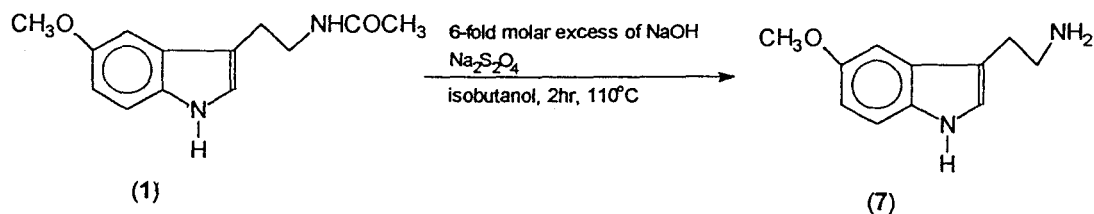
Figure 17: Deacetylation of Melatonin (43)

1.4.2. Iodination of a Suitable Precursor

Most reports describe halogenation of indoles under polar, electrophilic conditions. Because of the high electron density of the indole moiety, reactions are possible with weak electrophiles like alkyl halides. Electrophilic halogenations on indoles

have been reviewed by Remers (44) and by Sundberg (45).

In an unsubstituted indole the 3-position is preferably attacked under electrophilic conditions. If it is blocked, halogenation occurs at the 2-position. Electrophilic halogenations are complicated by the fact that indoles and their derivatives are unstable in acids (which are produced during the reaction). Therefore, an acid scavenger like pyridine is often added.

An electrophilic iodination in the 2-position of an indole has been reported (46), where the indole nitrogen was protected by a tert-butoxy-carbonyl group, which also served to direct iodine into the 2-position. The yield was 56% (Figure 18).
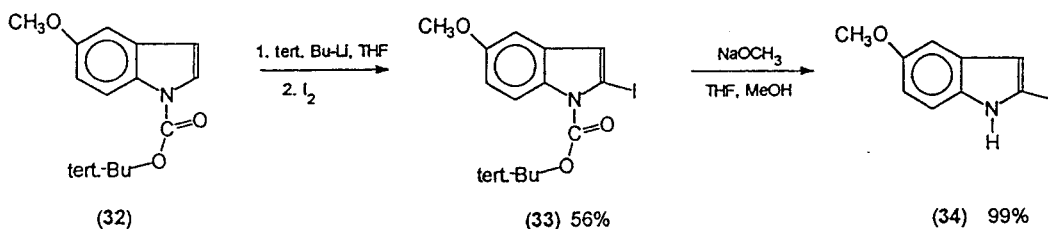
Figure 18: Electrophilic Iodination of an Indole (46)

Considering the polar and electron-rich character of the indole moiety, radical, homolytic substitutions do not proceed very well. Nevertheless, some recent reports favour 2-halogenation (X=Cl,Br) with radical mechanism over the electrophilic method (39,40,47). Because of the aprotic conditions the yields were higher than in the electrophilic reactions, since there occurred no product decomposition due to acid attack.

A radical chain mechanism for iodination is thermodynamically not favoured; the overall reaction is slightly endothermic and it has a large energy barrier for the H atom abstraction step (48). Nevertheless, the commercially available 2-iodomelatonin (Research Biochemicals Incorp.) has been prepared by a radical method using N-iodosuccinimide

in CHCl$_3$, although with low yield (Dr. Robert Milius, RBI, personal communication).
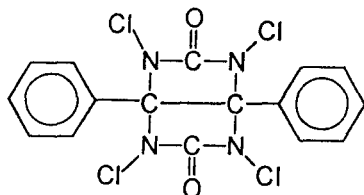
Recently, melatonin has been iodinated directly with NaI in the presence of an oxidizing iodination reagent, Iodo-gen (supplied by Pierce Co.)(26,27). Iodo-gen (1,3,4,6-tetrachloro-3α-6α-diphenyl-glycoluril, (35)) resembles a four-fold chloramine-T molecule (Figure 19) and is water insoluble.

Figure 19: Iodo-gen (35)

Glass walls can be coated with Iodo-gen and the iodination is then carried out in aqueous solution, minimizing contact of the oxidizing reagent with the reactant. The application is shown in Figure 20. With this method the authors prepared up to 6 mg of 2-iodomelatonin, labelled with ^{125}I per reaction vial with a yield of 20 to 30%.
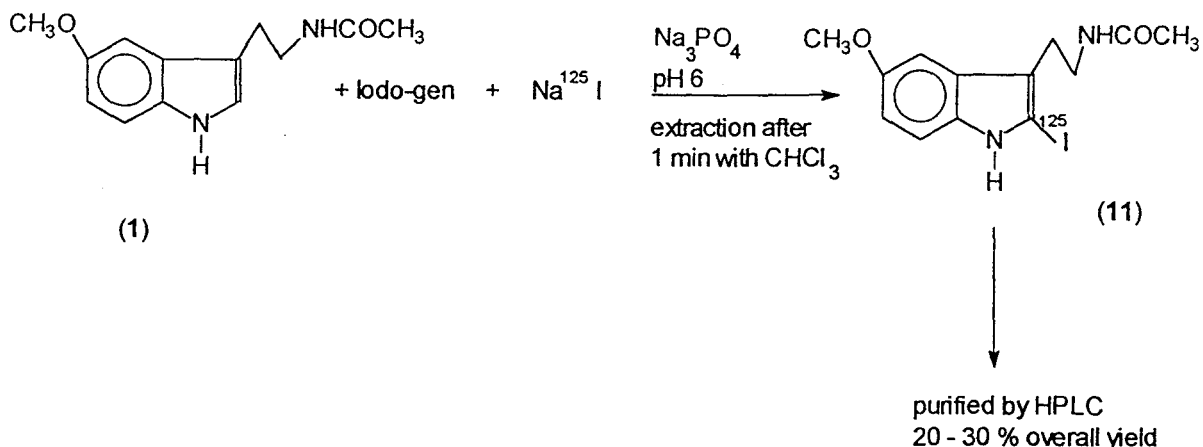
Figure 20: Radioiodination of Melatonin with Iodo-gen (27)

All these methods are not applicable to 5-methoxytryptamine because the free amino group would be oxidized. One conceivable solution would be the following sequence of steps (Figure 21):

(1) Protection of the amino group by an easily removable group, e.g., trifluoroacetylation according to Huang et al. (49)

(2) Iodination with the Iodo-gen method according to Vakkuri *et al.* (26,27)

(3) Hydrolysis of the trifluoro acetamide under mild basic conditions.

Considering the yield of each step, the overall yield of 2-iodinated 5-methoxytryptamine may be rather low.

1. Trifluoroacetylation
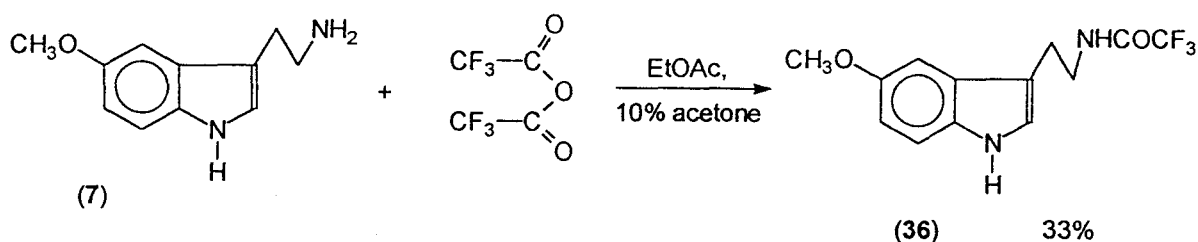
2. Iodination
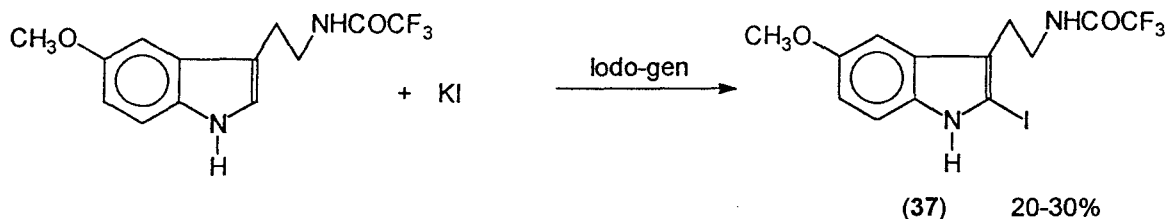
3. Hydrolysis
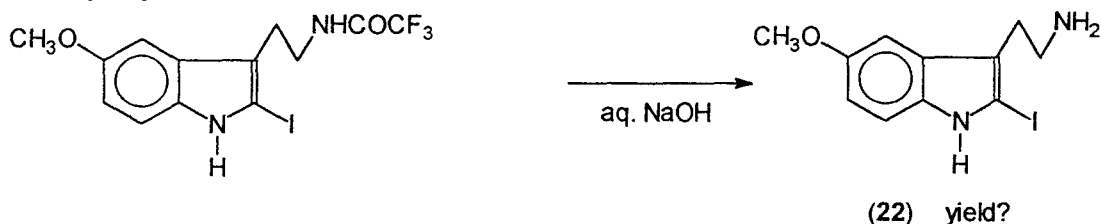
Figure 21: Sequence of Steps for Iodination of 5-Methoxytryptamine

1.4.3. Total Synthesis

The total synthesis of 2-iodo-5-methoxytryptamine (22) from smaller units seems to be the most laborious option. The steps in the procedure reported by Kline (46) are summarized in Figure 22.

The author gives several choices for protection of the N-function in the indole, of which the tert-butoxycarbonyl group gave the best results. This protecting group also

served to activate the 2-position for electrophilic substitution. Because of the sensitivity of the iodine in the 2-position towards acids and nucleophiles, the side chain was synthesized via a Mannich reaction, followed by reduction of the intermediate nitrile. The yields for each step were relatively high, making this procedure a practical alternative.
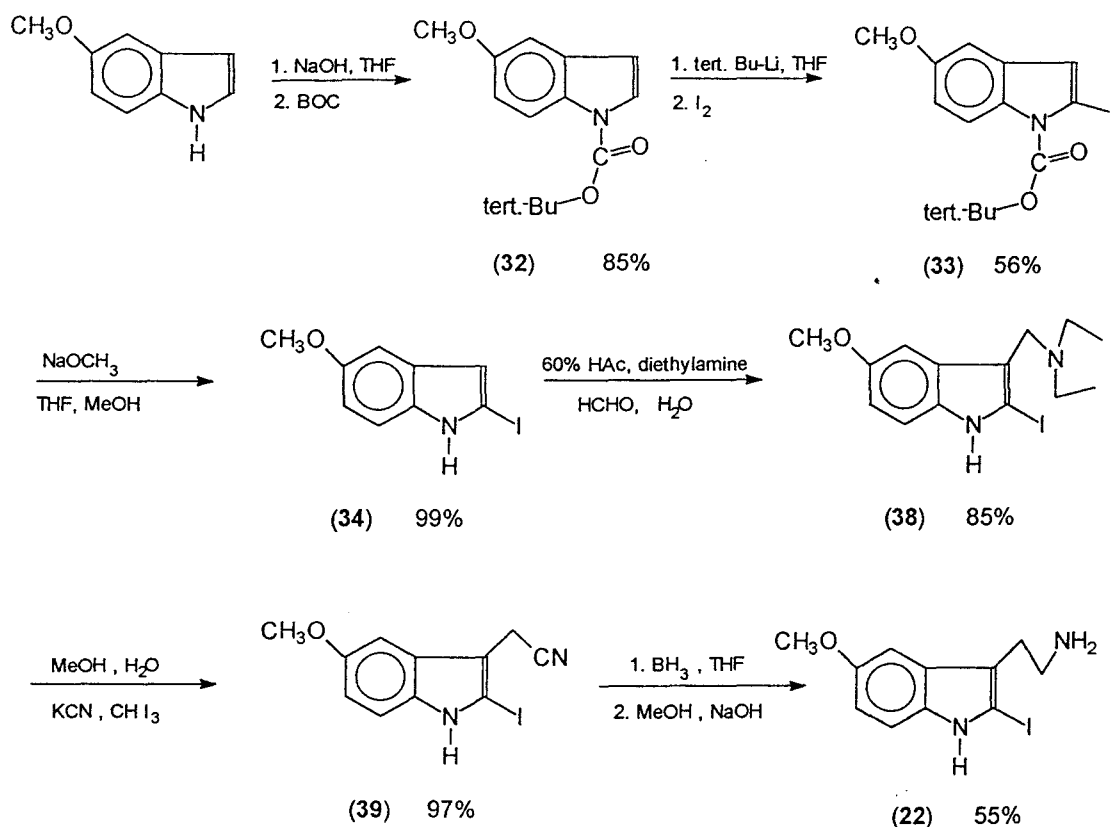
Figure 22: Synthesis of 2-Iodo-5-methoxytryptamine from 5-Methoxyindole (46)

1.4.4. Conclusions

The preparation of the iodotryptamine (22) by the hydrolysis of 2-iodomelatonin (11) under acid conditions must be excluded because the 2-iodomelatonin would be converted into 2-oxindole (38). The stability of 2-halogenated indoles under aqueous basic conditions depends on substituents and is difficult to predict (39,40).

A specific deacetylating enzyme for melatonin has been found, but has not yet

been isolated (4,41).

Direct iodination of an indole precursor would be possible by an electrophilic or radical mechanism after protecting the N-functions in the precursor. These approaches involve several steps and would probably result in a low yield.

The N-acetyl group of melatonin can be cleaved under basic aprotic conditions (43). It has also been shown that a halogen in 2-position is stable in basic aprotic medium (38). Therefore, hydrolysis of 2-iodomelatonin under basic aprotic conditions has been chosen as the best way to prepare 2-iodo-5-methoxytryptamine.

1.5. Thesis Objectives

The overall objectives of this thesis are:

(1) to develop and to test a generic radiochemical acylation procedure that uses ^{11}C-acyl chlorides prepared from $[^{11}C]CO_2$, based on a synthesis principle described by LeBars *et al.* (32). It is proposed to construct an apparatus that will allow these acetylation reactions to be carried out remotely.

(2) to develop a radioacetylation method for the acetylation of amines and to apply this method to the synthesis of the ^{11}C-labelled melatonin receptor ligands, 2-iodomelatonin (11) and S20098 (15).

(3) to optimize each step of the radiosynthesis in order to obtain compounds with high specific activities.

(4) to produce the above ^{11}C-labelled melatonin analogues as radiopharmaceuticals and to start *in vivo* imaging using PET. For PET studies ligands need to be synthesized and purified in a reproducible and reliable manner with a high radiochemical yield and must be provided as sterile, apyrogenic, isotonic solutions. Pilot studies are necessary with the two melatonin analogues to assess their ability to visualize melatonin receptors in the living human brain.

CHAPTER 2

EXPERIMENTAL

2.1. Instrumentation

2.1.1. Cyclotron

A Siemens CTI cyclotron (Radioisotope Delivery System, model 112/00) was used for production of ^{11}C. It produces protons with an energy of 11 MeV at a maximum intensity of 50 μA. The cyclotron can produce up to 1500 mCi of ^{11}C.

2.1.2. Mass Spectrometry

Low resolution mass spectra (MS) were obtained on a VG ZAB-E mass spectrometer with samples being introduced through a direct inlet system. Ions were created using electron impact (EI) or through chemical ionization (CI) with NH_3 as the reactant gas.

2.1.3. Nuclear Magnetic Resonance Spectroscopy

Proton magnetic resonance (^{1}H-NMR) spectra were recorded on a Bruker AM-500 spectrometer at 500.13 MHz. The spectra were accumulated in 16 to 120 scans in 16 K data points. A spectral width of 5000 Hz and a pulse width of 5 μs was used.

2.1.4. High Performance Liquid Chromatography

The HPLC system consisted of a Waters pump model M6000 and a UV detector (model 440, Waters) with a wavelength filter at 280 nm. Two different columns were

used:

(1) Waters Radial Compression Cartridge RP C18-PrepNovaPak, length: 11cm, diameter: 2.5 cm, particle size: 6 µm, pore size: 60 Å, flow: 6 mL/min

(2) C18 µ-Bondapak, length: 30 cm, diameter: 0.39 cm, particle size: 10 µm, flow: 1 mL/min.

2.1.5. Thin Layer Chromatography and Autoradiography

Silica Gel plates were used with fluorescence indicator (254 nm) for analytical and preparative TLC (Merck).

The compounds were visualized under short wave UV light, where they showed a dark, UV-absorbing spot on the fluorescing plate. When the sample contained radioactivity, the spots were visualized by autoradiography, that is, exposing a film (DuPont, Cronex video imaging film) for several minutes to the TLC plate. After development (Film Processor Kodak Model M7B) the film showed dark spots corresponding to radioactivity on the plate.

The following solvent systems were used:

Solvent A: 87% isopropanol, 9% water, 4% ammonia (25%)

Solvent B: 95% ethyl acetate, 5% triethylamine

2.1.6. Radioactivity Measurements

The radioactivity was measured using a radioisotope calibrator (Capintec CRC-12) manufactured by Capintec Inc., which consists of a measuring well (6 cm i.d. by 25 cm deep), surrounded by an ionization chamber filled with argon gas. In addition, a Geiger Müller tube was calibrated in parallel measurements with the Capintec and it was used to measure the activity of $^{11}CO_2$ when collected in the cold trap of the acetylation apparatus.

2.2. Materials, Precursors and Solvents

The following reagents were purchased from Aldrich and used without further purification: 2,6-di-t-butylpyridine, phthaloyl dichloride, anhydrous diethyl ether and dibutyl ether, 3M methylmagnesium bromide in diethyl ether, isobutanol and sodium dithionite ($Na_2S_2O_4$). For the acetylation apparatus helium gas (research grade, >99.999%) was used (Liquid Air). Melatonin and 5-methoxytryptamine (free base) were purchased from Sigma; 2-iodomelatonin was obtained from Research Biochemicals (RBI). 7-Methoxynaphthylenyl-1-ethyl-N-acetamide (S20098) and 7-methoxynaphthylenyl-1-ethylamine hydrochloride were donated to us by Servier Co., France. All other reagents and solvents were obtained from BDH and were of analytical or HPLC grade.

7-Methoxy-naphthylenyl-1-ethylamine hydrochloride (100mg, 0.5 mmol) was converted to the free amine by dissolving it in 100 mL water. In a separatory funnel the solution was made alkaline with an aqueous solution of K_2CO_3 and the resulting mixture was extracted with 100 mL CH_2Cl_2. The dichloromethane was then washed with water (30 mL), dried over Na_2SO_4 and evaporated under vacuum to afford the residue.

2.3. Synthesis of 2-Iodo-5-Methoxytryptamine (22)

The 2-iodo-5-methoxytryptamine (22) was obtained by deacetylation of the corresponding acetamide, 2-iodomelatonin (11). The procedure used has been described by Bertholet and Hirsbrunner (43) to deacetylate melatonin.

2-Iodomelatonin (11) (10 mg, 0.028 mmol), NaOH (6.6 mg, 0.165 mmol) and $Na_2S_2O_4$ (0.6 mg, 3.6 μmol) were dissolved in 80 μl isobutanol in a Reacti-Vial (Pierce Co.) under nitrogen in a glove bag and then heated at 110°C for 4 hours. The reaction mixture was cooled to room temperature and extracted with 100 μl water. The isobutanol layer was examined by TLC using solvents (A) and (B). TLC analysis showed the product with an R_f=0.72 (precursor, R_f=0.85) in solvent (A) and with an R_f=0.76 (precursor,

R$_f$=0.81) in solvent (B).

The product was isolated by HPLC using a Waters Radial Compression Cartridge C18-PrepNovaPak with a mobile phase consisting of 40% methanol, 60% water and 0.1% trifluoroacetic acid. Aliquots of the isobutanol phase were injected onto the column and the peak eluting at 15 to 16 minutes was collected and the solvent evaporated under vacuum to a volume of 30 mL. The aqueous solution was made alkaline with aqueous K$_2$CO$_3$ solution and the product extracted with 30 mL CH$_2$Cl$_2$. The dichloromethane phase was dried over Na$_2$SO$_4$ and evaporated to dryness. The product was redissolved in methanol for mass spectral analysis and in CD$_2$Cl$_2$ for NMR analysis. The yield was 15% (0.8 mg, 4.2 µmol).

The analysis of the compound showed:

^{1}H NMR: <u>σ (ppm) (splitting pattern, integral, coupling constant (Hz), assigned proton[A])</u>: 8.26 ppm (br, 1H, H1); 7.21 ppm (d, 1H, 8.81 Hz, H7); 6.99 ppm (d, 1H, 2.37 Hz, H4); 6.76 ppm (dd, 1H, 8.78 Hz and 2.42 Hz, H6); 3.82 ppm (s, 3H, H$_e$); 2.91 ppm (t, 2H, 6.4 Hz, H$_b$); 2.80 ppm (t, 2H, 6.7 Hz, H$_a$); spectra recorded at room temperature in CD$_2$Cl$_2$; in a subsequent experiment one drop of D$_2$O was added.

[A] refer to Figure 23 for proton assignment
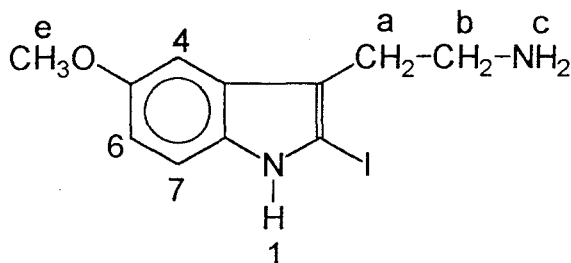
(22) 2-Iodo-5-methoxy-tryptamine

Figure 23: Proton Assignment for 2-Iodo-5-methoxytryptamine (22)

MS (EI):   **m/z (RI%)**; 316 [M$^+$] (2), 299 (6), 287 (54), 286 (98), 271 (16), 243 (12), 190 (15), 189 (100), 160 (24), 30 (24)

MS (CI):   317 (100), 300 (10), 261 (10), 191 (25), 162 (50), 160 (68)

UV: **λ_{max} (methanol)**; 283 nm, 220 nm; ϵ_{max}(283 nm) = 11,000 L mol^{-1} cm^{-1}

2.4. Acetylation of 2-Iodo-5-Methoxytryptamine (22)

To 2-iodo-5-methoxytryptamine (**22**), the product obtained from the hydrolysis of 2-iodomelatonin (**11**), (10 mg, 0.028 mmol) was added acetic anhydride (1.7 mg, 0.016 mmol). After 10 minutes (room temp.) an aliquot was removed and subjected to TLC analysis in solvent systems (A) and (B). The spot corresponding to the amine was no longer visible and a new spot (R$_f$=0.85 in (A) and R$_f$=0.81 in (B)) was observed. The new spot in both solvents had chromatographic properties identical to those of authentic 2-iodomelatonin (**11**).

2.5. Optimization of the Hydrolysis of 2-Iodomelatonin (11)

The influence of hydrolysis reaction time on the yield was investigated in the following experiment. 2-Iodomelatonin (**11**) (10 mg, 0.028 mmol), NaOH (6.6 mg, 0.165 mmol) and Na$_2$S$_2$O$_4$ (0.6 mg, 3.6 μmol) were dissolved in 80 μl isobutanol in a Reacti-Vial (Pierce Co.) under nitrogen in a glove bag and then heated at 110°C. The reaction was interrupted at specific times, the reaction mixture was cooled to room temperature and aliquots of 1 to 2 μl were removed in a nitrogen atmosphere (glove bag). The aliquots were analyzed by HPLC (C18 μ-Bondapak column) with a mobile phase consisting of 60% water (pH 3.8 with acetic acid) and 40 % methanol.

Next, several hydrolysis reactions of 2-iodomelatonin (**11**) (20 mg, 0.056 μmol) were carried out, each with NaOH (13.2 mg, 0.13 mmol) and Na$_2$S$_2$O$_4$ (1.2 mg, 7.2

μmol) in 160 μl isobutanol. After either 2 or 4 hours reaction time the crude hydrolysis product was cooled to room temperature and extracted with 200 μl water. The isobutanol phase was then purified by either preparative HPLC (as described in Section 2.3.) or by preparative TLC. When TLC was used, the product was spotted onto a plate for preparative TLC and developed in solvent (A). The area on the plate corresponding to the product was identified under UV light and scraped off. The product was eluted from the silica gel by washing it with 30 mL ethanol.

Yields were determined by analytical HPLC (C18 μ-Bondapak), calibrated with standard solutions of 2-iodomelatonin.

2.6. ^{1}H NMR and MS Spectra of Melatonin (1), 5-Methoxytryptamine (7), 2-Iodomelatonin (11) and 7-Methoxynaphthyl-1-ethyl-N-acetamide (15)

Authentic samples of melatonin, 5-methoxytryptamine, 7-methoxynaphtyl-1-ethyl-N-acetamide and 2-iodomelatonin were dissolved in methanol for mass spectral analysis and in CD_2Cl_2 for proton NMR spectroscopy, respectively (the naphthyl derivative (15) was only analyzed by mass spectrometry).

Melatonin (1) showed:

^{1}H NMR: σ (splitting pattern, integral, coupling constant, assigned proton): 8.14 ppm (br, 1H, H1); 7.27 ppm (d, 1H, 8.9 Hz, H7); 7.04 ppm (d, 2H, 2.1 Hz, H2 and H4); 6.83 ppm (dd, 1H, 8.8 and 2.4 Hz, H6); 5.61 ppm (br, 1H, H_c); 3.83 ppm (s, 3H, H_e); 3.53 ppm (dd, 2H, 6.8 Hz, H_b); 2.91 ppm (m, 2H, 6.8 and 0.5 Hz, H_a), 1.89 ppm (s, 3H, H_d)
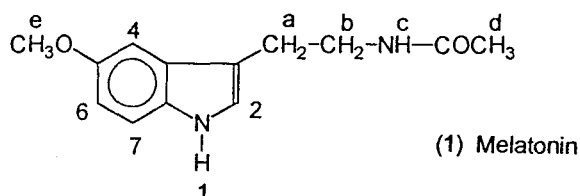
Figure 24: Proton Assignment for Melatonin (1)

MS (EI): **m/z (RI%):** 232 [M]⁺ (18), 173 (88), 160 (100), 145 (20), 117 (20)

MS (CI): 250 (35), 233 (100), 173 (8), 160 (10)

The following data were obtained with 5-methoxytryptamine (7):

MS (EI): 190 [M]⁺ (32), 161 (73), 160 (100), 145 (20), 117 (24)

MS (CI): 191 (100), 174 (9), 160 (8)

¹H NMR: 8.10 ppm (br, 1H, H1); 7.25 ppm (d, 1H, 8.9 Hz, H7); 7.03 ppm (d, 2H, 2.2 Hz, H2 and H4); 6.81 ppm (dd, 1H, 8.8 and 2.4 Hz, H6); 3.83 ppm (s, 3H, H_e); 2.97 ppm (t, 2H, 6.8 Hz, H_b); 2.83 ppm (t, 2H, 6.8 Hz, H_a), 1.12 ppm (br, 2H, H_c)
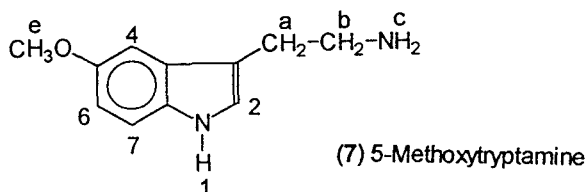
Figure 25: Proton Assignment for 5-Methoxytryptamine (7)

The following data were obtained with 2-iodomelatonin (11):

¹H NMR: 8.13 ppm (br, 1H, H1); 7.23 ppm (d, 1H, 8.9 Hz, H7); 7.00 ppm (d, 1H, 2.4 Hz, H4); 6.78 ppm (dd, 1H, 8.8 and 2.4 Hz, H6); 5.52 ppm (br, 1H, H_c); 3.83 ppm (s, 3H, H_e); 3.47 ppm (dd, 2H, 6.6 Hz, H_b); 2.87 ppm (t, 2H, 6.6 Hz, H_a); 1.88 ppm (s, 3H, H_d)
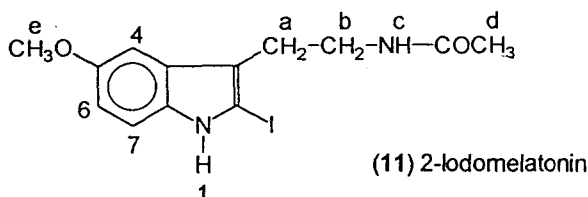
Figure 26: Proton Assignment for 2-Iodomelatonin (11)

MS (EI):   358 [M]$^+$ (20), 300 (15), 299 (100), 286 (82), 231 (63), 145 (20), 117 (20)

MS (CI):   376 (5), 359 (80), 299 (16), 286 (17), 232 (100), 178 (58), 160 (52)

The mass spectrometric analysis of 7-methoxynaphthyl-1-ethyl-N-acetamide (15) showed the following peaks:

MS (EI):   243 [M]$^+$ (25), 184 (100), 171 (71), 153 (20), 128 (27)

MS (CI):   261 (60), 244 (100)
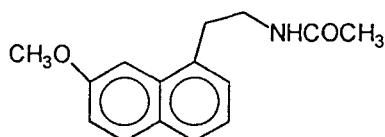
(15) 7-Methoxynaphthyl-1-ethyl-N-acetamide

Figure 27: Structure of (15)

2.7. Production of [^{11}C]CO$_2$

2.7.1. Procedure

The following procedure is written with reference to the computer-controlled target loading, irradiation and unloading procedures; the detail in this section is intended for researchers who will use the system in the future. Figure 28 shows a schematic of valves and tubings for loading and unloading the ^{11}C target, which is also used for the production of ^{15}O.

In the target support area, the hand-operated selector valve is switched to connect the ^{14}N$_2$ gas to the target. The hand valve before valve r90 must be opened. In the gas processing unit (GPU) the ^{15}O product line after flow regulator SAD5 is connected to the stainless steel line #3, which leads to the apparatus in the hot cell. From the maintenance system of the computer valve r83 is opened (command "on r83"). The C-11-Acetylation

program on the Macintosh Powerbook is started and valve #1 switched to target. For irradiation the following commands are given on the computer main terminal:

"Produce labelled product"

"Target zone #3"

"[O15]oxygen" (this command must be given to activate the ^{15}O target, which is used for production of ^{11}C)

The desired beam current and irradiation time are entered in the respective dialogue boxes. Irradiation is started by highlighting the last line and pressing "enter". At the end of bombardment (EOB) the product is automatically unloaded and the main menu on the computer screen can be accessed by pressing "enter".

A printout of the computer programs for loading and unloading is attached in the Appendix.

2.7.2. Flushing of the Target

After use of the target for production of ^{15}O-labelled compounds the target contains still some $^{15}N_2$, which is used for the production of ^{15}O. If the target were irradiated for production of ^{11}C, this $^{15}N_2$ gas would yield ^{15}O, which has shown to increase the amount of side products in a ^{11}C-acetylation reaction. Therefore the target must be flushed with $^{14}N_2$ as follows: all tubings were connected as outlined in Section 2.7.1.. On the second computer terminal ("Kimtron") the maintenance system was entered and the directory was changed by typing "cd /prod". After returning to the main menu, the submenu "Execute user command" was selected and there the target loading program "O15LOAD210" was executed. After completion, the target was unloaded with the user command file "O15BOLUS".
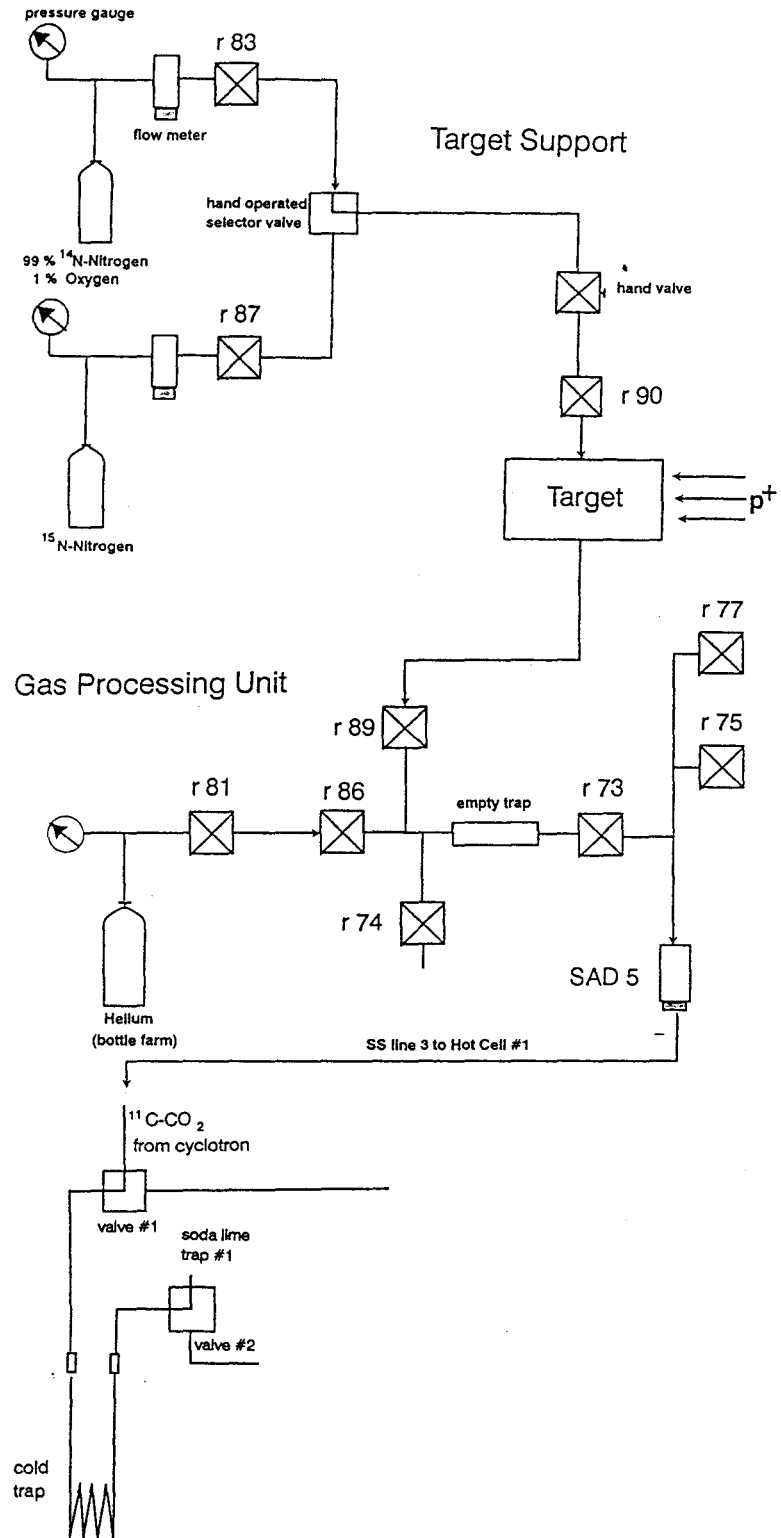
Figure 28: Schematic of Tubings, Valves and Target for [^{11}C]CO$_2$ Production

2.7.3. Optimization of the Target Unloading Procedure

The following processes to transfer the $[^{11}C]CO_2$ from the target to the apparatus (target unloading) were tested (changes are underlined):

a) - cycle valve r89[A) 0.2 s, 7.5 s for 180 seconds

(valve r89 is opened for 0.2 s, closed for 7.5 s),

then cycle r89, 0.5 s, 5.5 s for 10 s,

then open r89 for 10 s,

then open r81 and r86 for 60 s (allows to sweep line with helium)

b) - cycle r89 **0.1 s, 4 s** for 180 s, then cycle r89 0.5 s, 5.5 s for 10 s,

then open r 89 for 10 s, then open r81 and r86 for 60 s

c) cycle r89 0.1 s, 4 s for 180 s, then cycle r89 0.5 s, 5.5 s for 10 s,

then open r89 for 10 s,**no helium sweep**

d) cycle r89 0.1 s, 4 s for 180 s, then cycle r89 0.5 s, 5.5 s for 10 s,

then open r89 for 10 s, then open r 81 and **cycle r86 0.4 s, 4 s** for 60 s.

[A) refer to Figure 28

2.7.4. Saturation Yield and Saturation Activity

The saturation yield Y_S and saturation activity A_S were determined in the following way: one irradiation with a beam current of 10 μA was carried out for 4 minutes while a second irradiation with a beam current of 20 μA was carried out for 15 minutes. The radioactivity produced in each experiment was measured both in the cold trap and in the soda lime trap #1 of the apparatus (refer to Figure 29); the values were decay corrected to EOB and summed.

2.8. Apparatus for the Synthesis of ^{11}C-Labelled Amides

2.8.1. Description

The apparatus for remote-controlled synthesis of ^{11}C-labelled amides consists of two panels, designed and built by G. Firnau and B. Schulze. They are mounted in a hot cell, shown in the photograph in Figure 29 and schematically depicted in Figure 30.

Swagelok fittings (Teflon or stainless steel) have been used for all connections. From the target to reaction Vessel 1 the tubing is made of 1/16'' stainless steel. Vessels 1 and 2 are connected by 1/8'' Teflon tubing to facilitate better transfer during the distillation. For all other lines 1/16'' Teflon tubing was used. The cold trap ("loop") is made of stainless steel tubing, 12 cm long, 1/16'' in 10 turns. The electrically operated 2- and 3-way valves were obtained from Furon (Anaheim, Ca., USA), Delta Fluorocarbon Valves (Anaheim, Ca., USA) and from Skinner (Mississauga, Ont., Canada).

The signal for switching the valves and heaters is given by a Macintosh Powerbook, programmed in Hypercard by K. Chin. On the computer screen a schematic of the apparatus is displayed. Valves and the heaters are activated by clicking on the appropriate symbol.

A motorized moving jack (Swiss Boy, Grauer, Switzerland) is beneath panel one, operated from outside the hot cell. On its top is mounted a sheet of plexiglass (47 x 15 cm), on which can be placed two Dewar flasks for loop and Vessel 2 and the oil bath for Vessel 1. The plexiglass is large enough so that the heating and cooling devices can be moved from outside the hot cell with stick manipulators.

Gases and liquids are transferred between the reaction vessels by applying pressure with a helium gas stream.

With a calibrated Geiger-Müller detector (Vakutec, Dresden) the ^{11}C in the cold trap is measured, and a heat sensor measures the temperature of the oil bath. Both values are displayed on the computer screen.

Figure 29: Apparatus for ^{11}C-Acylation Reactions

Figure 30: Schematic of the Apparatus for ^{11}C Acylation Reactions

50
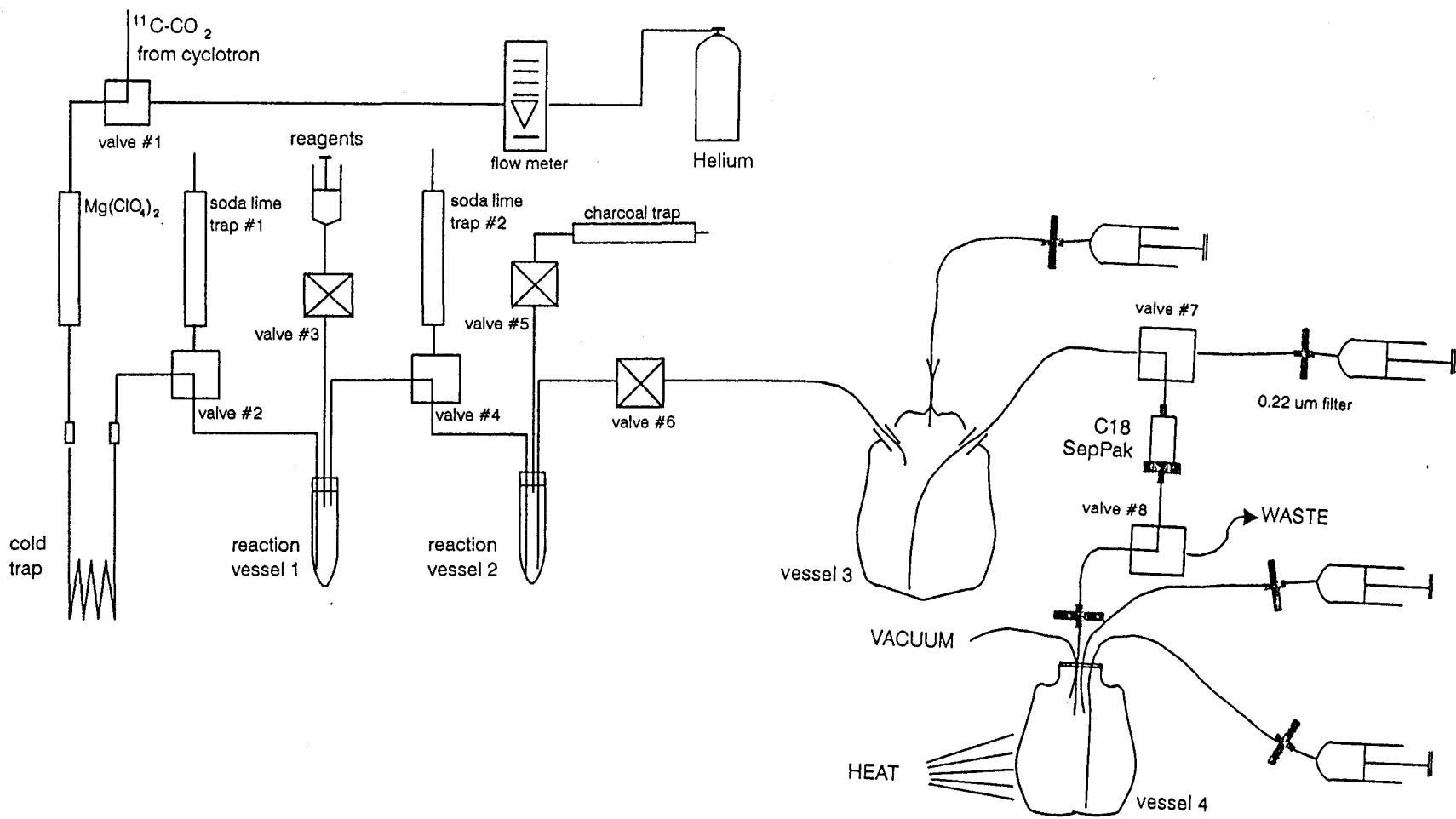
2.8.2. Selection of a Cold Trap for $^{11}CO_2$

Three different loops, all with a wall thickness of 0.7 mm, were tested for their

[^{11}C]CO_2 trapping efficiency:

(1) stainless steel tubing, 1/8'' o.d., 1.82 mm i.d., 5 turns with diameter of 4 cm,

cooled length of 120 cm $^{A)}$

(2) copper tubing, 1/8'' o.d., 1.82 mm i.d., 5 turns with diameter of 4 cm,

cooled   length of 60 cm

(3) stainless steel tubing, 1/16'' o.d., 0.26 mm i.d., 10 turns with diameter of 4

cm,   cooled length of 60 cm.

$^{A)}$ The cooled length indicates the length of tubing that was immersed in liquid nitrogen.

In subsequent experiments the loops were connected and the target was irradiated

for 4 minutes with 10 μA. The radioactivity was measured in the loop and in the soda

lime trap #1.

2.8.3. Maintenance

All three Teflon tubes leading into Vessel 1 were rinsed and dried after every

production run to eliminate any precipitate. The traps ($Mg(ClO_4)_2$ and $CaCO_3$) were

replenished after approximately 40 runs. With the same frequency, valves #2, 3, 4 and

5 were taken apart and the yellow and red precipitate removed. Reaction Vessels 1 and

2 were cleaned and oven dried after every reaction.

2.9. Syntheses of ^{11}C-Labelled Amides

2.9.1. Procedure

The synthesis was carried out remotely, using the apparatus described in Section

2.8. and Figures 29 and 30.

The irradiated target gas, containing [^{11}C]CO_2 (50 to 430 mCi, 5.5 to 50 pmol)

and $^{14}N_2$ was unloaded from the target of the cyclotron and released into the stainless steel loop, cooled in liquid nitrogen. When all the target gas had passed though the loop, $[^{11}C]CO_2$ was transferred into Vessel 1 containing methylmagnesium bromide (0.3M) in dibutyl ether (1mL). This was done by removing the Dewar flask with liquid nitrogen from the loop and warming up the loop with a hot air blower. During this transfer a gentle helium gas stream (5 mL/min) was passed though the loop. After 2 minutes the carbonation reaction was quenched by adding phthaloyl dichloride (100 μl, 0.7 mmol) and 2,6-di-t-dibutylpyridine (100 μl, 0.42 mmol) via a 1/16'' teflon tube. Any residual reagent in the teflon line was rinsed into Vessel 1 with 100 μl of diethyl ether. Vessel 1 was heated in an oil bath at 125°C. After 30 seconds Vessels 1 and 2 were connected and the gas stream was increased to 15 mL/min. Carbon-11 labelled acetyl chloride distilled into vessel 2, which contained the precursor amine (1.5 mg, 4.7 to 7.9μmol) in acetonitrile at -25°C. A cooling mixture of methanol and liquid nitrogen was prepared in a Dewar flask and adjusted to the appropriate temperature before the start of the reaction. Depending on the experiment, the amine was either 5-methoxytryptamine (7), 2-iodo-5-methoxytryptamine (22) or 7-methoxynaphthyl-1-ethylamine (43). After 6 to 7 minutes the distillation was stopped and the contents of Vessel 2 were transferred to Vessel 3 by a strong helium stream. Water (pH 2.9 with HCl) was added and the solution passed through a C18 solid phase extraction cartridge (SepPak, Waters). The SepPak column was washed (see Table 6 for the volumes and nature of the wash solvent), followed by an air flush. Valve #8 was then switched and the product eluted from the SepPak with 2 mL of 95% ethanol.

For HPLC and TLC analyses aliquots of the ethanolic eluate were used. For mass spectrometric analyses, the eluate was left for a few hours to allow decay of the isotope, then the ethanol was evaporated and the residue redissolved in methanol.

For studies in rats the ethanol was evaporated under reduced pressure and the

residue redissolved in saline (154 mM NaCl) with 1% TWEEN 80 (poly-oxyethylene sorbitol monooleate). The volume of the final solution was 0.5 mL per rat.

For use in a PET study, the tubing, the SepPak column and Vessel 3 in panel 2 were rinsed with sterile water prior to the synthesis. Reagent solutions were added through a sterile 0.22 μm filter. The ethanol eluate was collected in a sterile multidose vial and the solvent evaporated by heating the vial with a hot air blower and applying vacuum through a 16 gauge needle. After 5 minutes the dry residue was dissolved in saline solution with 0.5% TWEEN 80 (7 mL). The solution was withdrawn through a 0.22 μm filter into a sterile, lead-shielded syringe.

The synthesis time was 30 to 35 minutes.

Table 6: Conditions for Purification of ^{11}C-labelled Melatonin (**1**), 2-Iodomelatonin (**11**) and S20098 (**15**)

	[^{11}C]Melatonin (**1**)	[^{11}C]2-Iodo-melatonin (**11**)	[^{11}C]S20098 (**15**)
Amine Precursor	5-Methoxy-tryptamine (**7**)	2-Iodo-5-methoxy-tryptamine (**22**)	7-Methoxy-naphthyl-1-ethyl-amine (**43**)
Volume for Dilution with Water (pH 2.9) in Vessel 3	30 mL	13 mL	8.5 mL
Volume and Composition of H_2O (pH 2.9) / MeOH Mixture	0 mL	20 mL, 15% methanol	30 mL, 20 % methanol

2.9.2. Product Identification and Analysis

After each radiosynthesis as described in Section 2.9.1., aliquots of the ethanolic SepPak eluate were analyzed by TLC (autoradiography) and HPLC to determine the radiochemical purity and the amount of unlabelled material. For this purpose calibration curves with the respective authentic amide had to be established. In several runs for each compound, the whole ethanol eluate was evaporated to dryness and the residue redissolved in methanol for mass spectral analysis.

Table 7: HPLC, TLC and MS of Products

	$[^{11}C]$Melatonin (1)	$[^{11}C]$2-Iodo-melatonin (11)	$[^{11}C]$S20098 (15)
Mobile Phase for HPLC (C18 μ-Bondapak column)	25% Methanol, 75% Water, 0.02% TFA	40% Methanol, 60% Water, 0.02% TFA	50% Methanol, 50% Water, 0.02% TFA
HPLC; k' value[A]	3.1	5.0	4.2
TLC; R_f value in solvent (A)	0.82 (melatonin) 0.37 (precursor)	0.87 (2-iodo-mel.) 0.66 (precursor)	0.85 (S20098) 0.52 (precursor)
TLC; R_f value in solvent (B)	0.22 (melatonin) 0.05 (precursor)	0.41 (2-iodo-mel.) 0.09 (precursor)	0.4 (S20098) 0.06 (precursor)
EI MS; m/z (RI%)[B]	232 [M$^+$] (18), 173 (100), 160 (98), 141 (25), 115 (32), 77 (65)	358 [M$^+$] (20), 300 (8), 299 (100), 286 (92), 257 (33), 231 (36)	243 [M$^+$] (9), 184 (55), 171 (33), 149 (33), 129 (22), 69 (100)
CI MS; m/z (RI%)[B]	250 (20), 233 (100), 173 (8), 160 (10)	359 (54), 299 (14), 286 (17), 233 (65), 232 (95), 231 (62), 160 (82)	261 (30), 244 (100)

[A] k' value of precursor amine is in each case between 0 and 0.5
[B] The HPLC fraction pertaining to the peak with the respective k' value was collected, the solvent evaporated under reduced pressure and the residue redissolved in methanol.

The operating conditions for HPLC analysis and the signals pertaining to the respective products in HPLC, TLC and MS are summarized in Table 7.

The radiochemical yield of a typical synthesis of a ^{11}C-labelled amide (1, 11 or 15) was found to be 15 to 20%. The quantities of amide ranged from 6 to 20 μg (16 to 86 nmol) per production run.

In initial runs for each product, both the aqueous and ethanolic phase eluting from the SepPak cartridge were analyzed by HPLC for the respective amine and amide. For this purpose, the volume of the aqueous SepPak eluate was decreased under reduced pressure to approximately 1 mL. Aliquots were injected onto a C18 μ-Bondapak column and quantified.

2.9.3. Further HPLC Analyses

A solution of 2,6-di-t-butylpyridine in diethyl ether was analyzed by HPLC with a C18 μBondapak column with a mobile phase consisting of 60% methanol, 40% water and 0.02% trifluoroacetic acid. The compound showed a k' value of 2.9 and the detection limit at a UV detector sensitivity of 0.02 AUFS and at a wavelength of 280 nm was 20 ng (0.01 nmol).

To 7-methoxynaphthylenyl-1-ethylamine (43) (1.5 mg, 7.5 μmol) in 1mL acetonitrile was added phthaloyl dichloride (0.14 mg, 0.7 μmol) in 100 μl ether. HPLC analysis (same conditions as above) showed a peak at the k' value of the amine (0.2) and a new peak with a k' of 4.3. The HPLC peak was collected, evaporated under reduced pressure and redissolved in methanol. Mass spectral analysis showed:

MS (EI):   331 (10), 184 (15), 172 (12), 171 (25), 149 (9), 128 (8), 69 (40), 45 (100)

MS (CI):   332 (10), 214 (30), 202 (100), 214 (30)

The compound could not be identified unambiguously with these mass spectral data and the detection limit could therefore be expressed only in terms of phthaloyl

dichloride that was added to the amine sample and caused the peak in HPLC analysis with a k' value of 4.3. At a detector sensitivity of 0.02 AUFS a detection limit of 11.2 ng (0.56 nmol) phthaloyl dichloride was found.

A ^{11}C-acetylation reaction was carried out to synthesize [11C]S20098 as described (Section 2.9.1.). After the radioactivity had decayed, the ethanol eluate was evaporated to 20 μl and then the whole mixture was injected onto the HPLC column (same conditions as above). At 0.02 AUFS a peak was observed for the amide (k'=5.6), but no signals were detected at k' values of 2.9 or 4.3.

2.10. Optimization of C-11-Acetylation Reactions

2.10.1. Efficiency of [11C]CO_2 Trapping

Carbon-11-acetylation reactions were carried out as described in Section 2.9.1. In all of the following experiments the reaction conditions and reagents were kept constant except for the solution in Vessel 1, which contained methylmagnesium bromide in diethyl ether. The volume of this Grignard reagent in a series of independent experiments was varied as follows:

(1) 0.5 mL of 0.3M Grignard (150 μmol methylmagnesium bromide) in three runs

(2) 0.7 mL of 0.3M Grignard (210 μmol methylmagnesium bromide) in five runs

(3) 1 mL of 0.3 M Grignard (300 μmol methylmagnesium bromide) in one run

The radioactivity levels that were retained in Vessel 1 and that were trapped in the soda lime trap #1 (refer to Figure 30) were measured and were decay corrected to EOB.

2.10.2. Distillation Efficiency

Carbon-11-acetylation reactions were carried out as described in Section 2.9.1. In these experiments 5-methoxytryptamine (7) was used as the precursor amine in Vessel 2. All reaction conditions and reagents were kept constant except for the nature of the

ether in Vessel 1 and for the oil bath temperature during distillation of [^{11}C]CH$_3$COCl. Table 8 summarizes the parameters.

Table 8: Reaction Conditions in Experiments to Determine the Distillation Efficiency

Experiment	Oil Bath Temperature for Vessel 1 [°C]	Solvent in Vessel 1
1	100	diethyl ether
2	100	dibutyl ether
3	120	diethyl ether
4	120	dibutyl ether
5	160	diethyl ether
6	150	dibutyl ether

After formation of the [^{11}C]acetyl chloride in Vessel 1, its radioactivity was measured (time t = 0) and the distillation started by moving the vessel into the preheated oil bath. At various time intervals the distillation was interrupted (removing of the oil bath and stopping of the helium gas) and the activity in Vessel 2 was measured. Vessel 2 was then reattached to the apparatus and the distillation was continued.

Mass spectral analyses of the ethanolic SepPak eluates after distillations at temperatures higher than 135°C showed reproducibly peaks at m/z = 57 (electron ionization) and at m/z = 131 (chemical ionization).

2.10.3. Efficiency of [^{11}C]CH$_3$COCl Trapping

Carbon-11-acetylation reactions were carried out as described in Section 2.9.1.

In these experiments 5-methoxytryptamine (7) (1 mg, 5 μmol) was used as precursor amine in Vessel 2. The [^{11}C]acetyl chloride was distilled at 150°C for 10 minutes, using dibutyl ether as solvent in Vessel 1. All other reaction conditions and reagents were not changed except the cooling regime for Vessel 2. Vessel 2 was cooled by immersion in a mixture of methanol and liquid nitrogen in a Dewar flask, adjusted to the following temperatures:

(1) -40°C from target unloading until the end of distillation

(2) -10°C from target unloading until the end of distillation

(3) -40°C from target unloading until 5 minutes of distillation were over,

then the Dewar flask was removed and Vessel 2 was left at room temperature

(4) -40°C from target unloading until 5 minutes of distillation were over,

then the Dewar was removed and Vessel 2 was immersed in hot water (50°C)

(5) Vessel 2 was left at room temperature from target unloading until the end of distillation.

At the end of distillation the amounts of ^{11}C in Vessel 2 and in the charcoal trap connected to its outlet (refer to Figure 30) were measured and time corrected to EOB. Activity measurements of the tubing between Vessel 2 and the trap showed that it retained only negligible amounts of radioactivity.

2.10.4. Rate of Amide Formation

Four Reacti-Vials (Pierce Co.) were charged with a solution of the naphthylic amine (43) (1 mg, 5 μmol) in acetonitrile (0.7 mL). A solution of CH_3COCl (19 nl, 0.3 μmol) in diethyl ether (0.3 mL) was added at room temperature. The reactions were quenched after 0.25, 0.5, 1 and 3 minutes, respectively, by adding one droplet of trifluoroacetic acid (30 μl, 400 μmol).

In other series of experiments, the amine and acetyl chloride solutions were kept

at 0°C, -20°C and -40°C, respectively, before the reactants were mixed; the reactions were conducted and quenched at the reaction temperatures and times described above.

One reaction was carried out at room temperature and quenched after 60 minutes. In another experiment the effectiveness of quenching was tested by adding one droplet of TFA to the amine solution first, followed by acetyl chloride.

Aliquots of all of these quenched reactions were analyzed by HPLC with a C18 μ-Bondapak column using a mobile phase consisting of 40% methanol, 60% water and 0.02% TFA.

2.11. PET Imaging of the Human Brain

2.11.1. Imaging with 2-Iodo[^{11}C]melatonin (11)

A healthy male volunteer (50 years) was positioned in the tomograph so that all the brain was monitored that is located 15 centimetres above the orbito-meatal line (the orbito-meatal line goes transaxially through the brain at the eye-ear level). A transmission scan was performed for 5 minutes.

A sterile and isotonic solution of [^{11}C]2-iodomelatonin (20 mCi in a volume of 7 mL, specific activity 130 mCi/μmol at time of injection) was injected at 3 p.m. into the arm vein of the volunteer. Carbon-11 in the brain was monitored at 30 second intervals for the next 30 minutes.

Emission data, accumulated after injection of the radiopharmaceutical, and transmission data, accumulated during the transmission scan (see Section 1.2.3.), were used to reconstruct images that represent the distribution of [^{11}C]2-iodomelatonin in the brain of the subject.

2.11.2. [^{11}C]S20098 (15)

A healthy male volunteer (50 years) was positioned in the tomograph as described

in Section 2.11.1. He received a sterile and isotonic solution of $[^{11}C]S20098$ (15 mCi in a volume of 7 mL, specific activity 410 mCi/μmol at time of injection) at 11 a.m. Carbon-11 in the brain was monitored at 30 second intervals for the next 30 minutes.

Emission data and transmission data were used in the same manner as described in Section 2.11.1. to reconstruct images that represent the distribution of $[^{11}C]S20098$ in the brain of the subject.

CHAPTER 3

SYNTHESIS OF 2-IODO-5-METHOXYTRYPTAMINE (22)

3.1. Synthetic Approach

The reaction conditions established by Bertholet and Hirsbrunner (43) for hydrolysis of melatonin to the corresponding amine were successfully applied to the preparation of 2-iodo-5-methoxytryptamine (22) from 2-iodomelatonin (11). The amide (11) was hydrolysed under basic aprotic conditions at 105°C in the presence of sodium dithionite to prevent oxidative degradation. Whereas Bertholet and Hirsbrunner (43) claimed a quantitative yield of 5-methoxytryptamine hydrochloride after a reaction time of 2 hours and after purification, the hydrolysis of 2-iodomelatonin gave 2-iodo-5-methoxytryptamine with a yield of only 15% after a reaction time of 4 hours and after HPLC purification. Figure 31 shows the chromatogram of the crude reaction product (C18 PrepNovaPak, 40% methanol, 60% water, 0.1% trifluoroacetic acid), while Figure 32 shows an analytical chromatogram of the purified compound under the same conditions.

The purified product in Figure 32 still showed a small impurity, which was either collected together with the large product peak or arose from a deiodination reaction, forming 5-methoxytryptamine. The presence of a deiodinated product was also indicated by mass spectral analysis. The observed peak at m/z = 190 (electron impact) belongs to the molecular ion of 5-methoxytryptamine and that at m/z = 160 may be its fragment ion after loss of CH_2NH_2.

The proposed fragmentation scheme for electron impact mass spectrometry is shown in Figure 33. It is identical to fragmentation patterns proposed in the literature
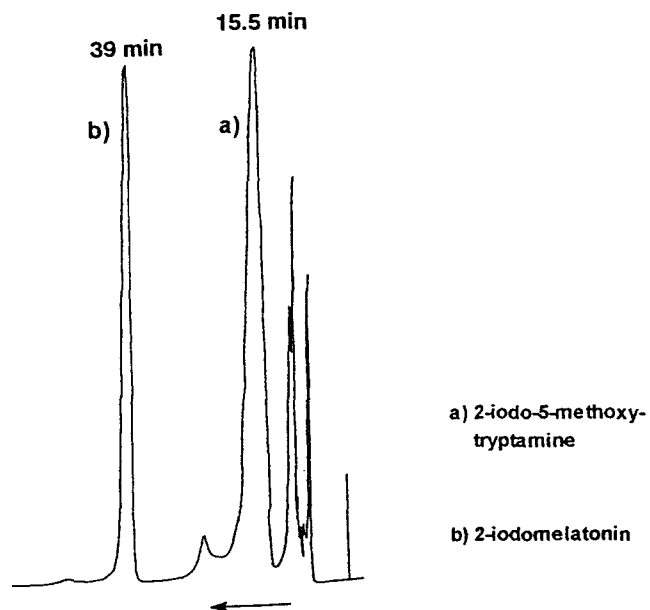
Figure 31: HPLC Analysis of Crude 2-Iodo-5-methoxytryptamine (**11**) after

Hydrolysis
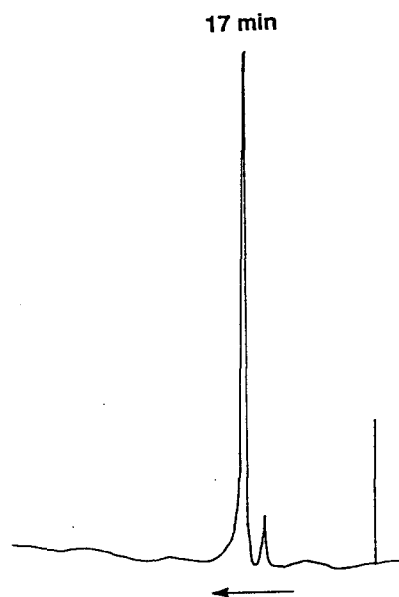
Figure 32: HPLC Analysis of 2-Iodo-5-methoxytryptamine (**11**) after Purification by

Preparative HPLC
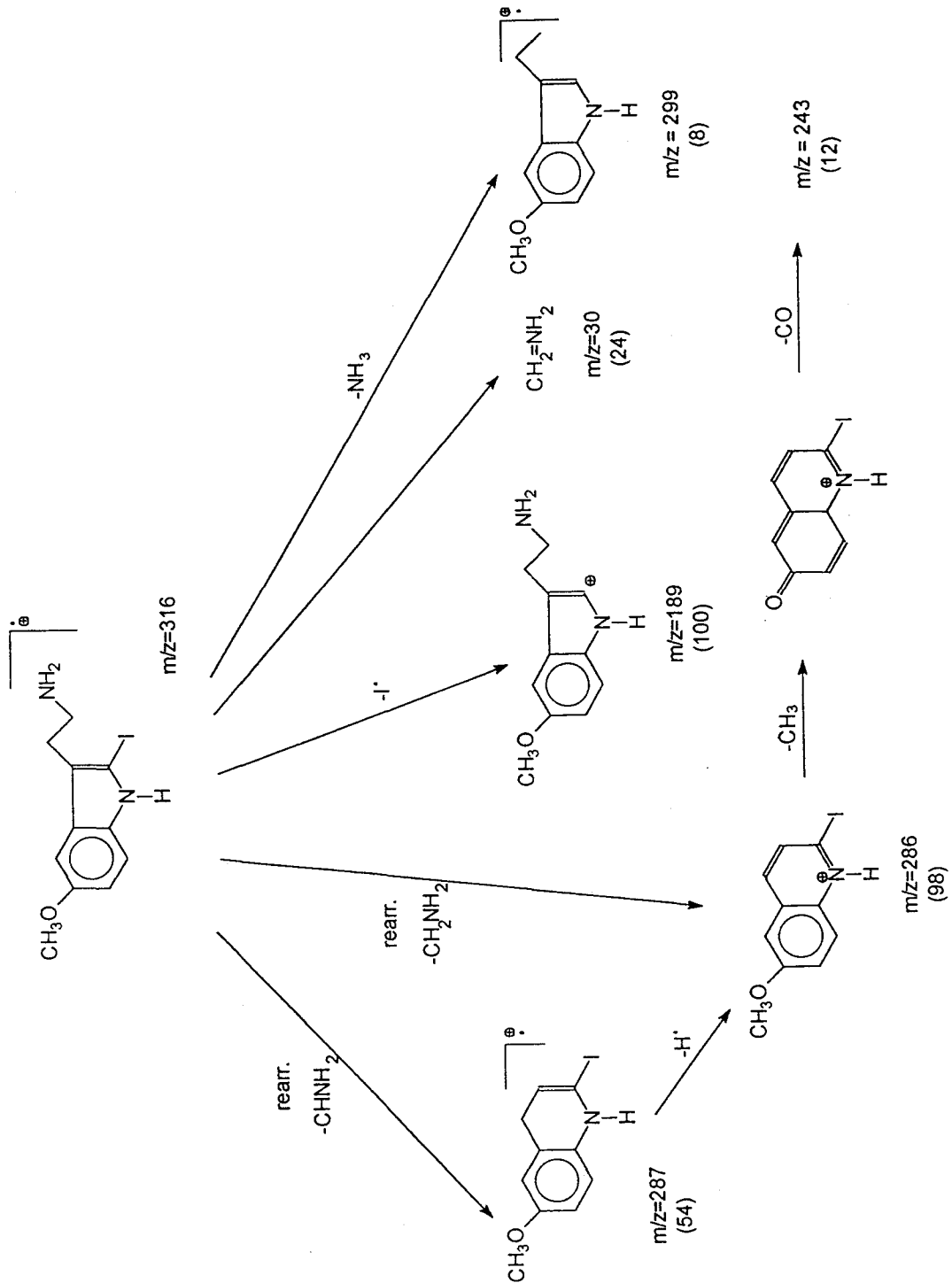
Figure 33: Proposed Fragmentation Scheme of 2-Iodo-5-methoxytryptamine (EI MS)

(50,51) for 5-methoxytryptamine (**7**), the only difference being the iodine in 2-position. The base peak at m/z = 189 results from loss of iodine. The ions at m/z = 287, 286 and 271 are probably due to ions with quinolinium structures, as has been proposed by Gynther *et al.* (51) and by Couch *et al.* (50) for 5-methoxytryptamine (**7**). Both authors based their interpretation only on comparisons of their observations with other reports in the literature describing fragmentations of similar tryptamines and quinolines. Only the formation of the ion at m/z = 160 for 5-methoxytryptamine (**7**) (corresponding to m/z = 286 for the iodotryptamine (**22**)) by direct bond cleavage has been confirmed by observation of a metastable ion (50). Chemical ionization mass spectrometry yielded the expected molecular ion at m/z = 317.

Figure 34 shows the NMR spectra from about 6.6 ppm to 8.4 ppm for four compounds: melatonin (**1**), 5-methoxytryptamine (**7**), 2-iodomelatonin (**11**) and 2-iodo-5-methoxytryptamine (**22**). For (**1**) and (**7**), the peaks due to H2 and H4 overlapped and coupling constants could not be determined unambiguously. Nevertheless, the integral confirmed that the signals at 7.04 and 7.03 ppm, respectively, arose from two protons. Also, in a spin decoupling experiment of the melatonin sample, irradiation at 7.035 ppm caused the coupling in the signals at 2.915 ppm (J=0.5 Hz, H_a) and at 6.83 ppm (J=2.4 Hz, H6) to collapse. This experiment proved that one of these two aromatic protons (H2) must be close to the side chain, while the other one must be coupling with H6 with a coupling constant of 2.3 Hz (H4). For 2-iodomelatonin (**11**) and 2-iodo-5-methoxytryptamine (**22**) the signal at 7.00 ppm had a symmetrical shape and the coupling constant of 2.4 Hz was in agreement with the coupling seen in H6. Also, the integral showed that the peak at 7.00 ppm corresponded to one proton. This result led us to conclude that the H2 proton in the latter two compounds had been replaced by iodine.
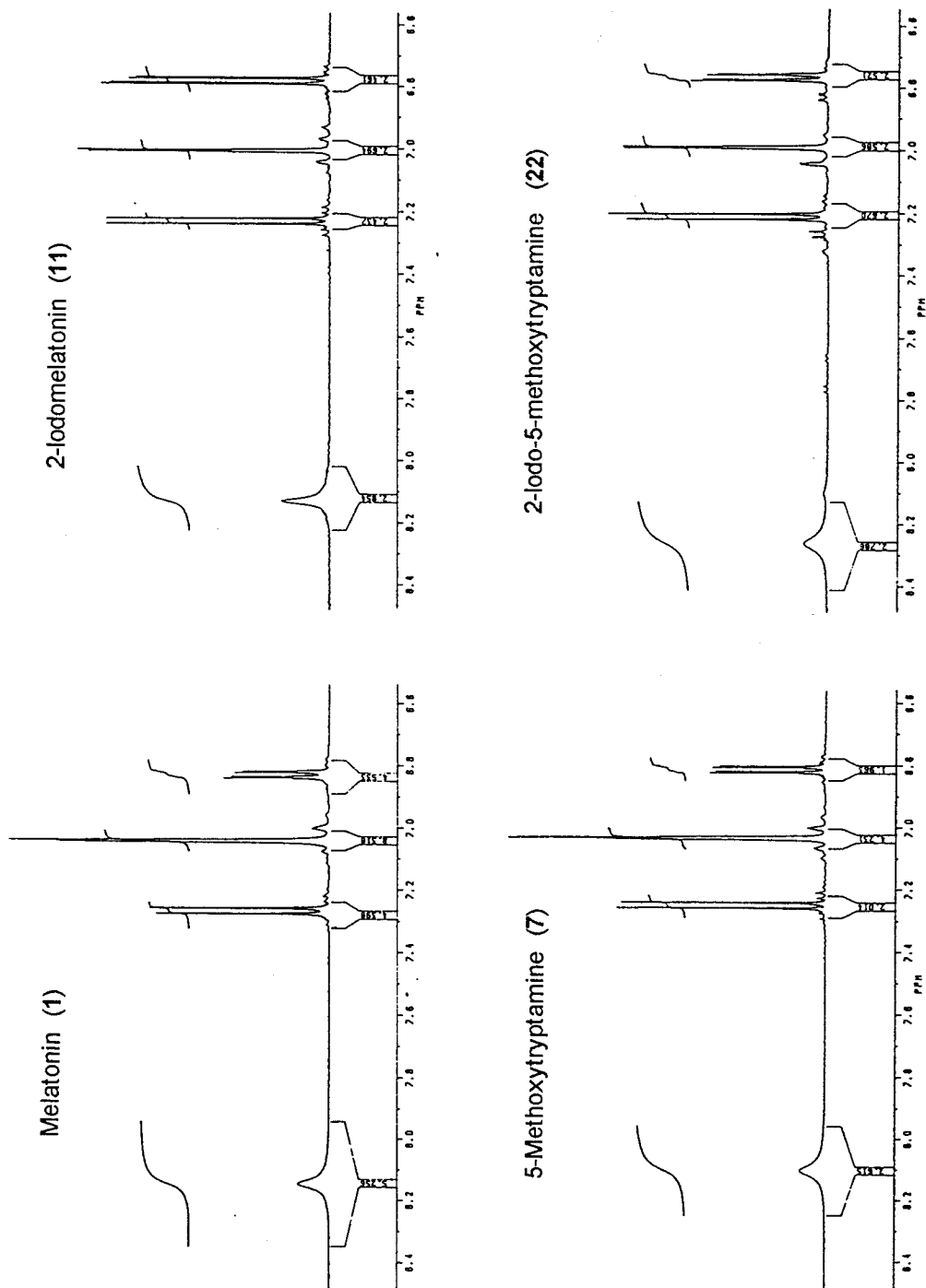
Figure 34: ^{1}H NMR of aromatic Region for **(1)**, **(7)**, **(11)** and **(22)**

Melatonin (1) and 2-iodomelatonin (11) also showed a three proton singlet at 1.89 and 1.88 ppm, respectively, resulting from the N-acetyl group. This signal was not observed in the tryptamines (7) or (22), confirming that the N-acetyl group was absent.

Reacetylation of the amine (Section 2.4.) also confirmed that the hydrolysis product was 2-iodo-5-methoxytryptamine (22). Upon reaction with acetic anhydride the free amine group was converted into an acetamide function and in two TLC solvents the R_f values of the reaction product and of 2-iodomelatonin were found to be identical.

3.2. Optimization of the Hydrolysis of 2-Iodomelatonin (11)

Since routine preparations of ^{11}C-labelled 2-iodomelatonin (11) would require repeated syntheses of 2-iodo-5-methoxytryptamine (22), the hydrolysis reaction and purification methods to afford the desired amine were investigated with the goal of optimizing the yield.

First, a hydrolysis reaction was carried out as described previously (Section 2.5.); at certain time intervals the reaction was interrupted and aliquots were taken and then analyzed by HPLC on a C18 μ-Bondapak column with a mobile phase consisting of 60% water (pH 3.8 with trifluoroacetic acid) and 40% methanol. Figure 35 shows chromatograms at several times during the reaction while Figure 36 shows the relative peak areas, corresponding to the relative concentrations of 2-iodomelatonin (11) and 2-iodo-5-methoxytryptamine (22). Note in Figure 35 that the retention time of the amine is longer than that of the amide; these chromatographic analyses were done with a very low concentration of acetic acid in the mobile phase, an amount which was insufficient to convert all of the amine into a charged and more polar compound. (Subsequent analyses using higher concentrations of trifluoroacetic acid (0.02% in the mobile phase) caused the amine to elute significantly earlier than the corresponding acetamide.)

Care must be taken in the interpretation of the chromatograms in Figure 35
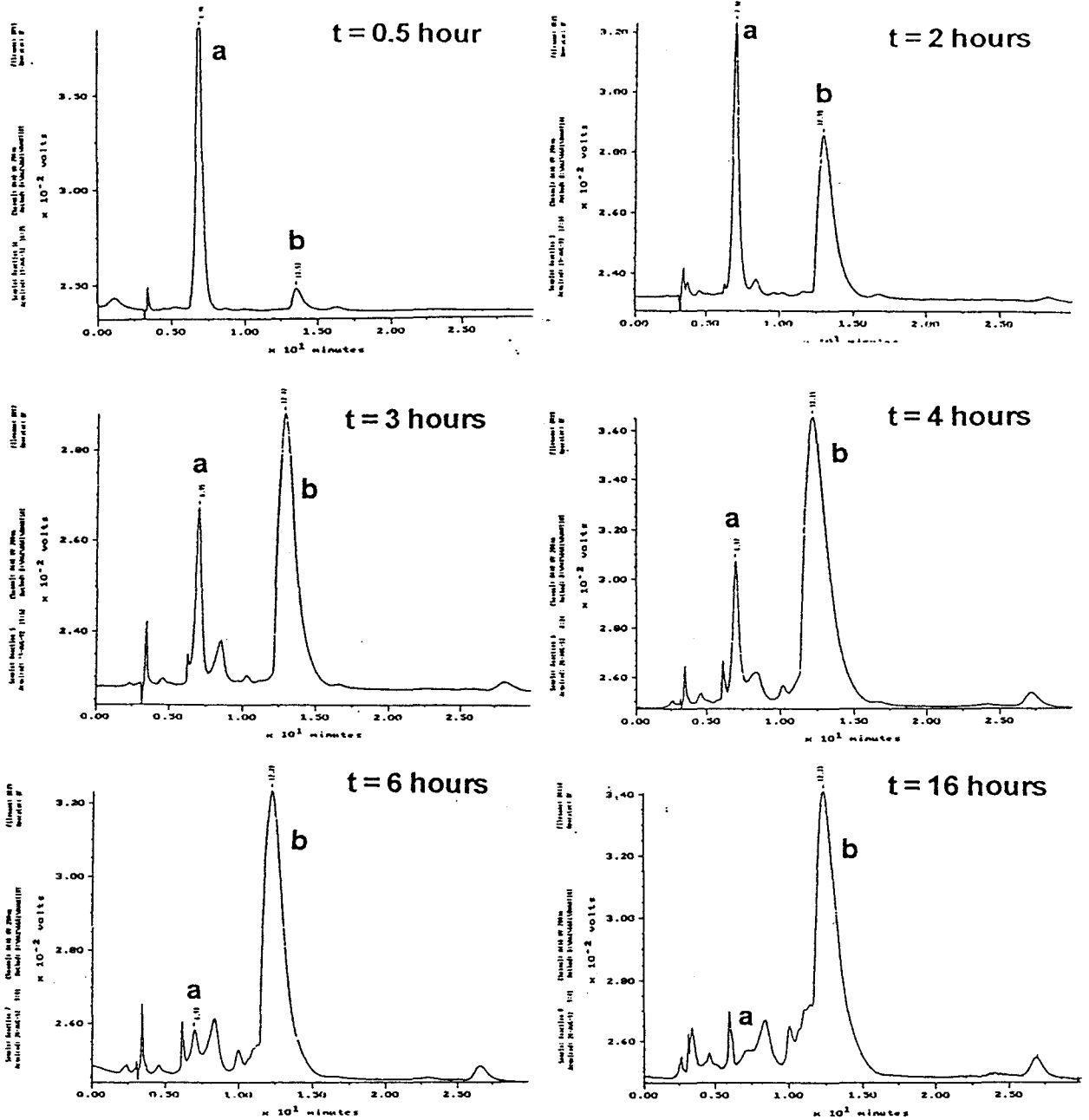
a = 2-iodomelatonin

b = 2-iodo-5-methoxytryptamine

t = reaction time

Figure 35: HPLC of Aliquots from the Hydrolysis Reaction at Various Time Points

relative peak area percent (absorption at 280 nm)
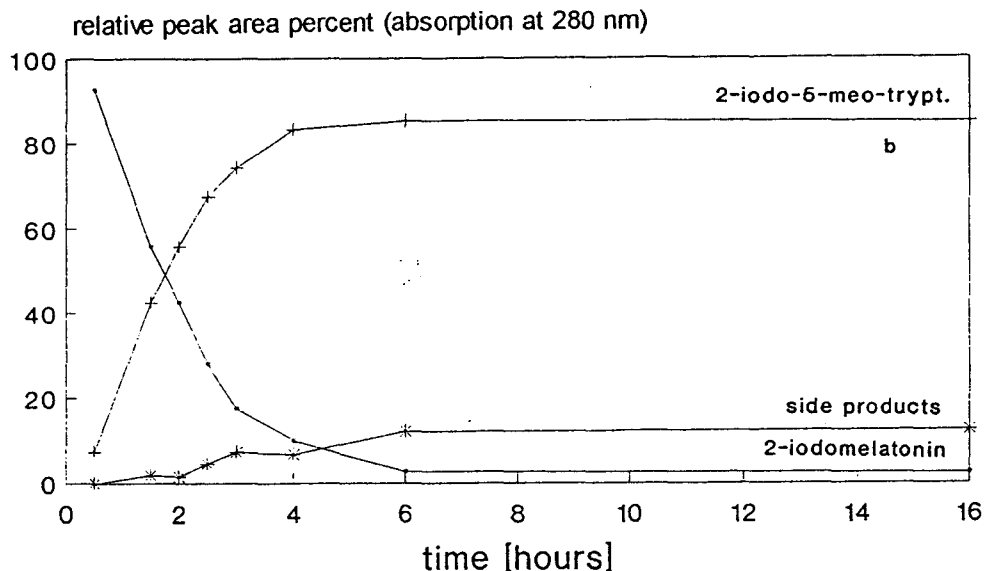
Figure 36: Change of Relative Peak Areas of 2-Iodomelatonin (a), 2-Iodo-5-methoxytryptamine (b) and Side Products during the Hydrolysis

because the computer program that was used for recording the spectra normalized the highest peak in each run. Therefore, Figures 35 and 36 illustrate only that the ratio of the peak areas of 2-iodomelatonin and 2-iodo-5-methoxytryptamine changed constantly during the first four hours of hydrolysis in favour of the iodotryptamine (**22**), whereas after four hours no more conversion of 2-iodomelatonin to the corresponding amine occured.

From Figures 35 and 36 it can not be concluded whether 2-iodomelatonin can be hydrolyzed to the corresponding amine (**22**) without significant degradation reactions. Therefore, a comparison was done of the yields of hydrolysis after two and four hours. The goal was to establish whether the yield can be maximized by extending the hydrolysis time up to six hours (until no more 2-iodomelatonin precursor is present, see Figure 35) or whether the degradation reactions proceed so fast that a compromise is necessary and the hydrolysis time must be shorter than six hours in order to minimize losses by degradation.

Reaction times of two and four hours were chosen in the next set of experiments;

all other conditions (reagent concentrations, hydrolysis temperature) were kept constant. After both reaction times the products were purified by either preparative HPLC or by TLC as described in Section 2.5. Table 9 summarizes the yields obtained by analytical HPLC.

Table 9: Yields of Hydrolysis Reactions of 2-Iodomelatonin (**11**) under Varying Conditions

Reaction and Purification	Yield of crude 2-Iodo-5-methoxy-tryptamine (**22**)	Yield of purified 2-Iodo-5-methoxy-tryptamine (**22**)	Yield of recovered 2-Iodomelatonin (**11**)
2 hour reaction time, prep. TLC (5 experiments)	not measured	7.5%	not measured
4 hour reaction time, prep. TLC (1 experiment)	24%	11.2%	6.5%
2 hour reaction time, prep. HPLC (2 exp.)	17%	9%	35% (20% after prep. HPLC)
4 hour reaction time, prep. HPLC (1 experiment)	25%	15%	7.5%

The table shows that after two hours of reaction about 17% 2-iodo-5-methoxytryptamine (**22**) was present in the crude reaction mixture, whereas after four hours this yield increased to 25%. After two hours the precursor and the product still accounted for 52% of the contents of the initial reaction mixture (i.e., 48% loss by degradation), whereas after four hours they amounted only to 32% of the initial mixture

and losses had risen to 68%. These results confirm that the rates of the decomposition reactions are faster (decrease by 20% in two hours) than the rate at which the iodotryptamine (22) is formed (increase by 8% in two hours, see Table 9).

Therefore, a hydrolysis time of four hours was found as the optimal procedure, with a yield of crude 2-iodo-5-methoxytryptamine of 25%; the increase in losses from two to four hours of reaction time suggests that the decomposition reactions are proceeding faster than the hydrolysis and that a longer reaction time would not give an increased yield. The most likely decomposition reactions are:

(1) cleavage of iodine (visible during some hydrolysis reactions because of the yellowish to dark brown/violet colour of the solution), followed by oxidation of the indole moiety

(2) oxidation of the free amine group by oxygen or by iodine that was cleaved off, followed by degradation of the whole molecule.

Philips and Cohen (40) also noted instability of α-N-(trifluoroacetyl)-2-halo-L-tryptophan methyl esters (29) in aqueous alkaline solution, but Hinman and Bauman reported that 2-bromoskatole (25) was relatively stable in ethanolic alkaline solution (38). Therefore, the dryness of reagents and solvent in the hydrolysis of 2-iodomelatonin is probably the most influential factor. An increase in the amount of $Na_2S_2O_4$ (which is supposed to prevent oxidation) by up to 100% did not influence the results significantly.

When preparative TLC was compared with preparative HPLC, a higher loss was observed with TLC, probably because the compound is exposed to both air and to a strongly alkaline chromatographic medium for more than one hour. Isolation by TLC gave an amine product with a slightly lower yield than isolation by HPLC, but with a lower purity.

3.3. Conclusions

Purification of the iodotryptamine (**22**) by HPLC is preferred to purification by TLC and the optimal reaction time was found to be four hours. While the overall yield under these conditions was only 15%, it represents a near maximal yield given the competition between a relatively slow hydrolysis and the lability of the iodinated indole nucleus. This procedure can be carried out rapidly and easily. Thus, the hydrolysis of 2-iodomelatonin (**11**) was found to be more practicable than any multistep synthesis because the quantities required for ^{11}C labelling are small (1.5 mg of 2-iodo-5-methoxytryptamine for each radiochemical synthesis).

CHAPTER 4

SYNTHESES OF ^{11}C-LABELLED MELATONIN ANALOGUES

4.1. Production of $[^{11}C]CO_2$

Carbon dioxide labelled with ^{11}C was produced by irradiating a gas target in the on-site cyclotron at the McMaster PET centre. The target contained $^{14}N_2$ at a pressure of 210 psi. The nuclear reaction $^{14}N(p,\alpha)^{11}C$ created the radionuclide ^{11}C which reacted with traces of oxygen in the nitrogen to give $^{11}CO_2$. It has been shown that at the proton energy of 11 MeV all of the isotope is present in the form of $^{11}CO_2$; $^{11}CN^-$ or ^{11}CO are not present. After irradiation the high pressure gas was automatically transferred from the target through 23 metres of stainless steel tubing to the stainless steel loop of the ^{11}C-acetylation apparatus, which was immersed in liquid nitrogen. The $[^{11}C]CO_2$ was frozen out, whereas both the $^{14}N_2$ and the helium sweep gas passed through the loop.

The saturation yield Y_S and the saturation activity A_S were determined at two different irradiation currents of the cyclotron and were calculated with equations 10 and 11, respectively.

$$(11) \qquad Y_S = \frac{activity}{I_{irr.} \times \left(1 - \exp\left(\frac{-0.693 \times t}{20}\right)\right)}$$

activity = produced radioactivity during irradiation

$I_{irr.}$ = irradiation current   t = irradiation time

$$(12) \qquad A_S = \frac{activity}{1-\exp\left(\frac{-0.693 \times t}{20}\right)}$$

activity = produced radioactivity during irradiation

$I_{irr.}$ = irradiation current   t = irradiation time

Table 10: Saturation Yield and Saturation Activity during Production of $^{11}CO_2$

Irradiation Current [μA]	Irradiation Time [min]	mCi produced	Saturation Activity A_s [mCi]	Saturation Yield Y_s [mCi/μA]
10	4	60	464	46.4
20	15	301	752	37.7

The results are summarized in Table 10. The saturation yield gives information about the radioactivity (in mCi) that can be produced per μA of beam current. The saturation activity is the maximal radioactivity that can be produced with the respective beam current. Both values allow us to estimate by extrapolation the amount of radioactivity that can be produced with the cyclotron.

In this thesis the calculated saturation activity was used for comparison with radioactivity values measured with a Geiger-Müller tube.

4.2. Apparatus for ^{11}C-Acylation Reactions

A Geiger-Müller detector for measuring the trapped radioactivity was positioned close to the stainless steel loop and was calibrated with the experimental setup by comparison measurements with the Capintec radioactivity detector. After installation of

the detector the measured value of radioactivity was constantly displayed on the screen of the Macintosh Powerbook.

The tubing had to be rinsed and dried carefully and checked regularly for deposits or bends. If the tubing was plugged or leaking during a synthesis involving radioactivity, the production had to be aborted because of the potentially high radiation dose; in addition, a time loss of only 5 minutes that may arise while attempting to repair a leaking line would already result in a loss of 16% in radiochemical yield because of the decay of the ^{11}C isotope. Also, a regular check of the valves was necessary to ensure that they were functioning. For example, a precipitate in Valve 5 can be the cause for its not closing properly, in which case the reaction mixture from Vessel 2 could not be transferred into Vessel 3.

In recent years increasing efforts have been made to design radiochemical syntheses for PET tracers that can be handled in a remote way, either with computer control or with robots. The amounts of radioactivity in preparations of PET radiopharmaceuticals are in the range of several hundred millicuries and often there are gaseous radioactive precursors involved, for example $[^{11}C]CO_2$ or $[^{18}F]F_2$. Therefore, safety and protection of personnel have to be considered in the choice of possible chemical reactions and procedures.

4.3. Synthetic Approach

The synthesis of the ^{11}C-labelled acetamides in this thesis is based on the procedure described by LeBars et al. (32), who used it to label melatonin (32,33) and 6-fluoromelatonin (35). Figure 37 shows the reactions used to prepare the compounds in this project.

Phthaloyl dichloride was used to convert the $[^{11}C]CO_2$-Grignard adduct into its corresponding acid chloride. The mechanism is shown in Figure 38. The reaction was
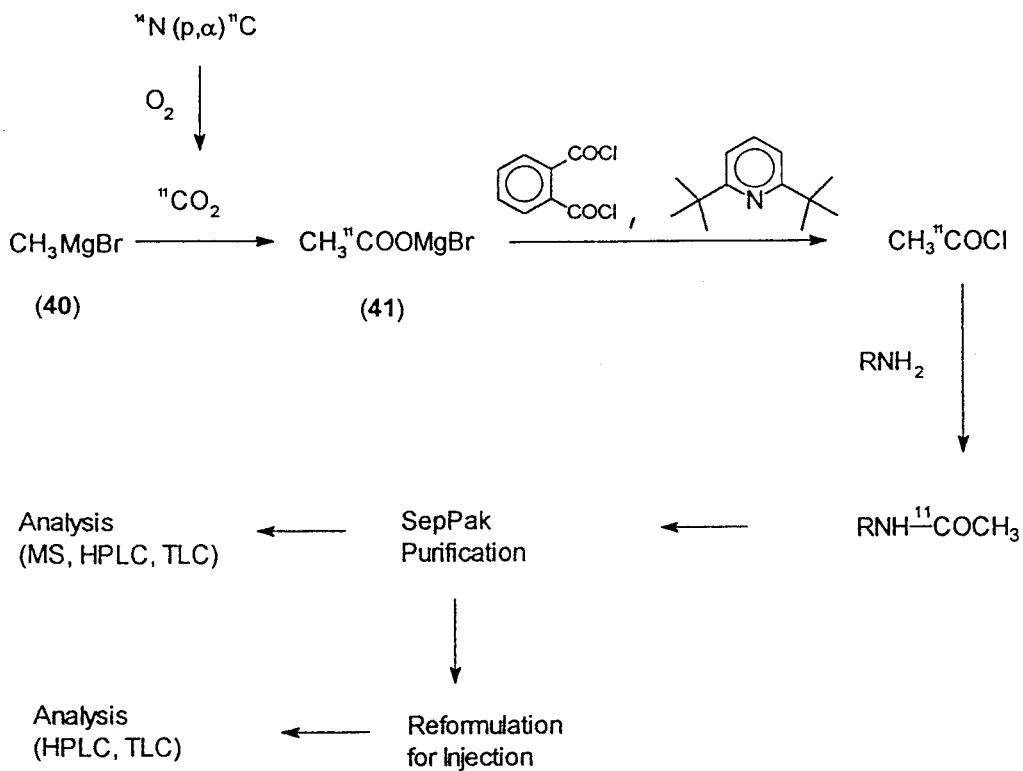
Figure 37: Synthesis and Purification of ^{11}C-Labelled Amides
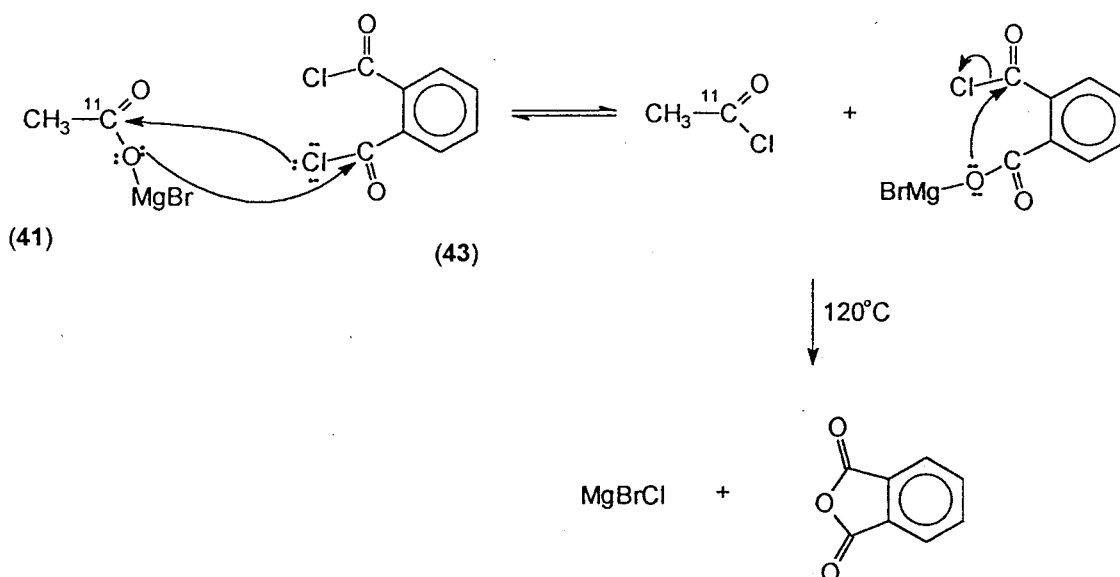
Figure 38: Mechanism for Formation of Acetyl Chloride

driven by ring formation of phthalic acid anhydride, especially at higher temperatures.

The advantage of this method is that, because of the high boiling point of phthaloyl dichloride (275°C), the acetyl chloride product could be separated from the reaction mixture relatively easy by distillation into a second vessel (b.p. of CH₃COCl 56°C). Although the reaction proceeded without addition of 2,6-di-t-butylpyridine, this hindered base served two purposes: to scavenge any trace acid and to keep the solution homogeneous. During the addition of phthaloyl dichloride a white precipitate formed, which became yellow and, upon heating, red; simultaneously the solution became increasingly viscous and tarry.

Whereas LeBars et al. (32,33) prepared fresh methylmagnesium bromide prior to every acetylation reaction, we found that the commercially available Grignard reagent (Aldrich) gave good results, if stored and handled properly.

Acetonitrile was preferred over dichloromethane (32,33) as the solvent for the amide formation in Vessel 2 of the ^{11}C-acetylation apparatus. Both the charged transition state and formation of HCl as side product can be better accommodated by a more polar solvent such as acetonitrile than a less polar solvent such as by dichloromethane. Figure 39 shows the mechanism of amide formation.
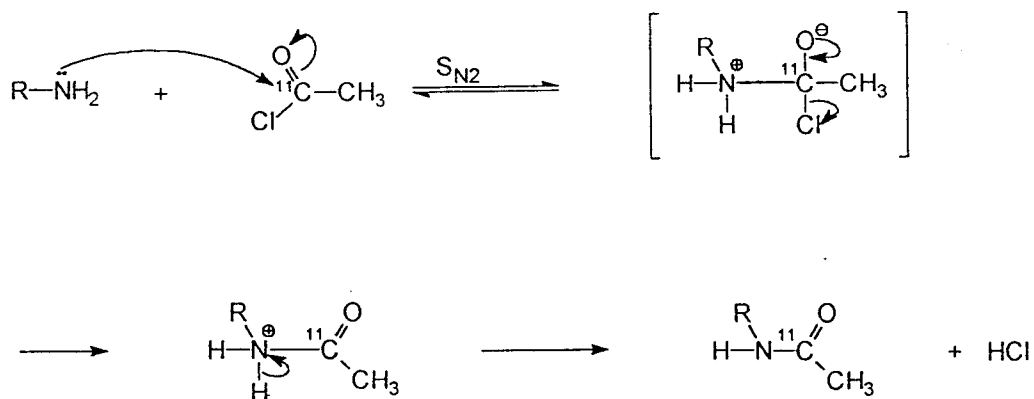
Figure 39: Mechanism of Amide Formation

The use of acetonitrile also allowed dilution of the reaction mixture (contained in Vessel 2 and transferred into the larger Vessel 3 of the apparatus) with water (pH 2.9 with HCl) during the SepPak purification. This dilute mixture was loaded directly onto a reversed-phase solid phase extraction column with ease, then the column was washed with a mixture of water (pH 2.9) and methanol before the final product was eluted with a small volume of 95% ethanol. A purification protocol was established for each of the ^{11}C-labelled amides (1), (11) and (15); the optimal volumes of washing mixture, the pH value of the aqueous phase and the percentage of methanol were determined in order to ensure that there was neither a loss of product during the washing step nor were there any impurities in the final ethanol eluate. Thus, both the aqueous methanolic and the ethanolic SepPak eluates resulting from syntheses of the respective ^{11}C-labelled amides melatonin (1), 2-iodomelatonin (11) and S20098 (15) were analyzed by HPLC, as described in more detail in Section 4.4.

Figure 40 is an example of an HPLC analysis of an aliquot taken from Vessel 2 of the acetylation apparatus and chromatographed on a C18 PrepNovaPak column with a mobile phase consisting of 60% water (pH 3.3 with trifluoroacetic acid) and 40% methanol. Unreacted precursor amine (in Figure 40, 5-methoxytryptamine (7)) gave a large peak in the UV trace; several signals were observed in the radioactivity channel, of which one peak ([^{11}C]melatonin) corresponded to the melatonin signal in the UV trace. After SepPak purification the radioactive and UV-absorbing impurities were eliminated. This is illustrated in Figure 41, which shows a radiochromatogram of [^{11}C]2-iodomelatonin (11), analyzed with a C18 PrepNovaPak column and a mobile phase consisting of 60% water, 40% methanol and 0.02% trifluoroacetic acid.

Note that the acid concentration was increased between Figure 40 and Figure 41. Therefore, in Figure 40 the amine elutes after the amide, but in Figure 41 the amine is converted into an ionic species and it elutes before the amide.
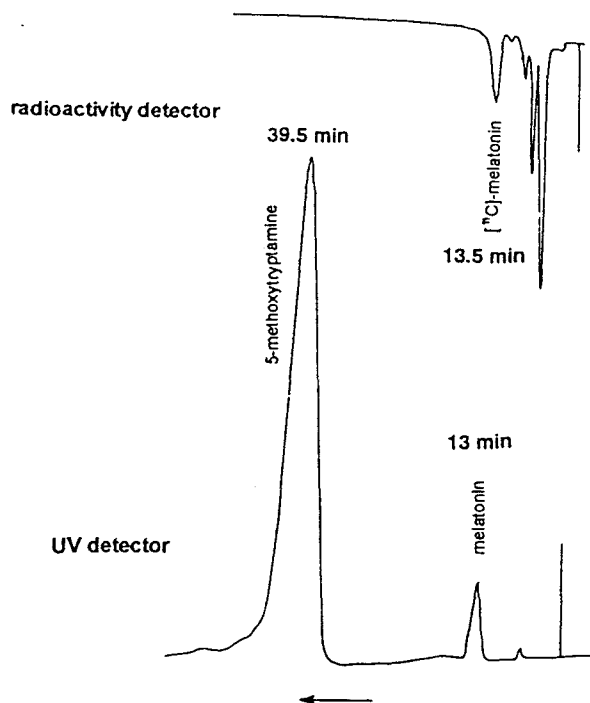
Figure 40: HPLC Analysis of [^{11}C]Melatonin before SepPak Purification
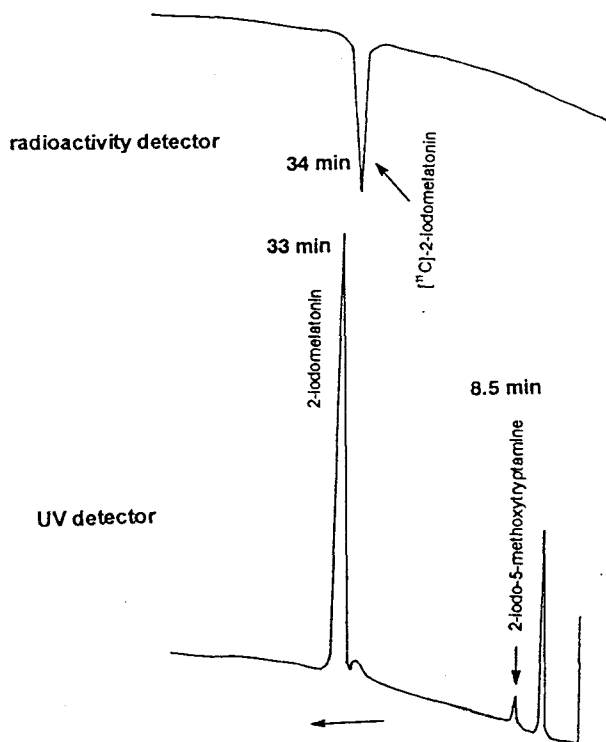
Figure 41: HPLC Analysis of [^{11}C]2-Iodomelatonin after SepPak Purification

4.4. Product Identification and Analysis

In order to identify the products of the radiochemical syntheses, the HPLC fraction containing the UV peak that was observed simultaneously with the radioactive peak was collected and prepared for mass spectral analysis. As explained in Section 1.2.4, the amount of radioactive material is at most in the picomole range and therefore the chemical species corresponding to this radioactive peak cannot be identified positively. However, the quantity of unlabelled material produced simultaneously is much larger (micromole range); the unlabelled material can be identified and it is assumed that the radioactive and the unlabelled compound are otherwise identical.

The unlabelled "byproducts" that arose during the production of ^{11}C-labelled melatonin (1), 2-iodomelatonin (11) and S20098 (15) were prepared for mass spectral analysis; the spectra were compared with those of the respective authentic materials. Although there were slight deviations in some ion intensities and in some of the less intense fragment ions, the characteristic peaks resulting from bond cleavages and from McLafferty rearrangements were always present with reproducible intensities (m/z = 232, 173 and 160 for melatonin, m/z = 358, 299, 286 and 231 for 2-iodomelatonin, m/z = 243, 184 and 171 for S20098).

Solvents for TLC were chosen so that either the amine or the amide showed an R_f value in the region between 0.2 and 0.7 (see Table 6). In all cases the observed R_f values in TLC and k' values in HPLC agreed with those of the respective authentic materials.

The unlabelled synthetic acetamides (1), (11) and (15) were identical in all respects with authentic samples leading us to conclude that the ^{11}C-labelled acetamides were also identical to the authentic acetamides.

For each of the ^{11}C-labelled products (1), (11) and (15) quantitative analyses were carried out on both the ethanolic and the aqueous SepPak eluates to assure that the

desired product had not been lost in the SepPak purification step. As an example, the results from three production runs for [^{11}C]melatonin are discussed here. Both the aqueous phase and the ethanolic phase eluting from the SepPak cartridge were analyzed by HPLC for the respective amine and amide. Table 11 shows the averaged results of the analyses obtained from three [^{11}C]melatonin production runs and SepPak purifications.

Table 11: HPLC Analysis of SepPak Eluates after Production of [^{11}C]Melatonin (mean of three independent experiments)

	5-Methoxytryptamine (7) [μg]	Melatonin (1) [μg]
Starting Material in Vessel 2	1100	0
Aqueous Eluate	952	0.2
Ethanolic Eluate	22.5 [A]	8.4

[A] This amount was later decreased to undetectable quantities by increasing the elution volume slightly.

These data show that only 2.4% of the amide eluted in the load and wash steps prior to the ethanol elution. In these experiments a small quantity of amine (22.5 μg, 2.3% of the recovered amine) was found in the ethanol eluate. Following these experiments the volume of the aqueous wash was increased slightly; with this modified protocol the amount of amine recovered in the aqueous wash became virtually quantitative while melatonin recoveries were unaffected.

On average, 90% of the amine placed in Vessel 2 was recovered by HPLC analysis (sum of quantities in aqueous and ethanolic eluate). This proved that the described quantitative analysis was reliable and correct.

The results also confirmed that the overall procedure was reproducible and efficient for the purification of the ^{11}C-labelled acetamides. The ethanolic eluates from the SepPak purification were found to contain the pure acetamides by HPLC analysis. Thus, the SepPak ethanolic eluent provided acetamides of sufficient purity that further purification was unnecessary and the compounds could be injected into humans.

4.5. Radiochemical Yield and Specific Activity

HPLC analysis of the reaction mixture in Vessel 2 showed that even under optimal conditions only approximately 40% of the radioactivity was found in the amide, whereas 60% was found in the more polar side products (see Figure 40). This observation is of significant importance because a minimum radiochemical yield is necessary in order to carry out PET studies at all. There are two explanations possible:

(1) The amine was not present as its free base or the solution was contaminated with another base (ammonia, other polar amine), competing for the acid chloride.

(2) The acetyl chloride was hydrolysed before it could react with the amine.

In initial experiments the naphthylic amine (43) was obtained by extraction from an aqueous, alkaline solution (containing ammonia) into dichloromethane. Later, this procedure was changed to avoid the introduction of ammonia; the aqueous solution was made alkaline with potassium carbonate prior to extraction with dichloromethane (see Section 2.2). The yield improved significantly to the above mentioned amount (30-40% of activity in Vessel 2). This indicates that in the initial experiments influences listed under (1) were likely to have led to decreased yields. With the present extraction procedure neither amine hydrochloride nor a competing base should be present in Vessel 2.

The second explanation is not very likely under the given circumstances. The helium gas stream that was passed through the apparatus during the experiment was dried

over $Mg(ClO_4)_2$; therefore it should not contain water that could condense into Vessel 2 when it is cooled to -20°C or below. Also, the primary amine is a stronger nucleophile than water, making it much more likely to react with the acetyl chloride.

TLC analyses showed the presence of a polar radiochemical impurity with an R_f value of zero when an aliquot from Vessel 2 was chromatographed in solvent system (B). When an aliquot from Vessel 2 was spotted together with a droplet of water and then developed in solvent (B), its R_f value increased from zero to 0.3, an R_f value identical to that exhibited by [14C]acetate. This result implies that unreacted acetyl chloride was still present in the reaction medium. It remains unclear what factors prevented further reaction between the excess amine and the acid chloride. Interestingly, radiochromatograms pertaining to ^{11}C-labelled melatonin and 6-fluoromelatonin and their respective precursors, published by LeBars *et al.* (32,35), show the same feature: the peak area arising from the radioactivity of polar compounds is about twice as high as the peak area pertaining to the radiolabelled product.

Table 12 shows values for the radiochemical yields and specific activities for the compounds discussed in this thesis and compares them with results from the literature. These results are quite comparable; whereas the radiochemical yield is of less importance (as long as 10 to 15 mCi are available at EOB), the specific activity is very critical. As discussed in section 1.2.4, *in vivo* there is competition between the labelled ligand and naturally occurring melatonin for a limited number of high affinity receptor binding sites. In section 1.3.2 it was estimated that a specific activity of at least 460 mCi/μmol <u>during</u> the PET scan must be available. This was not even quite achieved with [11C]S20098 (15). If the specific activity is too low, the concentration of the radioactive ligand at the receptor sites is not sufficient to give a signal that can be detected with the PET scanner.

Table 12: Radiochemical Yields and Specific Activities of Labelled Melatonin Receptor Agonists

Compound	Radiochemical Yield [%]	Specific Activity [mCi/μmol]
[^{11}C]Melatonin **(1)** (Average of 5 Productions with low Activity)	12.8	323 (EOB)
2-Iodo-[^{11}C]Melatonin **(11)** (for PET Study)	20	545 (EOB) 130 (at Start of PET Study)
[^{11}C]S20098 **(15)** (for PET Study)	14.5	2090 (EOB) 410 (at Start of PET Study)
[^{11}C]Melatonin **(1)** (for PET), (33)	25	700 (EOB) 268 (EOS)
6-Fluoro-[^{11}C]melatonin **(21)** (35)	35	141 (EOB)

The strong variations in the specific activities reported in this thesis illustrate that reaction conditions are of critical importance. Therefore, a series of optimization experiments were carried out to further investigate the influence of the reaction conditions on the radiochemical yield and specific activity of the syntheses (see Section 4.7). Although no carrier added $^{11}CO_2$ is produced, at the end of synthesis the ratio of ^{11}C-amide versus ^{12}C-amide was between 1:20,000 and 1:70,000. It has been found that $^{11}CO_2$ generated by nuclear reactions in a nitrogen gas target is diluted more than 1000 times with trace amounts of $^{12}CO_2$ contained in the nitrogen gas (52). A relatively minor dilution (1:20 to 1:70) occurs later because of dissolved $^{12}CO_2$ in the Grignard reagent. The varying quality of the Grignard reagent is probably sufficient to cause the observed changes (see also Section 4.7.2). Also, when too much time elapses

between $^{11}CO_2$ transfer and addition of phthaloyl dichloride, more $^{12}CO_2$ from the atmosphere and from the helium gas used for transfer can enter the Grignard solution.

In this project only two syntheses were done with higher amounts of $^{11}CO_2$ and the specific activities obtained in these production runs were rather low (130 and 410 mCi/μmol). Nevertheless, with syntheses performed using routine or sub-optimal conditions, it should be possible to decrease the amount of unlabelled material to *ca.* 10 nmol (see also Section 4.7.1). Furthermore, the produced amount of $[^{11}C]CO_2$ in these two runs was only 450 mCi; by increasing the irradiation current from 10 μA up to 40 μA it can be estimated that a production of *ca.* 900 mCi of $[^{11}C]CO_2$ is possible. With a radiochemical yield of 20% after a synthesis time of 35 minutes 54 mCi of ^{11}C-labelled product would then be available. A product with a radioactivity of 54 mCi and with 10 nmol of unlabelled material would have a specific activity of 5400 mCi/μmol. Thus, the evaluation of the current data allowed us to conclude that it should be possible to increase the specific activity by a factor of 10.

4.6. Analysis for Contaminants

Several experiments were carried out to determine whether some of the reactants that had been added to Vessel 1 (2,6-di-t-butylpyridine and phthaloyl dichloride) were being carried over into Vessel 2. Although their boiling points are considerably higher than the temperature used in Vessel 1 (100°C at 23 mm Hg for 2,6-di-tert-butylpyridine and 275°C for phthaloyl dichloride), small amounts may have been carried over by the helium gas stream at 15 mL/min.

Standard solutions of 2,6-di-t-butylpyridine were prepared and a detection limit of 20 ng (0.1 nmol) was established at a detector sensitivity of 0.02 AUFS and at a wavelength of 280 nm (see Section 2.9.3). The product amide (15) of a ^{11}C-acetylation reaction was analyzed by HPLC under conditions identical to those used for the analysis

of 2,6-di-t-butylpyridine. In this chromatogram there was no peak with a k' value of 2.9, which allowed us to conclude that 2,6-di-t-butylpyridine was not present in Vessel 2 in an amount equal to or exceeding 20 ng (0.1 nmol).

If phthaloyl dichloride distilled into Vessel 2, it would have reacted with the amine present in large excess to form the amide (41), the diamide (42) and perhaps the phthalimide (44) according to Figure 42. Contamination of Vessel 2 with only 0.025% of the phthaloyl dichloride present in Vessel 1 would result in approximately a 1:10 molar ratio of phthaloyl dichloride to amine, yielding 0.7 μmol of diamide.
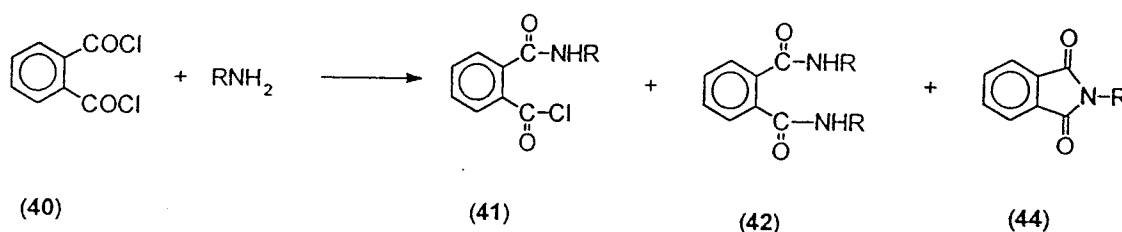
Figure 42: Reaction between Phthaloyl Dichloride and Amine

This situation was simulated by adding phthaloyl dichloride (0.7 μmol) to a solution of the amine (43) (7.5 μmol) as described in Section 2.9.3. This reference solution was chromatographed on a C18 μ-Bondapak column with a mobile phase consisting of 60% water, 40% methanol and 0.02% TFA, where the solution showed a peak belonging to the amine (k'=0.2) and a new peak with a k' of 4.3.

Although attempts were made to identify the compound that caused the peak at k' = 4.3 in HPLC analysis of the mixture containing phthaloyl dichloride and the amine, the structure of this product could not be established unambiguously by mass spectral analysis. An apparent molecular weight of 331 was found; this may be due to the

phthalimide (44) in Figure 42, but it is also possible that (44) was formed from the amide (41) or from the diamide (42) while being introduced into the heated ion source of the mass spectrometer.

Therefore, in this case the detection limit could only be expressed in terms of phthaloyl dichloride that entered Vessel 2 and reacted with the amine to form either one of compounds (41), (42) or (44). The detection limit was found to be 11 ng (0.56 nmol) for phthaloyl dichloride.

The product amide (15) of a ^{11}C-acetylation reaction was then chromatographed under conditions identical to those that were used for the analysis of the mixture containing the phthalic acid derivative as described in Section 2.9.3. The ^{11}C-reaction mixture did not show a peak at the k' value of 4.3; this allowed us to conclude that Vessel 2 contained not more than 11 ng (0.56 nmol) phthaloyl dichloride.

In the future, if the distillation temperature is increased, e.g., when attempting to distil at a higher temperature, this type of analysis should be repeated.

4.7. Optimization of the Acetylation Procedure

4.7.1. Optimization of Target Unloading and of [11C]CO_2 Trapping in the Cold Trap The term "target unloading" refers to a procedure to transfer the irradiation product, for example [11C]CO_2 from the target of the cyclotron to the reaction apparatus. During unloading, the gas stream from the target must be gentle enough so that the maximum amount of [11]CO_2 is trapped in the cold trap. Furthermore, the target must be unloaded rapidly so as to minimize losses due to radioactive decay. Experiments were carried out to optimize this procedure (Section 2.10.1). Table 13 summarizes the radioactivity measured in the stainless steel loop and soda lime trap #1 (refer to Figure 30) under varying target unloading conditions.

Table 13: Activity in Stainless Steel Loop and in Soda Lime Trap #1 under Varying Target Unloading Conditions

Unloading Process [A] (n=number of exp.)	^{11}C in Loop, corrected to EOB [mCi]	^{11}C in Loop [%] [B]	^{11}C in Soda Lime, corr. to EOB [mCi]	^{11}C in Soda Lime [%]
a) ; n=3	51.8	80	12.9	20
b) ; n=2	46.8	78	13.1	22
c) ; n=1	46.5	88	6.6	12
d) ; n=3	55.0	87	8.0	13

[A] refer to Section 2.7.3. for description

[B] the percentage is calculated as follows: (activity in loop/sum of activ. in loop and soda lime) x 100%

These experiments show that the target gas must be released slowly, otherwise the $[^{11}C]CO_2$ is not trapped efficiently in the loop and appears in the soda lime trap (conditions a) and b)). If the line is not swept with helium, a considerable amount of $[^{11}C]CO_2$ remains in the 23 metres of gas transfer line between the target in the cyclotron and the cold trap (condition c)). The best results were obtained when the line was swept with a pulsed helium gas stream (condition d)), which created a slow and gentle flow.

Therefore the computer program for target unloading was changed accordingly (see Appendix, program "O15BOLUS") and this program was used for all experiments reported in this thesis except those performed during the testing of the cold trap (Section 2.10.1).

In another set of experiments the influence of the design of the cold trap on the amount of retained ^{11}C was investigated by using three different loops and measuring the

amount of radioactivity that was trapped in each of the loops. For these runs unloading procedure a (see Section 2.10.1) was used. Table 14 displays the results.

Table 14: Radioactivity Trapped in three different Cold Trap Loops

Trap	^{11}C produced [mCi] [A]	^{11}C in trap, corr. to EOB [mCi]	^{11}C in trap [%] [B]
1/8'' SS Loop, 60 cm cooled length, 1.82 mm i.d.	61	31	51
1/8'' Copper Loop, 60 cm cooled length, 1.82 mm i.d.	61	42	69
1/16'' SS Loop, 120 cm cooled length, 0.26 mm i.d.	61	58	85

[A] calculated from irradiation time (4 min) and current (10 μA) and saturation yield (47 mCi/μA at 10 μA):

$$Activity = 47\frac{mCi}{\mu A} \times 10\mu A \times (1-\exp\left(\frac{-0.693\times 4min}{20min}\right) = 61mCi$$

[B] calculated as (activity in loop) / (produced amount) x 100%

The trapping experiments provided the basis for selecting the optimal loop size. The wall thickness was the same in all three loops, but because of their different outer diameters their inner diameters differed significantly. The 1/16'' tubing could be bent in 10 turns with an approximate diameter of 4 cm, thus *ca.* 120 cm were immersed in liquid nitrogen. The 1/8'' tubing was more difficult to bend and only 5 turns could be accommodated in the Dewar flask, thus only 60 cm of tubing were cooled. The copper loop was chosen to investigate whether this material would be more efficient in cooling.

The best results were obtained with stainless steel tubing of 1/16'' o.d. and a cooled length of approximately 120 cm. The diameter of the other loops (1/8'' o.d.) and their shorter cooled length (*ca.* 60 cm) may not have been optimal for efficient trapping of [^{11}C]CO$_2$. The quantity of radioactive [^{11}C]CO$_2$ to be trapped is in the pico- to femtomole range; this small amount must interact with the walls of the trap as much as possible so that it can cool beneath its melting point of -56°C and crystallize. All three types of tubing that were used had the same wall thickness, therefore the more effective cooling in the 1/16'' tubing can be attributed to its smaller inner diameter. Therefore, all experiments reported in this thesis were carried out using the loop made from 1/16'' stainless steel.

4.7.2. Trapping Efficiency of [^{11}C]CO$_2$ in Vessel 1

In Section 2.10.1 experiments were described that were aimed at improving the amount of [^{11}C]CO$_2$ retained in the methylmagnesium bromide solution in Vessel 1. This solution was prepared by diluting 3 M Grignard reagent solution (Aldrich) about 10-fold with an appropriate volume of either diethyl ether or dibutyl ether in a multidose vial with a rubber septum. The volume of 0.3 M methylmagnesium bromide solution in Vessel 1 was varied and both the radioactivity in Vessel 1 and the radioactivity in soda lime trap #2 (refer to Figure 30) were measured. These values (Vessel 1 and soda lime trap #2) were summed and were taken as 100%. Figure 43 displays the radioactivity in Vessel 1, decay corrected to EOB and expressed as percentage of starting activity (also corrected to EOB) that was measured in the cold trap.

We expected to find an increase in trapped [^{11}C]CO$_2$ with an increased volume of the Grignard reagent because of a more efficient interaction of the gas with the solution. This can not be seen clearly in Figure 43. For example, in the experiments represented by bars A, B and C the same solution of 0.3 M Grignard reagent was used; the solution
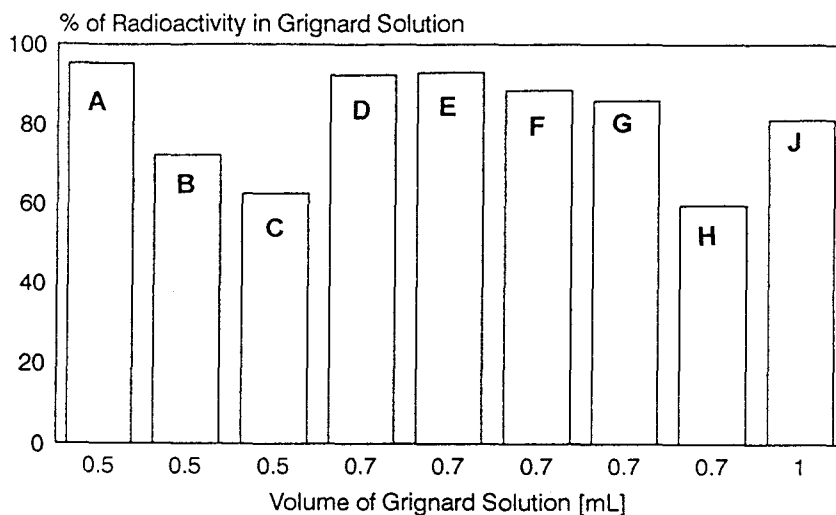
Figure 43: Amount of [^{11}C]CO$_2$ in Vessel 1 at various Volumes of Grignard Solution as Percentage of Starting Activity

was fresh in experiment A, in experiment B it was 2 days old and in experiment C it was 5 days old. These data illustrate that the quality of a diluted Grignard solution decreases over time and that its reactivity towards the incoming carbon dioxide decreased. Consequently, the amount of trapped [^{11}C]CO$_2$ decreased probably because decomposition of the methylmagnesium bromide had decreased the actual concentration of the Grignard reagent. In the experiments represented by bars D, E, F, G, H and J the 0.3 M Grignard solution was either freshly prepared or one day old (E and F). If we assume that the low amount of trapped [^{11}C]CO$_2$ in experiment H was caused by another influence (e.g., moisture in needle, reaction vessel or tubing), we can conclude that with a freshly prepared Grignard solution more than 90% of [^{11}C]CO$_2$ can be trapped. Therefore, despite the observed results further experiments were carried out with a volume of 1 mL, but usually with freshly diluted Grignard solutions.

As described in Section 4.5, the specific activity was reduced by dilution of ^{11}CO$_2$ with ^{12}CO$_2$ in the target and to a lesser degree during the first minutes of the radiosynthesis (until the carbonation of the Grignard is quenched by reaction with

phthaloyl dichloride). In the introduction chapter it was explained that in PET studies aimed at imaging hormone receptors there is a competition between labelled and unlabelled ligands for the receptors; therefore, the less dilute the radioactive tracer with unlabelled material (i.e., the higher its specific activity), the better its ability to bind to the receptors and to yield a detectable signal in the tomograph. This ratio of labelled and unlabelled material is of critical importance and may have been the most limiting factor in the studies reported later in this thesis (see Chapter 5). The experiments discussed in this section did not explicitly demonstrate that repeated use of the same Grignard dilution will cause an increase of the amount of $[^{12}C]CO_2$ introduced into the multidose vial and absorbed in the solution, leading to a decreased specific activity. Nevertheless, they show that both the Grignard reagent and the ether for its dilution must not be exposed to air. Therefore, it will be worthwhile in future experiments to use fresh or freshly distilled ether for diluting the Grignard reagent before each experiment.

4.7.3. Distillation Efficiency

A series of ^{11}C-acetylation reactions was carried out to investigate the influence of oil bath temperature, distillation time and the type of solvent in Vessel 1 on the transfer of $[^{11}C]CH_3COCl$ into Vessel 2 (see Section 2.10.2).

Distillations were done at various oil bath temperatures, using two different ethers as the solvent in Vessel 1. The distillation efficiency has been defined as the current activity in Vessel 2 divided by the starting activity in Vessel 1, multiplied by 100%:

$$(13) \qquad distillation\ efficiency = \frac{(activity)_{v2,t}}{(activity)_{v1,t=0}} \times 100\%$$
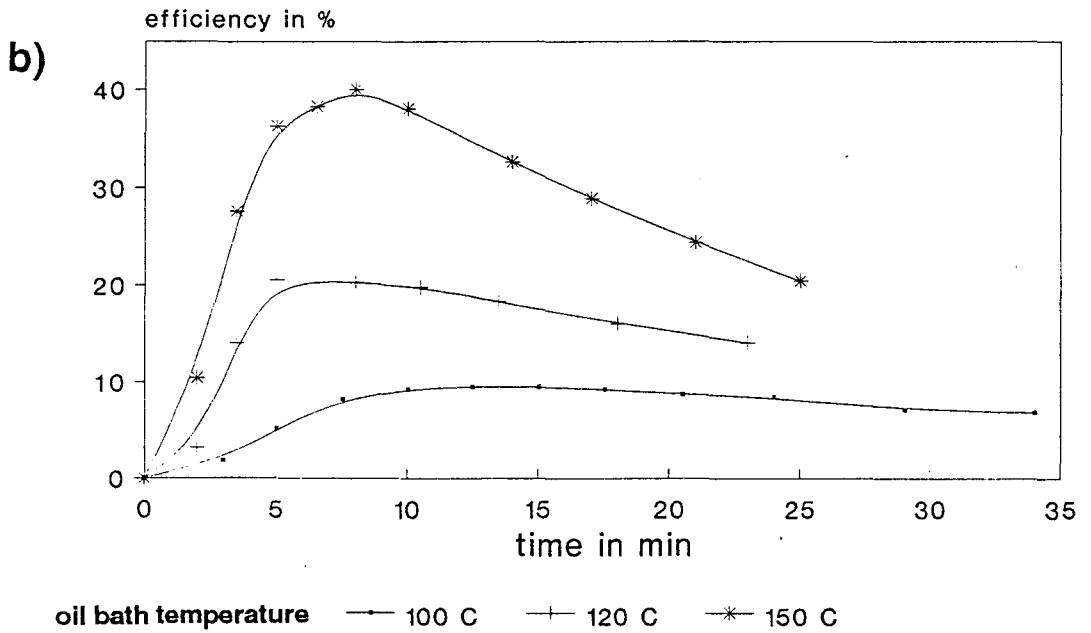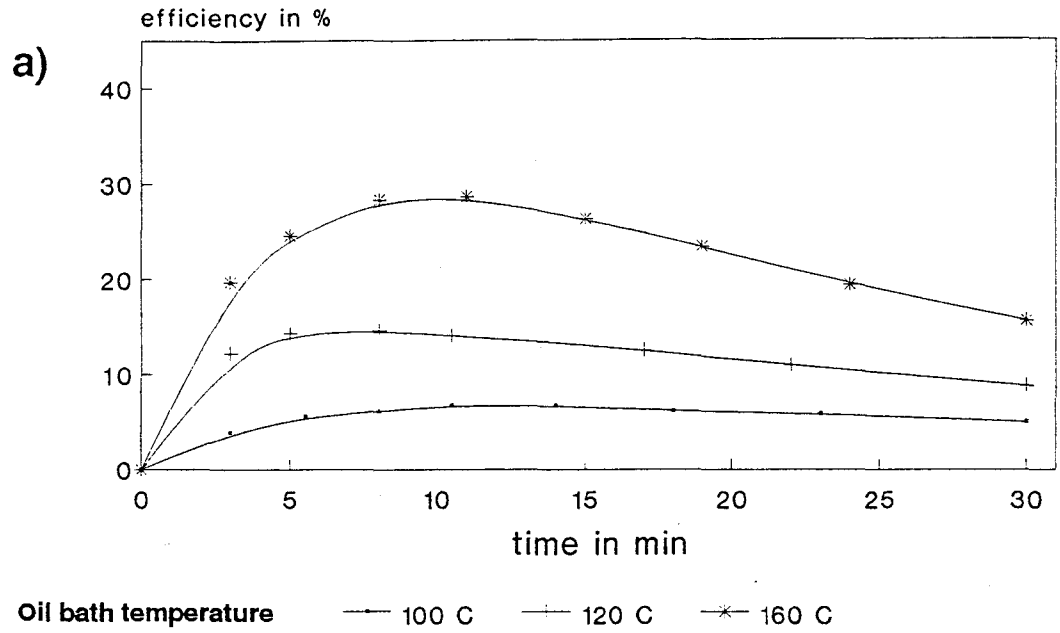
Figure 44: Distillation Efficiency at various Temperatures with a) Diethyl Ether and

b) Dibutyl Ether

Because the distillation efficiency is calculated from the actual values of radioactivity in Vessel 2 and not from the respective decay-corrected activity values, it gives information about the effectiveness of the distillation itself and about the influence of the time on the yield of ^{11}C in Vessel 2. Therefore, the distillation efficiencies calculated according to equation (13) reflect more accurately the actual situation during the distillation of [^{11}C]CH$_3$COCl and are of higher practical relevance than distillation efficiencies that could have been calculated from decay-corrected activity data.

Figure 44 shows the distillation efficiencies over time and at various temperatures using diethyl ether and dibutyl ether as solvents. Some experimental error might have been introduced during these measurements because the distillation had to be interrupted for ca. 30 seconds so that the activity at each time point was measured. Since this influence was approximately constant in each experiment, it is unlikely to have changed the overall outcome drastically.

These graphs show that distillations using dibutyl ether as the solvent in Vessel 1 gave consistently higher yields than distillations using diethyl ether. When diethyl ether was used as solvent, it evaporated during the first 30 to 60 seconds of distillation because of its low boiling point (35°C), leaving behind a tarry residue that contained [^{11}C]CH$_3$COCl. Dibutyl ether, with a boiling point of 142°C, did not distil as readily and a homogeneous solution remained until the end of the distillation. The helium gas stream at 15 mL/min was less efficient in removing [^{11}C]CH$_3$COCl from the diethyl ether residue compared to distillations where dibutyl ether was used as a solvent.

Figure 44 also shows the importance of the distillation time. Each curve has a peak, after which the decay of ^{11}C in Vessel 2 becomes faster than the rate of distillation. With dibutyl ether the peak activity occurred between 6 and 8 minutes. Because of the nature of this experiment and the time losses during each activity measurement, in reality the peak of activity will be shifted to even shorter time (5-6 minutes).

Figure 45 shows again the three curves obtained for the distillation efficiency with

dibutyl ether and for each of these graphs a curve for the radioactive decay of the peak activity (occuring at 8 minutes at 150°C, at 5 minutes at 120°C and at 12 minutes at 100°C). The decay of the peak activity A_0 has been calculated with equation (10), yielding the activity A_t for each time point after the peak maximum:

(10)
$$A_t = A_0 \times \exp\left(-\frac{0.693 \times t}{t_{1/2}}\right)$$
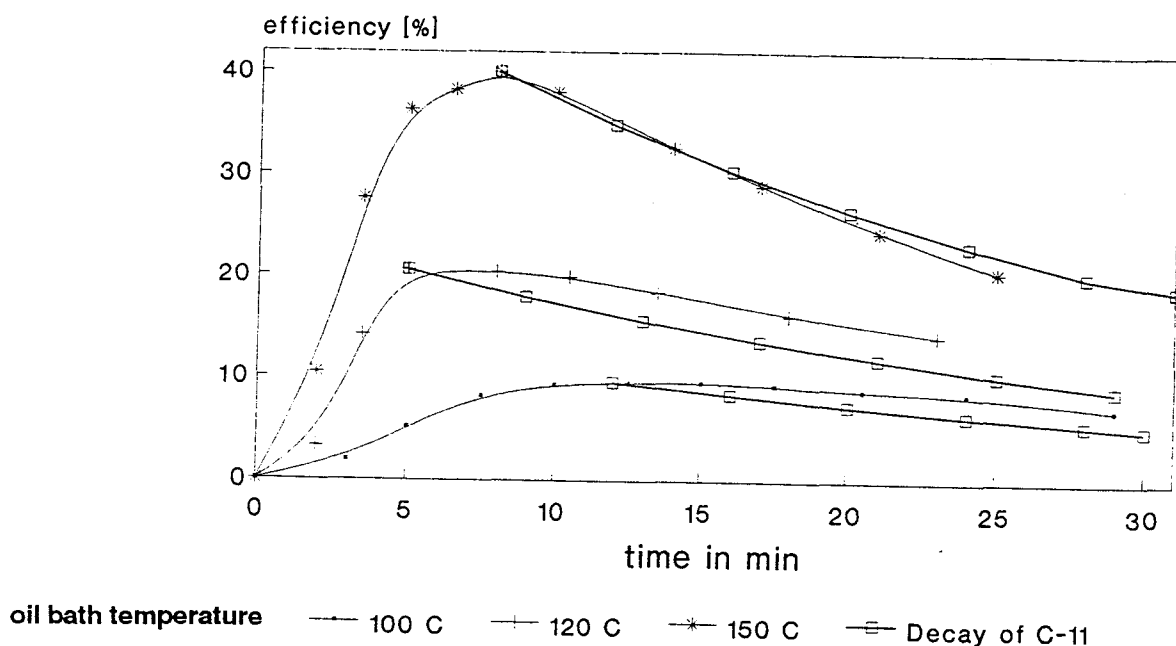
Figure 45: Comparison of Distillation Efficiency (Dibutyl Ether) with the Decay of [11]C

In each case the calculated curve starts at the respective point for the observed peak activity. The graphs illustrate that when distilling at 150°C, after about 8 minutes the observed decay in Vessel 2 approximately equalled the radioactive decay of ^{11}C, calculated with equation (10). This allowed us to conclude that after about 8 minutes at a distillation temperature of 150°C little or no more [11C]acetyl chloride distilled into Vessel 2. On the other hand, the calculated curves for the decay of the peak activities at 100°C and at 120°C, respectively, have steeper slopes than the curves for the observed

decay in Vessel 2 at 100°C and at 120°C, respectively. Therefore, at both temperatures the distillation was less efficient in the first minutes and even after the peak activity had been observed, some [^{11}C]acetyl chloride distilled into Vessel 2.

In reactions using dibutyl ether, where the distillation temperature equalled or exceeded 135°C, mass spectral analyses of the ethanolic SepPak eluate gave signals indicating the presence of some dibutyl ether in the reaction product. In electron impact mass spectra a peak at m/z = 57 due to the $CH_3(CH_2)_3^+$ fragment was observed, while in chemical ionization experiments a peak at m/z = 131 was attributed to the protonated molecular ion of dibutyl ether. At a distillation temperature of 120-125°C these ions were undetectable. The observations in mass spectral analysis do not allow a conclusion about the quantities of dibutyl ether that were present in the product at distillation temperatures equal or above 135°C; nevertheless, we can assume that in the products of reactions with a distillation temperature below 135°C dibutyl ether was present at a concentration of less than 100 ng (the detection limit in mass spectrometry is usually in the nanogram range, depending on the volatility of the analyte and its ability to form ions). Therefore, the amount of dibutyl ether that might have been injected with a product (125°C distillation) into a human with a body weight of 70 kg was at most 100 ng, which is 10^{-8} times the LD_{50} of the compound in rats (the LD_{50} value of dibutyl ether in rats is 7.4 g per kg of body weight (Material Safety Data Sheet)). This quantity will not have toxic effects. Nevertheless, if the radiochemical yield of the reaction is not sufficient, an increase in the distillation temperature must be considered because at a distillation temperature of 150°C the yield in Vessel 2 could be doubled (see Figure 44). In that case gas chromatography will be necessary to quantify the amounts of dibutyl ether found at higher distillation temperatures and after the respective distillation time. The toxicity of these quantities must then be evaluated.

Therefore, a distillation protocol of 120 to 125°C for 6 minutes with dibutyl ether

as solvent was settled upon as the optimal procedure to maximize [^{11}C]acetyl chloride production while minimizing the transfer of dibutyl ether.

4.7.4. Trapping Efficiency of [^{11}C]CH$_3$COCl

In a series of acetylation reactions (see Section 2.10.3) the cooling regime for Vessel 2 was varied to find the optimal cooling temperature for Vessel 2. The acid chloride is distilled at a high temperature (150°C in these experiments) and Vessel 2 must be cooled well below the boiling point of acetyl chloride (56°C), otherwise some of the acid chloride may be carried by with the helium gas stream.

At the end of each distillation the ^{11}C was measured both in Vessel 2 and in a downstream charcoal trap connected to its outlet (refer to Figure 30) and decay corrected to EOB. The sum of these two values was taken as 100%; the distribution of ^{11}C in percent between Vessel 2 and the trap is shown in Figure 46. In all experiments the acid chloride was distilled for 10 minutes. Vessel 2 was kept at the indicated temperatures throughout the whole radiosynthesis (i.e., from target unloading until end of distillation). However, in experiments #3 and #4 Vessel 2 was kept at the lower temperature only from target unloading until the first 5 minutes of distillation; then the cooling bath was removed and the vessel was either left at room temperature (experiment #3) or immersed in a hot water bath (experiment #4). In all other cases the reported temperature refers to that of the cooling mixture in the Dewar flask. In all experiments the actual temperature in Vessel 2 was not measurable and probably it was slightly above the reported values because of the incoming stream of hot gas (distillation temperature of 150°C).

As expected, the most favourable distribution of activity between Vessel 2 and the trap was found at the lowest temperature for Vessel 2 (-40°C throughout, experiment #1). If the cooling was removed after 5 minutes (experiment #3), the loss of [^{11}C]CH$_3$COCl doubled. Further losses were encountered when Vessel 2 was cooled to

only -10°C (experiment #2) or left at room temperature (experiment #5). In fact, these two experiments gave identical results. The results led us to conclude that Vessel 2 should be kept at -40°C to allow optimal retainment of the incoming hot [^{11}C]CH$_3$COCl gas.
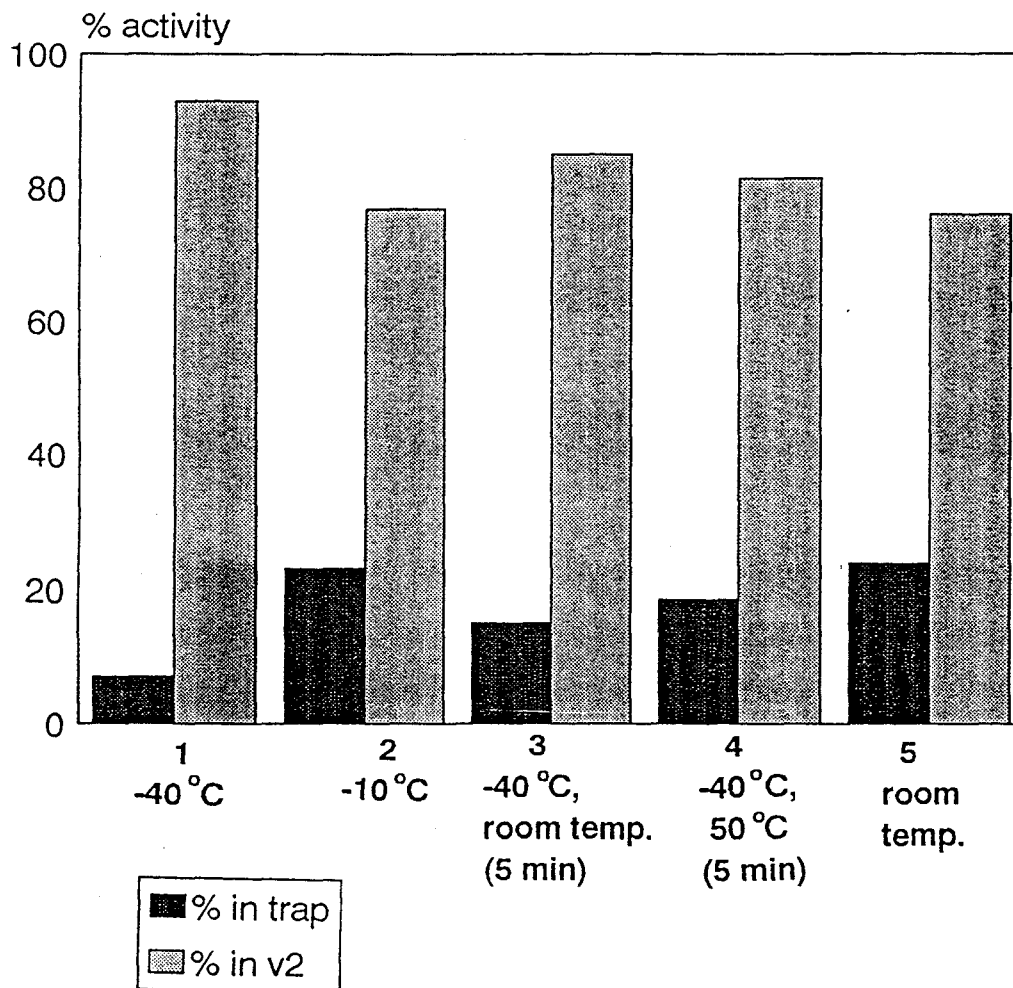

Figure 46: Distribution of ^{11}C between Vessel 2 and the Charcoal Trap

4.7.5. Rate of Amide Formation

Experiments were carried out to determine the dependency of amide formation on reaction time and temperature (see Section 2.10.4). One additional reaction was carried out for one hour to determine the maximum yield. In another reaction

trifluoroacetic acid was added to the amine before addition of the acetyl chloride to ensure the efficiency of the trifluoroacetic acid to convert the amine into its salt, thus preventing further reaction of the amine. Aliquots of all reactions were analyzed by HPLC and showed a peak for the desired amide with the same area as the peak arising from the reaction that proceeded for one hour. The peak areas were quantified and corresponded to 0.3 μmol $\pm$ 0.03 μmol (73 μg) amide. Analysis of the sample where trifluoroacetic acid was added before CH_3COCl did not show any trace of the peak for the amide.

These data proved that the reaction between acetyl chloride and the amine is complete in less than 30 seconds at temperatures down to -40°C and the yields at each time point were equal to the maximum yield. In the experiment where trifluoroacetic acid was added to the amine before the acetyl chloride it was demonstrated that protonation of the amine completely prevented any reaction of the amine with another electrophile such as acetyl chloride.

In the reactions conducted at -20°C and at -40°C, the handling of the samples might have introduced some experimental error by slight warming of the acetyl chloride solution for a few seconds when transferring it from its reservoir into the vial containing the amine. It is unlikely that this altered the overall result significantly. A similar situation existed in the remote controlled synthesis of [^{11}C]amides. The solution in Vessel 2 of the acetylation reaction apparatus was cooled to low temperature; during its transfer to Vessel 3 this solution would probably be warmed up to a similar extent before reaching Vessel 3.

These studies showed that after distillation of the acid chloride into Vessel 2, this vessel does not need to be warmed for several minutes as proposed by Luthra *et al.* (53), even if the vessel had been cooled to -40°C. This modification saves time when working with ^{11}C and simplifies the remote synthesis considerably. Although these experiments

were carried out using 7-methoxynaphthylenyl-1-ethylamine (**43**), these results will be valid for other primary amines that have similar reactivities and nucleophilicities (e.g., 5-methoxytryptamine (**7**), 2-iodo-5-methoxytryptamine (**22**)).

4.8. Summary

The results presented in Chapter 4 are summarized with respect to the thesis objectives established in Section 1.5.

(1) A generic method has been developed to produce ^{11}C-labelled amides. First, ^{11}C-labelled acetyl chloride was produced by the reaction of CH_3MgBr with $[^{11}C]CO_2$, followed by reaction with phthaloyl dichloride. Second, the resulting $[^{11}C]$acetyl chloride was reacted with various amines to give ^{11}C-labelled acetamides; in this thesis the acetamides were biologically active melatonin analogues. The apparatus designed for this work allowed for the remote and computer-operated synthesis of ^{11}C-labelled compounds with large amounts of activity on a routine basis. This apparatus resulted in a substantially lower radiation dose for the chemist.

(2) Two melatonin agonists, 2-iodomelatonin (**11**) and 7-methoxynapthylenyl-1-N-acetyl-ethylamine (**15**) have been labelled with ^{11}C for the first time.

(3) A series of experiments was conducted to determine the reproducibility of the synthesis steps and to optimize the overall procedure. The trapping of $[^{11}C]CO_2$ in Vessel 1 and the trapping of $[^{11}C]CH_3COCl$ in Vessel 2 depended strongly on reaction conditions and affected the overall yield significantly. Distillation at 120°C for approximately 6 minutes with dibutyl ether as solvent in Vessel 1 was settled upon as a compromise to minimize transfer of dibutyl ether and to maximize transfer of $[^{11}C]CH_3COCl$ into Vessel 2. If the distillation temperature needs to be raised to increase the radiochemical yield of the syntheses, the amounts of dibutyl ether found in Vessel 2 must be quantified to evaluate its toxicity. The rate of amide formation is rapid, even at -40°C such that Vessel

2 can be kept at -40°C to optimize [^{11}C]CH$_3$COCl trapping without slowing the rate of amide formation. The quality of the Grignard reagent can cause variations in the yield; when a product with a high specific activity is needed, freshly distilled dry ether should be used.

As a result of the optimizations of these steps, the described method including the SepPak workup can be carried out remotely in 30 to 35 minutes, which is close to the reaction time of 30 minutes published by LeBars *et al.* (32,33) for the directly handled procedure. Thus, the remote operation of the apparatus has been achieved without a trade-off in reaction time.

Under the established reaction conditions, a radiochemical yield of 15 to 20% was achieved, which is comparable to the yields cited in the literature (32,33). Two syntheses were carried out with high starting activities and they allowed an estimation of the specific activity that is achievable with the described procedure. In these two syntheses specific activities of 410 and 130 mCi/μmol at the end of synthesis were achieved; with higher irradiation currents it should be possible to achieve specific activities of 5400 mCi/μmol. In the future PET studies must be carried to determine whether such specific activities will be sufficient to visualize melatonin receptors *in vivo*.

(16) R = CF$_3$ K$_d$ = 10^{-13} M
(45) R = cyclopropyl   K$_d$ = 10^{-13} M
(46) R = ethyl   K$_d$ = 10^{-11} M
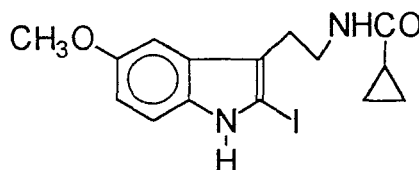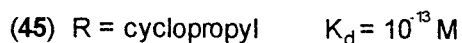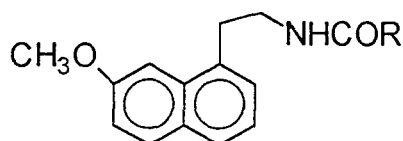
(47)

Figure 47: Melatonin Analogues for Future ^{11}C-Labelling

Further efforts should also be made to develop the radiochemical syntheses of new melatonin analogues with lower binding dissociation constants; for example, it has been shown that variation of the amide function effects the binding of the ligand to the receptor (12,13) and there are recent reports (19) about several compounds (e.g., **16, 45, 46** in Figure 47) where the N-acetyl moiety is replaced by a cyclopropyl, ethyl or trifluoro acetyl group. Also, the cyclopropyl amide of 2-iodomelatonin (**47**) may be a potent melatonin receptor agonist and its labelling with ^{11}C should be attempted.

In principle, the acetylation apparatus can be used for a variety of acylation reactions; one obvious problem that may arise is the higher boiling point for acid chlorides with a longer carbon chain, but attempts to distil ^{11}C-labelled propionyl and butyryl chlorides have already been reported in the literature (53).

If further experiments show that the half-life of ^{11}C is too short to allow imaging of the receptors, labelling with ^{18}F must be invoked; in that case electrophilic fluorination must be avoided because of the low specific activities (see Section 1.3.1).

CHAPTER 5

BIOLOGICAL STUDIES

This chapter describes preliminary results obtained in PET studies with the ^{11}C-labelled melatonin agonists 2-iodomelatonin (11) and S20098 (15). With each tracer a pilot PET scan was done to assess the quality of the scan (count rates in the brain, contrast) and the tracer's ability to visualize melatonin receptors *in vivo*.

5.1. PET Images

[11C]2-Iodomelatonin (11) was prepared for intravenous injection as described in Section 2.9.1. A sterile, isotonic solution of the radiopharmaceutical (7 mL, 20 mCi, specific activity of 130 mCi/μmol at time of injection) was injected and the subject's brain was monitored as described in Section 2.11.1. Figure 48 shows images that were obtained from the PET scan.

All slices displayed in Figure 48 are taken coronally, which means parallel to the face and thus cutting the brain bilaterally and symmetrically. The bottom of each slice is the orbito-meatal line, which is approximately the eye-ear line. The distance from the bottom to the top of a slice is 15 cm. The person's right side is at the readers left side. Slice 1 is in the back of the brain, slice 21 is in the front of the brain; a depth of approximately 15 cm is covered by these 21 slices, therefore each slice has a thickness of about 0.7 cm. Figure 48a (left side) displays coronal slices through the brain with radioactivity accumulated during the first two minutes of the scan, Figure 48b (right side) shows coronal slices with radioactivity observed between 20 and 30 minutes after
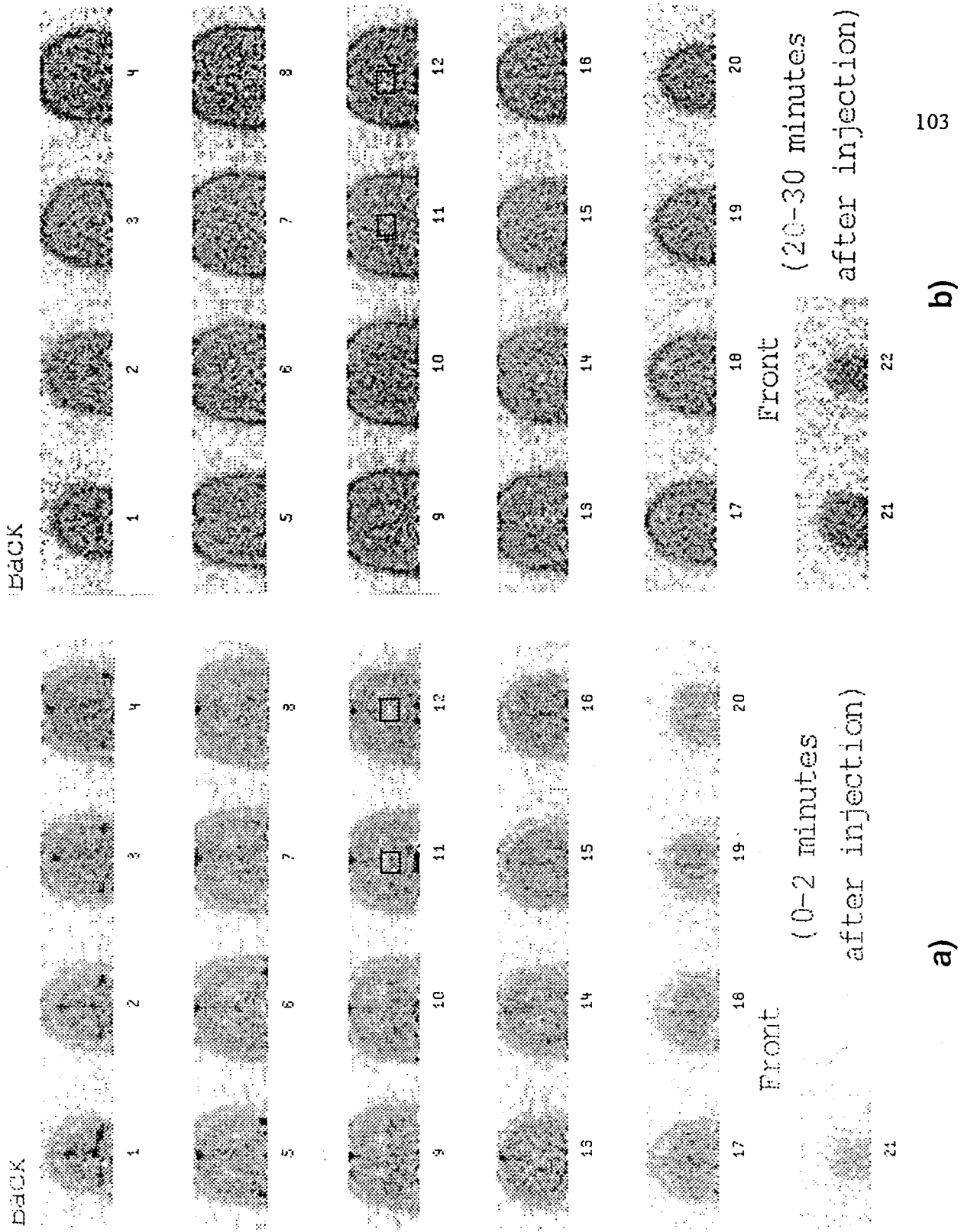
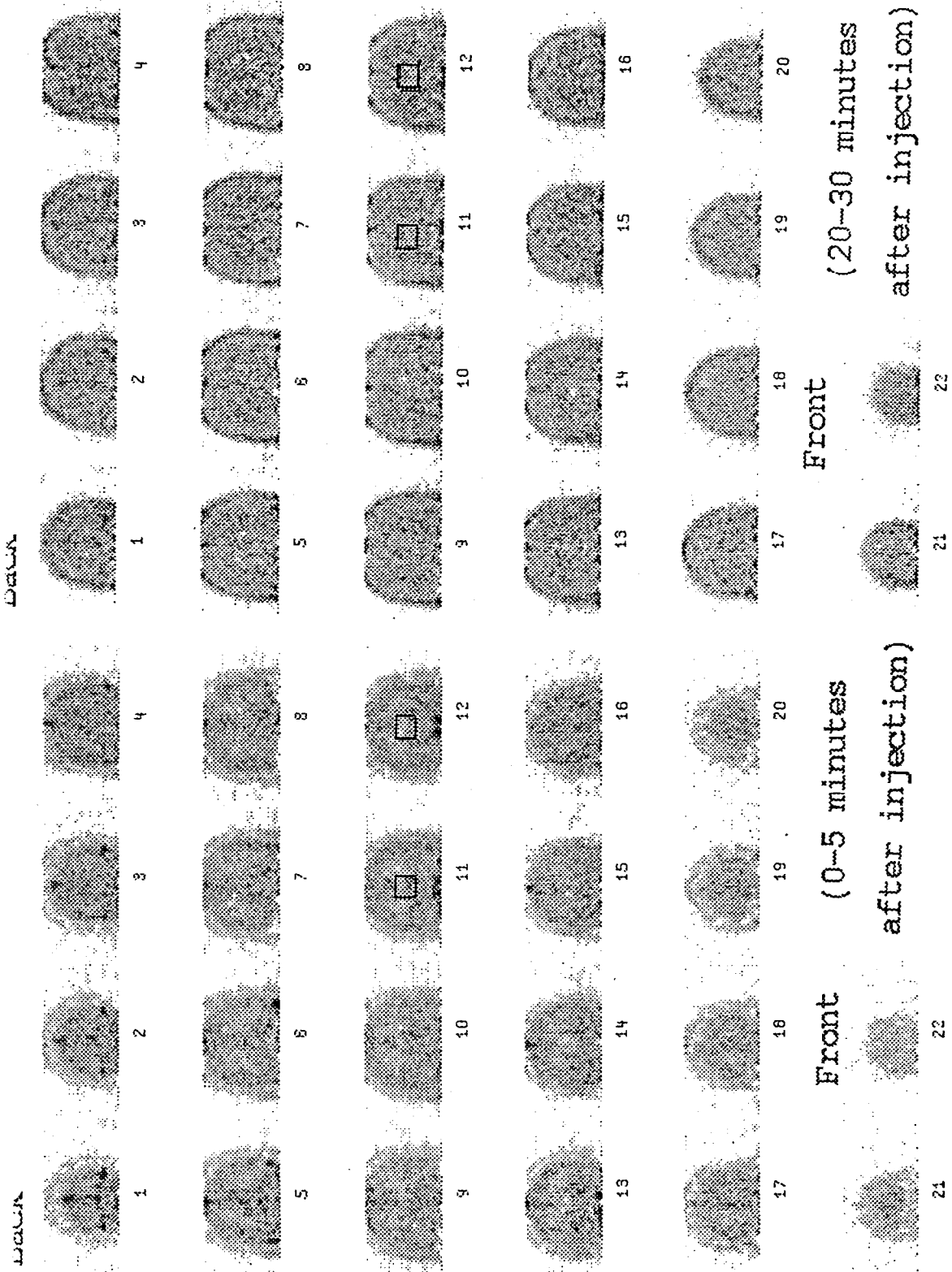**Figure 48:** Coronal Slices of a Human Brain after Injection of [^{11}C]2-Iodomelatonin and Scanning of the Areas by PET

Figure 49: Coronal Slices of a Human Brain after Injection of [^{11}C]S20098 and Scanning of the Areas by PET

injection. The stronger the black contrast, the more counts that were recorded. A relative colouring scale was used: in each slice the pixel with the highest count rate was set to 100% and the other pixels were adjusted accordingly.

Similarly, [^{11}C]S20098 (15) was prepared for intravenous injection as described in Section 2.9.1. A sterile, isotonic solution of the radiopharmaceutical (7 mL, 15 mCi, specific activity of 460 mCi/μmol at time of injection) was injected and the subject's brain was monitored as described in Section 2.11.1.

Figure 49 shows the images that were obtained from the PET study with this compound. As in Figure 48, coronal slices are displayed with the same orientation as in Figure 47. The images in Figure 49a (left side) display the observed radioactivity during the first five minutes of scanning, whereas the images in Figure 49b (right side) were obtained between 20 and 30 minutes after injection of the tracer. The black contrast is proportional to the observed count rates and a relative scale was used for each slice.

5.2. Discussion

Figures 48 and 49 show that both 2-iodomelatonin (11) and the naphthyl derivative S20098 (15) cross readily the blood-brain-barrier. The biological half-life of 2-iodomelatonin has been reported to be 60 minutes (54); therefore, in the case of [^{11}C]2-iodomelatonin we can assume that during the 30 minutes of scanning the majority of the observed counts were caused by the radiopharmaceutical and not by any of its metabolites. There is no information available about the biological half-life of S20098 (15); because this is a synthetic compound we assume that a fast catabolism in the human organism is not very likely and therefore, during the 30 minutes of PET scanning the observed counts were mainly due to S20098 and not to any of its metabolites. These assumptions are valid for a qualitative discussion of the images, but for quantitative investigations they will have to be confirmed in animal experiments.

The PET images of both [^{11}C]2-iodomelatonin and of [^{11}C]S20098 are featureless; only blood vessels are outlined (with a higher intensity in Figures 48a and 49a, respectively, because at the beginning of the scan most of the radioactivity was still in the blood).

In all figures the hypothalamus is expected to be in the middle of slices 11 or 12 within the small frame. The hypothalamus contains the suprachiasmatic nuclei (SCN), which have the highest concentration of melatonin receptors (see Section 1.3.1). These nuclei have been found in autoradiographic studies of coronal slices of the human brain (orientation identical to that described in Section 5.1 for the PET images) as 2 oval spots, approximately 0.5 mm wide, 2 mm long and 4 mm apart from each other (30). The PET images displayed in Figures 48 and 49 do not show an obvious accumulation of ^{11}C in the area of the hypothalamus. The melatonin receptors in the SCN have not been visualized with either of these two ^{11}C-labelled compounds. This observation is probably the result of relatively high levels of nonspecific binding of these compounds to brain tissues leading to a substantial background noise.

Nevertheless, there seems to be an accumulation of radioactivity in two "spots" in the lower part of slice 12 in Figure 48b ([^{11}C]2-iodomelatonin between 20 and 30 minutes after injection). These spots have been identified as the Circle of Willis, one of the blood supply system for the brain, which is outside the brain. The fact that the radioactivity remained there even at 20 to 30 minutes after injection suggests that this accumulation was due to specific binding; binding sites for melatonin in the Circle of Willis of the rat have been reported with K_d values between 10^{-10} and 3×10^{-11} M (55). These binding dissociation constants are similar to those reported for 2-iodomelatonin in the SCN of the hypothalamus (see Table 5), but the number of binding sites in the Circle of Willis has been reported to be 15 to 19 fmol/mg protein (55), which is 3 to 4 times higher than in the SCN (31). In addition, the arteries in the brain sections in Figures 48

and 49 have a larger size than the SCN which makes it plausible that more labelled compound was specifically bound in the Circle of Willis and therefore visualized.

The failure to visualize the SCN on the basis of its melatonin receptor contents may be due to the following reasons:

(1) The size of the SCN is below the spatial resolution volume of the PET technology, which is 4 mm^3. Therefore, we will not be able to resolve the actual shape of the SCN. If there were a sufficient accumulation of radioactive ligand in the brain volume pertaining to the SCN, this radioactivity would be detected by the scanner as a volume with a dimension equal to the resolution of the scanner (4 mm^3). This means that the original accumulation of count rates in the small volume of the SCN becomes more diffuse when displayed as a larger volume and therefore more difficult to detect at all.

(2) The ^{11}C-labelled tracers used in these preliminary studies had specific activities that were too low to visualize receptors. Therefore ligands with higher specific activities are required.

(3) The levels of nonspecific binding in all tissues were very high. Therefore, longer scanning times will be necessary to allow the nonspecifically bound ^{11}C-labelled ligands to clear away. In order to satisfy this goal ^{11}C-labelled ligands of even higher specific activities will be needed. Alternatively, the observation times can be extended by labelling with the longer-lived isotope, [18]F.

(4) The compounds tested are quite lipophilic. Less lipophilic ligands with high receptor affinities (low K_d value) may be more appropriate. Unfortunately, all known melatonin agonists have a similar structure (indoles, naphthalene derivatives and tetracyclines, see Figure 5 in Section 1.1.3.), and none of these is expected to have a significantly different nonspecific binding behaviour.

5.3. Summary

Two ^{11}C-labelled melatonin agonists, 2-iodomelatonin (11) and the naphthyl derivative S20098 (15), were produced with a sufficient radiochemical yield (15 to 20 mCi) to be used as radiopharmaceuticals for PET imaging. With each of these compounds a pilot PET study was performed. It was shown that both ligands penetrate the blood-brain barrier. The SCN could not be visualized with these compounds because of dominating nonspecific binding, but there are indications that [11C]2-iodomelatonin showed specific binding to receptors in the Circle of Willis.

These PET studies showed that both the specific activities of the radiopharmaceuticals must be increased and that the procedures of the PET study have to be optimized. It was estimated in Section 4.5 that an increase in the specific activity to approximately 5400 mCi/μmol may be possible. This specific activity should be sufficient to allow us to extend the duration of the PET study significantly and thus decrease the relative amount of nonspecific binding. Further PET scans under these optimized conditions will then allow us to determine whether labelling with ^{11}C is feasible to visualize melatonin receptors in the human brain or whether the synthesis of ^{18}F-labelled tracers will be necessary.

<u>REFERENCES</u>

1. Krause, D. N. and Dubocovich, M. L. (1990) Regulatory sites in the melatonin system of mammals. *TINS* **13**, 464-470

2. Kopin, I. J.; Pare, C. M. B.; Axelrod, J. and Weissbach, H. (1961) The fate of melatonin in animals. *J. Biol. Chem.* **236**, 3072-3075

3. Beck, O. and Jonsson, G. (1981) *In vivo* formation of 5-methoxytryptamine from melatonin in rat. *J. Neurochem.* **36**, 2013-2018

4. Cahill, G. M.; Grace, M. S. and Beshare, J. C. (1991) Rhythmic regulation of retinal melatonin: metabolic pathways, neurochemical mechanisms, and the ocular circadian clock. *Cell. Mol. Neurobiol.* **11(5)**, 529-560

5. Clemens, J. A.; Flaugh, M. E.; Parli, J. and Sawyer, B. D. (1980) Inhibition of luteinizing hormone release and ovulation by 6-chloro- and 6-fluoromelatonin. *Neuroendocrinology* **30**, 83-87

6. Cassone, V. M. (1990) Effects of melatonin on vertebrate circadian systems. *TINS* **13**, 457-463

7. Moore, R. (1983) Organization and function of a central nervous system circadian oscillator: the suprachiasmatic hypothalamic nucleus. *Federation Proc.* **42**, 2783-2789

8. Armstrong, A. M.; Cassone, V. M.; Chesworth, M. J.; Redman, J. R. and Short, R. V. (1986) Synchronization of mammalian circadian rhythms by melatonin. *J. Neur. Transm.* **21**, S375-S394

9. Silman, R. (1992) Melatonin: the clinical perspective in man. *Biochem. Soc. Trans.* **20**, 315-317

10. Arendt, J.; Aldhous, M. and Wright, J.(1988) Synchronization of a disturbed sleep-wake cycle in a blind man by melatonin treatment. *Lancet* 772-773

11. McGonigle, P. and Molinoff, P. B. (1989) Quantitative aspects of drug-receptor interactions. *Basic Neurochemistry* (Siegel, G. J., Agranoff, B. W., Wayne Albers, R., and Molinoff, P. B., eds) pp. 183-202, Raven Press, New York

12. Heward, C. B. and Hadley, M. E.(1975) Structure - activity relationship of melatonin and related indoles. *Life Sci.* **17**, 1167-1178

13. Frohn, M. A.; Seaborn, C. J.; Johnson, D. W.; Phillipou, G.; Seamark, R. F.and Matthews, C. D. (1980) Structure - activity relationship of melatonin analogues. *Life Sci.* **27**, 2043-2046

14. Laudon, M. and Zisapel, N.(1986) Characterization of central melatonin receptors using [^{125}I]iodomelatonin. *FEBS Lett.* **197**, 9-12

15. Niles, L.; Pickering, D. S. and Sayer, B. G. (1987) HPLC-purified 2-[^{125}I]iodomelatonin labels multiple binding sites in hamster brain. *Biochem. Biophys.*

Res. Commun. **147**, 949-956

16. Dubocovich, M. L. (1988) Luzindole (N-0774): a novel melatonin receptor antagonist. *J. Pharmac. Exp. Ther.* **246**, 902-910

17. Laudon, M.; Yaron, Z. and Zisapel, N. (1988) N-(3,5-dinitrophenyl)-5-methoxytryptamine, a novel melatonin antagonist: effects on sexual maturation of the male and female rat and on oestrous cycles of the female rat. *J. Endocr.* **116**, 43-53

18. Pevet, P.; Masson-Pevet, M.; Chantegrel, J.; Marsura, A.; Luu-Duc, C.and Claustrat, B. (1989) Failure of N-(2,4-dinitrophenyl)-5-methoxytryptamine (a putative melatonin antagonist) and of N-(3,5-dinitrophenyl)-5-methoxytryptamine to prevent the effects of injections of melatonin in the late afternoon on testicular activity of the golden hamster. *J. Endocr.* **123**, 243-247

19. Yous, S.; Andrieux, J.; Howell, H. E.; Morgan, P. J.; Renard, P.; Pfeiffer, B.; Lesieur, D. and Guardiola-Lemaitre, B. (1992) Novel melatonin ligands with high affinity for the melatonin receptor. *J. Med. Chem.* **35**, 1484-1486

20. Copinga, S.; Tepper, P. G.; Grol, C. J.; Horn, A. S. and Dubocovich, M. L. (1993) 2-Amido-8-methoxytetralines: a new series of nonindolic melatonin-like agents. *J. Med. Chem.* **36**, 2891-2898

21. Pike, V. W. (1988) Organic synthesis with short-lived positron-emitting radioisotopes. *Isotopes: essential chemistry and Applications II* (Jones, J. R., ed) pp. 1-39, Royal Society of Chemistry

22. Siemens CTI, (1989) *RDS Model 112/00. Radioisotope delivery system, technical description*

23. McGeer, P. L., Eccles, J. C., and McGeer, E. G. (1987) *Molecular Neurobiology of the mammalian brain* Plenum Press, New York, London

24. Cardinali, D. P.; Vacas, M. I. and Boyer, E. E. (1979) Specific binding of melatonin in bovine brain. *Endocrinology* **105**, 437-441

25. Cassone, V. M.; Roberts, M. H. and Moore, R. Y. (1987) Melatonin inhibits metabolic activity in the rat suprachiasmatic nuclei. *Neurosci. Lett.* **81**, 29-34

26. Vakkuri, O.; Leppaeluoto, J. and Vuolteenaho, O. (1984) Development and validation of a melatonin radioimmunoassay using radioiodinated melatonin as tracer. *Acta Endocrinol. (Copenhagen)* **106**, 152-157

27. Vakkuri, O.; Laemsae, E.; Rahkamaa, E.; Ruotsalainen, H. and Leppaeluoto, J. (1984) Iodinated melatonin: preparation and characterization of the molecular structure by mass and 1H NMR spectroscopy. *Anal. Biochem.* **142**, 284-289

28. Vanececk, J.; Pavlík, A. and Illnerová, H. (1987) Hypothalamic melatonin receptor sites revealed by autoradiography. *Brain Res.* **435**, 359-362

29. Williams, L. M. and Morgan, P. J. (1988) Demonstration of melatonin-binding sites on the pars tuberalis of the rat. *J. Endocr.* **119**, R1-R3

30. Reppert, S. M.; Weaver, D. R.; Rivkees, S. A. and Stopa, E. G. (1988) Putative melatonin receptors in a human biological clock. *Science* **242**, 78-80

31. Yuan, H.; Lu, Y. and Pang, S. F. (1991) Binding characteristics and regional distribution of [^{125}I]iodomelatonin binding sites in the brain of the human fetus. *Neurosci. Lett.* **130**, 229-232

32. LeBars, D.; Luthra, S. K.; Pike, V. W. and Luu Duc, C. (1987) The preparation of a carbon-11 labelled neurohormone - [^{11}C]melatonin. *Appl. Radiat. Isot.* **38**, 1073-1077

33. LeBars, D.; Thivolle, P.; Vitte, P. A.; Bojkowski, C.; Chazot, G.; Arendt, J.; Frackowiak, R. S. J. and Claustrat, B. (1991) PET and plasma pharmacokinetic studies after bolus intravenous administration of [^{11}C]melatonin in humans. *Nucl. Med. Biol.* **18**, 357-362

34. Chirakal, R.; Sayer, B. G.; Firnau, G. and Garnett, E. S. (1988) Synthesis of F-18 labelled fluoromelatonins and 5-hydroxyfluorotryptophans. *J. Labelled Compd. Radiopharm.* **25**, 63-71

35. LeBars, D.; Luthra, S. K.; Pike, V. W. and Kirk, K. L. (1988) Radiosynthesis of NCA [carbonyl-^{11}C]6-fluoromelatonin. *Appl. Radiat. Isot.* **39**, 287-290

36. Niles, L. P.; Wong, Y. -W.; Mishra, R. K. and Brown, G. M. (1979) Melatonin receptors in brain. *Eur. J. Pharmac.* **55**, 219-220

37. O'Connor, C. (1970) Acidic and basic amide hydrolysis. *Q. Rev. Chem. Soc.* **24**, 553-564

38. Hinman, R. L. and Bauman, C. P. (1964) Reactions of N-bromosuccinimide and indoles. A simple sythesis of 3-bromooxoindoles. *J. Org. Chem.* **29**, 1206-1215

39. Phillips, R. S. and Cohen, L. A. (1983) Synthesis of 2-bromo-1-tryptophan and 2-chloro-1-tryptophan. *Tetrahedron Lett.* **24**, 5555-5558

40. Phillips, R. S. and Cohen, L. A. (1986) Intramolecular general acid and general base catalysis in the hydrolysis of 2-halotryptophans and their analogues. *J. Am. Chem. Soc.* **108**, 2023-2030

41. Cahill, G. M. and Beshare, J. C. (1989) Retinal melatonin is metabolized within the eye of Xenopus laevis. *Proc. Natl. Acad. Sci. USA* **86**, 1098-1102

42. Grace, M. S.; Cahill, G. M. and Beshare, J. C. (1991) Melatonin deacetylation: retinal vertebrate class distribution and Xenopus laevis tissue distribution. *Brain Research* **559**, 56-63

43. Bertholet, R. and Hirsbrunner, P. (1985) Preparation of serotonin and derivatives. *Europ. Pat. Off.* **130 303 A1**,

44. Remers, W. A. (1972) *The chemistry of heterocyclic compounds. Indoles, part 1* (Houlihan, W. J., ed) pp. 71-78, Wiley-Interscience, New York

45. Sundberg, R. J. (1970) *The chemistry of indoles* (Anonymous, ed) pp. 14-17, Academic Press, New York

46. Kline, T. (1985) Preparation of 2-iodotryptamine and 2-iodo-5-methoxytryptamine. *J. Heterocyclic Chem.* **22**, 505-509

47. Porter, W. L. and Thimann, K. V. (1965) Molecular requirements for auxin action - 1. Halogenated indoles and indoleacetic acid. *Phytochemistry* **4**, 229-243

48. Carey, F. A. and Sundberg, R. J. (1990) *Advanced organic chemistry. Part A: structure and mechanism* Plenum Press, New York and London

49. Huang, H. T. and Niemann, C. (1952) The enzyme-inhibitor dissociation constants of alpha-chymotrypsin and three series of competitive inhibitors derived from d-tryptophan. *J. Am. Chem. Soc.* **74**, 101-105

50. Couch, M. W. and Williams, C. M. (1972) Mass spectrometry of tryptamines and acetylated tryptamine derivatives. *Anal. Biochem.* **50**, 612-622

51. Gynther, J.; Peura, P. and Salmi, S. (1985) Electron impact and chemical ionization fragmentation of 5-methoxytryptamine and some 6-methoxy-beta-carbolines. *Acta Chem. Scand.* **B39**, 849-859

52. Harada, N. and Hayashi, N. (1993) Measurement of the carbon source which is responsible for dilution in carbon-11 labelling reactions. *Appl. Radiat. Isot.* **44**, 629-630

53. Luthra, S. K.; Pike, V. W. and Brady, F. (1990) Preparation of some NCA [1-^{11}C]Acid chlorides as labelling agents. *Appl. Radiat. Isot.* **41**, 471-476

54. Stankov, B.; Gervasoni, M.; Scaglione, F.; Perego, R.; Cova, D.; Marabini, L. and Fraschini, F. (1993) Primary pharmaco-toxicological evaluation of 2-iodomelatonin, a potent melatonin agonist. *Life Sci.* **53**, 1357-1365

55. Viswanathan, M.; Laitinen, J. T. and Saavedra, J. M. (1990) Expression of melatonin receptors in arteries involved in thermoregulation. *Proc. Natl. Acad. Sci. USA* **87**, 6200-6203

APPENDIX

A) Program for Loading the Gas Target "O15LOAD210"

```
;O15LOAD210.CMD - /PROD version
;
;        HISTORY:
;                 14 May 1988 - Addition of logging function by FAR
;                 22 May 1988 - General clean-up
;                 06 Jan 1989 - Shortened leak check wait from 30 to 60 sec
;                               Commented out logging
;                 06 Feb 1989 - Modified for full energy target (210 psi load)
;
WATCH OFF              ; Clear any previous WATCH ZONE entries
WATCH R87             ; N-15 bottle valve
WATCH R90             ; Target load valve
WATCH SAD2,4          ; Target pressure (0-1000 psia)
WATCH F1BC,6          ; Watch foil current #2 (should be 0)
WATCH F3BC,7          ; Watch foil current #3 (should be 0)
WATCH F4BC,8          ; Watch foil current #4 (should be 0)
ON R87               ; Open [N-15] bottle valve
ON R90               ; Open target load valve
WAIT 15              ; Wait to pressurize
;CHECKVALUE  SAD2,210,10,@/TEST/O15OFF  ; if not 210 psia, abort
OFF R87              ; Close [N-15] bottle valve
WAIT 30              ; Wait 1 minute
WAITVALUE    SAD2,130,1,0.01,@/TEST/O15OFF  ; if < 130 psia, abort
OFF R90              ; Close target load valve
WATCH OFF,1          ; Stop watching R87
WATCH OFF,2          ; Stop watching R90
;@/TEST/LOGON1.cmd   ; Begin logging data to printer
```

B) Program for Unloading the Gas Target "O15BOLUS"

```
;O15BOLUS.CMD - /PROD version
;
; HISTORY:
; 22 May 1986 - General clean-up
; 27 Jul 1988 - Add WATCH OFF at end
; 09 Jan 1989 - Modified by J.Bida/D.Schlyer
; 17 Sep 1990 - General clean-up [DVa]
; 1. Oct 1992 - Modification to add cycling for use with O15WATER
; 5. Oct.1992 - G.Firnau, Modification to sweep with open bolus valve.
; 12.Febr.93 - G.Firnau, eliminate all WAITC-commands,helium sweeps also cycles
WATCH SHD2,7                            ; Display tube target pressure
WAT SHD3,8                             ; Display GFU flow rate
WATCH R83,9                            ; Watch bolus valve status
WATCH R86,10                           ; Watch He sweep valve
BEAMOFF                               ; Turn cyclotron beam off
WAIT 5                                 ; Wait to observe target pressure with beam off
on r61                                 ; Turn on Helium bottle valve
on r/3
cycle r83,ON,.1,4.0                         ;cycle the bolus valve, releases O-15.

wait 150
;text 21,0,Hit Enter to increase dispensing rate!
;waitc (D)
;cycle r89,on,.5,5
;text 21,0,Hit Enter to discontinue dispensing!
;waitc (D)
cycle r83,off                            ; Stop cycling bolus valve.
off r83
on r89
wait 15
cycle r86,ON,.4,4.0                                 ; Turns on heliu
m sweep gas.
wait 60
cycle r86,OFF
off r86
;text 21,0,Has O-15WATER arrived in HOT CELL No.1, if yes hit Enter.
;waitc (D)
off r89
off r61
off r/3
text 21,0,
text 22,0,Hit Enter to exit programme!
waitc (D)
WATCH OFF                    ; Clear watch zones
```